FACULTY OF SCIENCE
DEPARTMENT OF CHEMISTRY
MOLECULAR DESIGN & SYNTHESIS
Celestijnenlaan 200F box 2404
B-3001 Heverlee, Belgium
thupten.palden@.kuleuven.be

Thupten Palden

ORGANIC LIXIVIANTS FOR METAL RECOVERY FROM INDUSTRIAL PROCESS RESIDUES

June 2021

**ARENBERG DOCTORAL SCHOOL**
FACULTY OF SCIENCE

# Organic lixiviants for metal recovery from industrial process residues

**Thupten Palden**

Supervisor(s):

Prof. Dr. Koen Binnemans

Dr. Mercedes Regadìo

Dissertation presented in partial fulfilment of the requirements for the degree of

Doctor of Science (PhD): Chemistry

June 2021

# ORGANIC LIXIVIANTS FOR METAL RECOVERY FROM INDUSTRIAL PROCESS RESIDUES

**Thupten Palden**

Supervisor(s):
Prof. Dr. Koen Binnemans
Dr. Mercedes Regadìo

Members of the Examination Committee:
Prof. Dr. Annelies Delabie (Chairperson)
Prof. Dr. Ir. Bart Blanpain
Dr. Jeroen Spooren (External member)
Dr. Lieven Machiels
Prof. Dr. Ir. Tom Van Gerven
Prof. Dr. Valérie Cappuyns

Dissertation presented in partial fulfilment of the requirements for the degree of Doctor of Science (PhD: Chemistry)

June 2021

Uitgegeven in eigen beheer, Thupten Palden, Celestijnenlaan 200F, B-3001 Leuven (Belgium)

མཁས་པ་སྨོབ་པའི་དུས་ན་སྨྲུག།

བདེ་བར་སྩོད་ལ་མཁས་མི་སྲིད།

བདེ་བ་ཆུང་ལ་ཚགས་པ་དེས།

ཆེན་པོའི་བདེ་བ་ཐོབ་མི་སྲིད།

*“Speak with honesty, think with sincerity, and act with integrity”*

*To my son and daughter*

# Acknowledgements

This PhD thesis would not be complete without expressing gratitude to the people who showered upon me ample love, support and guidance.

First of all, I want to thank my supervisor *Prof. Koen Binnemans* for changing my life for good. You gave me the opportunity to do my PhD in a group filled with positivity and passion and guided and supported me through the years to be a good scientist. The last four years have been enriching, uplifting, and unforgettable, and I will always cherish them with a big smile on my face. All these would not have happened without your trust, patience and support. You have been an incredible mentor, and I will always be grateful to you.

Thank you, *Mercedes,* for being the best co-supervisor that one can ask. You welcomed me with open arms from the first day and then guided me daily to give me a strong foothold in a new research field and a new work environment. Your guidance with generosity, patience and experience has been instrumental in taking me to the finish line in my PhD. Thank you very much.

I would like to thank Tom, Bart, Valérie, Jeroen, and Annelies for agreeing to be my jury members. I am looking forward to your feedback. Special thanks go to *Tom* and *Bart* for being my assessor.

Thank you, *Bieke,* for your supervision and guidance after Mercedes left our group for good. Your ideas and suggestion during the meetings, revision of my manuscripts truly improved the quality of my works. Thank you for always being accessible and ready to help. Your support has been invaluable during my PhD. Thank you very much.

Thank you, *Lieven,* for always checking on my research progresses and seeing if it is on track or not with respect to the requirements of SOCRATES milestones. You always made important suggestions and brought an industrial perspective to my work. Thank you for being helpful whenever I needed it.

Many thanks go to *Tom, Piet, Lucian and Lieven* for helping me with fulfilling the requirements of the SOCRATES project and making the network-wide events (NWE) fun and educational at the same time. I always felt that I have friends to ask for help when it comes to the SOCRATES matters. Thank you,

*Piet,* for the good memories of touring new places (such as Helsinki ☺) and hanging out together like a buddy during the NWEs.

*Rita and Elisabeth,* thank you for all your support, kindness and encouragement, for everything you do to make sure things get done properly and on time. *Dirk, Paul, Bart and Dominik*, thank you for your help in the labs and with the orders; without you, everything would be much more complicated.

I would like to thank the members of the supervisory board of the SOCRATES project for fruitful meetings, interesting conversation during coffee breaks: Tom, Bart, Wim, Yiannis, Philippe, Annelies, Georgios, Andy, Carl, Gawen, Mathias, Mika, Eero, Barbara, Oldamur, Ratana, Herve, Bert, Robin, Markus, Päivi, Mari, Justin, Christina, Simon and Romain.

A big thanks to my dear friends and colleagues from the SOCRATES projects: Ioanna, Samant, Pelin, Stylianos, Ivan, Giacomo, Roberto, Gwydyon, Jennifer, Christina, Shuang, Nikos, Alejandro, Nikki and Ioannis. What wonderful memories we shared! We helped and learned from each other during the NWEs and explored different cities, played fun games and had many wonderful dinners and drinks together. Thanks to Stelios, we have all these great memories captured, and I treasure the pictures dearly.

I want to thank everyone I met during my secondment at Metallo and Leicester university: Mathias, Rafik, Samant, Maarten, Yves, Bert, Mark, Stef and Abbot.

Many thanks go to Federica, Dzenita, Clio, Michiel, Kumar, Lukas, Pieter, Isadora, Liubov, Nerea, Martina, Simona, Thomas, Stijn R, Stijn VR, Raju, Babu, Sharron, Bram, Nand, Brecht, Lukas, Zheng, Arne, Jonas, Jeroen, Sven, Tom VDH, Tu, Sofia, Willem, Rayco, Panagiotis, Pieter, Brent and Jakob, for being good friends and colleagues. Special mention goes to my office mates. Thank you, Dzenita, for your friendship and kindness. It was always nice to talk to you about work and personal stuff. You are a wonderful human being, and keep it that way. It was a pleasure knowing you and Semir. Thank you, Martina, for being so accessible and kind. Thank you, Federica, for being big-hearted and easy to talk to. Thank you, Simona and Matij, for being a good friend and inviting me for dinner. Thank you, Kumar and Sharron, for your kindness and being the person to go to when I am stuck in my research. Thank you, Nand, Jakob and Panagiotis, for joking around and keeping a light-hearted environment in the office. Thank you, Brecht, for always being helpful and inviting me and others to your home and showing me around your beautiful city of Ypres.

Thank you, Peter Kim, for your friendship. I will always remember cooking together and going out for drinks late at night at Oude Markt. You are a true friend and a very good cook. Thank you, Matthais Holemans, for always showing interest in my stories. I will remember the night when I got totally wasted in your apartment after tasting 20+ beers. Thank you, Samant, for your friendship. It was a pleasure exploring Helsinki, Oslo and London together with you. Remembering our road trip with Stef around Oslo on a snow-covered road gives me a smile and happiness.

Thanks to my Tibetan friends: Kunsel, Kunkyab, Garwang, Thinley, and zomzom, Dawa, Thongdol, Passang and Dhukar for always being there for me. I am eternally grateful for your friendship.

Thanks to Aya Tsering and Senghe for your support and generosity.

Thanks to my parent and family for always cheering for me from far. You motivated and inspired me to continue with my education, and I hope I made you proud.

I want to thank my son, my future daughter and my wife. You mean the whole world to me, and I hope I made you proud.

Lastly, I want to express my deepest gratitude to Ashang Thuptop and Aya Gyalten. You have been my inspiration as well as my backbone, ever since I left Tibet as a nine year old. I could not have come this far in my life without your love and support. I hope to continue making you proud. I want to thank my brother and partner-in-crime Pachi. We have come a long way together through ups and down since we were little kids. Your unconditional love and confidence has been uplifting and heartening. I also want to thank Cho Namkha, Ashang Damdul, Gen Dakpa Sherab, Cho Pema Wangyal, Aku Phuntsok Tashi and Acha Namgyal for showering me with abundance of love and care.

# Abstract

Rapid depletion of high-grade ores, stringent environmental regulations and global movement towards a circular economy has highlighted the importance of metal recovery from waste materials, including the residues generated by the metallurgical industry. Recovery of toxic and valuable metals from the industrial process residues is complex because the metals are often present in very low concentrations and often locked in complex matrices. Hence it is important to develop a process that can selectively recover the metal(s) of interest, while the undesired metals remain in the solid residue. Pyrometallurgical methods are economically viable to process only high-grade ores or ore concentrates, due to the high capital and operational expenditures (CAPEX and OPEX). Hydrometallurgical methods are often used to treat low-grade ores due to their lower CAPEX and OPEX, and occasionally higher selectivity than the pyrometallurgical methods. However, hydrometallurgical methods using acids for leaching (generally HCl, $H_2SO_4$ or $HNO_3$ dissolved in water), still suffer from poor selectivity as they dissolve large amounts of the matrix elements. Alkaline leaching (e.g. NaOH or $NH_3$ dissolved in water) and salt leaching (e.g. $Na_2CO_3$ dissolved in water) are more selective, but not all metals of interest can be leached by these hydrometallurgical lixiviants. In this PhD thesis, organic lixiviants were used to selectively recover valuable metals from industrial process residues. By selecting a suitable organic lixiviant, it is possible to attain high reactivity and selectivity towards the metal(s) of interest because non-hydrated anions have a great affinity to bind to certain metal ions. If required, water can be added to the organic lixiviant to avoid precipitation of the dissolved metal complexes because the high solvating power of water can keep them solubilized. If the lixiviants are composed mainly of organic solvents with no or very limited water, the process can be referred to as a solvometallurgical process. Solvometallurgy is a new branch of extractive metallurgy that uses non-aqueous solvents instead of aqueous solutions.

The first part of this PhD thesis shows the development of novel solvometallurgical processes to selectively recover lead and zinc from jarosite of the zinc industry. Jarosite is a by-product of zinc hydrometallurgy plants. It contains iron, lead, zinc, and low concentrations of valuable metals such as indium, germanium and silver. Two processes were developed to recover valuable metals from the jarosite. In the first process, ionic liquids

Aliquat 336 ([A336][Cl]) and Cyphos IL 101 ([C101][Cl]), equilibrated with 0.5 mol $L^{-1}$ hydrochloric acid, were used to selectively leach lead and zinc from the iron-rich residue. The dissolved metals were recovered from the pregnant leach solution (PLS) by selective precipitation-stripping with an aqueous ammonia solution, and the ionic liquid was reused for leaching a new batch of jarosite. In the second process, concentrated methanesulfonic acid (MSA) was used to leach lead and zinc from jarosite. The solubilized lead and zinc remained dissolved in the PLS whereas the solubilized iron precipitated due to the low solubility of iron methanesulfonate salts in pure MSA. The dissolved metals were recovered by vacuum distillation and the MSA was successfully reused for three leaching cycles.

In the second part of the PhD thesis, organic lixiviants were used to recover valuable metals from secondary lead smelter residues. Two processes were developed: one on iron-rich matte and slag, and the other on lead-rich dross. In the first process, EDTA was used as a lixiviant to recover lead from the matte and slag. These residues are composed mostly of iron and lead, with some amounts of tin, antimony, nickel and zinc. By using 0.05 mol $L^{-1}$ EDTA solution in water, highly selective leaching of lead over iron was achieved: the lead was fully leached from the residues when contacted three times by a fresh EDTA solution, with minimal co-dissolution of iron. The dissolved lead was recovered by precipitation using ammonium sulfide, and the EDTA was successfully reused for leaching of fresh residues. In the second process, antimony was selectively leached from a lead-rich dross, using 2 mol $L^{-1}$ hydrochloric acid in ethanol as a lixiviant. The antimony in the PLS was recovered by hydrolytic precipitation using water, producing a pure antimony(III) oxide chloride ($Sb_4O_5Cl_2$). The ethanol in the remaining PLS was distilled to be reused for leaching of more drosses.

In conclusion, leaching by organic lixiviants exhibited high selectivity towards the metal(s) of interest with minimal co-dissolution of matrix metals. The high selectivity of the organic lixiviant was due to the selective reactivity of the organic lixiviant towards the target mineral, or the selective solubility of the dissolved metal in the organic lixiviants. The high cost of using organic lixiviants was offset by recycling and reusing them several times.

# Samenvatting

De snelle uitputting van hoogwaardige ertsen, strengere milieuwetgeving en de wereldwijde transitie naar een circulaire economie stimuleren terugwinning van metalen uit afvalmaterialen. Tot deze afvalstromen behoren ook de residu's die door de metallurgische industrie worden gegenereerd. Het terugwinnen van waardevolle metalen uit industriële procesresidu's is een uitdaging omdat de metalen vaak in heel lage concentraties aanwezig zijn en in complexe matrices vervat zitten. Daarom is het belangrijk om een proces te ontwikkelen dat selectief de gewenste metalen kan terugwinnen, terwijl de ongewenste metalen in het vaste residu achterblijven. Pyrometallurgische methoden zijn enkel economisch haalbaar voor het verwerken van hoogwaardige ertsen en concentraten, vanwege hun hoge investeringskosten en operationele kosten (CAPEX en OPEX). Hydrometallurgische methoden worden vaak gebruikt voor het behandelen van laagwaardige ertsen, gezien hun lagere CAPEX end OPEX, en hun soms hogere selectiviteit in vergelijking met pyrometallurgische methoden. Hydrometallurgische methoden die gebruik maken van zure uitloging (meestal met watering HCl, $H_2SO_4$ of $HNO_3$) lijden nog steeds aan lage selectiviteit aangezien er een grote hoeveelheid matrixelementen opgelost worden. Alkalische uitloging (met bijvoorbeeld watering NaOH of $NH_3$) en uitloging met zouten (met bijvoorbeeld watering $Na_2CO_3$) zijn selectiever, maar niet alle beoogde metalen kunnen in oplossing gebracht worden door deze uitloogmiddelen. In dit doctoraatsproefschrift werden organische uitloogmiddelen gebruikt om selectief waardevolle metalen terug te winnen uit industriële procesresidu's. Door een gepast organisch uitloogmiddel te kiezen, is het mogelijk om een hoge reactiviteit en selectiviteit te bekomen voor de beoogde metalen, gezien niet-gehydrateerde anionen een grote affiniteit hebben om met bepaalde metaalionen te binden. Indien nodig kunnen kleine hoeveelheden water toegevoegd worden aan het organische uitloogmiddel om neerslaan van de opgeloste metaalcomplexen te voorkomen, omdat het hoge solvaterende vermogen van water de complexen in oplossing kan stabiliseren. Als de uitloogmiddelen voornamelijk zijn samengesteld uit organische oplosmiddelen, zonder of in zeer beperkte aanwezigheid van water, kan het proces worden aangeduid als een solvometallurgisch proces. Solvometallurgie is een nieuwe tak van de extractieve metallurgie die niet-waterige solventen gebruikt in plaats van waterige.

Het eerste deel van dit doctoraatsproefschrift omvat de ontwikkeling van nieuwe solvometallurgische processen om selectief lood en zink terug te winnen uit jarosiet, afkomstig van hydrometallurgische processen in de zinkindustrie. Het bevat ijzer, lood, zink en lage concentraties aan waardevolle metalen zoals indium, germanium en zilver. Twee processen zijn ontwikkeld om deze waardevolle metalen uit het jarosiet terug te winnen. In het eerste proces werden ionische vloeistoffen, Aliquat 336 ([A336] [Cl]) en Cyphos IL 101 ([C101] [Cl]) in evenwicht gebracht met 0,5 mol $L^{-1}$ waterstofchloride oplossing, gebruikt om selectief lood en zink uit het ijzerrijke residu te logen. De opgeloste metalen werden teruggewonnen uit de uitloogoplossing door middel van selectief neerslagstrippen met een waterige ammoniakoplossing. De ionische vloeistof werd hergebruikt voor het uitlogen van een nieuw staal jarosiet. In het tweede proces werd geconcentreerd methaansulfonzuur (MSA) gebruikt om lood en zink selectief te logen uit het jarosiet. Het opgeloste lood en zink bleven opgelost in de loogoplossing, terwijl het opgeloste ijzer als ijzermethaansulfonaat neersloeg vanwege de lage oplosbaarheid in zuiver MSA. De opgeloste metalen werden teruggewonnen met behulp van vacuümdestillatie en de MSA werd met succes hergebruikt gedurende drie opeenvolgende uitloogcycli.

In het tweede deel van het doctoraatsproefschrift werden organische uitloogmiddelen gebruikt om waardevolle metalen terug te winnen uit de residu's van secundaire loodsmelterijen. Opnieuw zijn er twee processen ontwikkeld: één voor ijzerrijke matten en slakken, en één voor loodrijke krassen. In het eerste proces werd EDTA gebruikt als uitloogmiddelen om lood uit de matten en slakken terug te winnen. Deze residu's zijn voornamelijk samengesteld uit ijzer en lood, maar bevatten ook kleine hoeveelheden tin, antimoon, nikkel en zink. Door gebruik te maken van een 0,05 mol $L^{-1}$ EDTA-oplossing in water, werd een zeer selectieve uitloging van lood over ijzer bereikt. Het lood werd volledig uit de residu's geloogd nadat het driemaal in contact werd gebracht met een verse EDTA-oplossing, met minimaal mede oplossen van ijzer. Het opgeloste lood werd teruggewonnen door neerslagvorming met ammoniumsulfide, en de EDTA oplossing werd met succes hergebruikt voor het uitlogen van verse residu's. In het tweede proces werd antimoon selectief uitgeloogd uit loodrijke gestolde slakken, waarbij 2 mol $L^{-1}$ waterstofchloride in ethanol als uitloogmiddel werd gebruikt. Het antimoon in de loogoplossing werd teruggewonnen door neerslagvorming met water, waarbij zuiver antimoonoxidechloride ($Sb_4O_5Cl_2$) werd gevormd. De ethanol in de resterende loogoplossing werd gedestilleerd voor hergebruik.

Er kan besloten worden dat de uitloging door organische uitlogingsmiddel een hogere selectiviteit vertoont voor de gewenste metalen met minimale mede oplossen van de matrixmetalen. De hoge selectiviteit van het organische uitlogingsmiddel was te wijten aan de selectieve reactiviteit van de organische uitlogingsmiddel ten opzichte van het gewenste metaal, of de selectieve oplosbaarheid van het opgeloste metaal in het organische uitlogingsmiddel. De hoge kosten van het gebruik van organische uitlogingsmiddel werden gecompenseerd door ze meermaals te recyclen en te hergebruiken.

# Abbreviations and symbols

| | |
|---|---|
| [A336][Cl] | Aliquat 336 |
| [C101][Cl] | Cyphos IL 101 |
| ATR | Attenuated total reflectance |
| $c_{Fe.I}$ | Concentration of iron in the industrial process residue |
| $c_{Fe.L}$ | Concentration of iron in the leachate |
| CHN | Carbon hydrogen nitrogen |
| $C_{m.I}$ | Metal concentration in initial solid |
| $c_L$ | Metal concentration in leachate before stripping |
| $c_{M.L}$ | Metal concentration in the leachate after leaching |
| CRM | Critical raw material |
| $c_S$ | Metal concentration in the aqueous phase after stripping |
| $c_{S.L}$ | Metal concentration in the organic phase after stripping |
| D2EHPA | Bis(2-ethylhexyl)phosphoric acid |
| DES | Deep-eutectic solvent |
| EAF | Electric-arc-furnace |
| EC | European Commission |
| EDS | Energy-dispersive X-ray spectroscopy |
| EDTA | Ethylenediaminetetraacetic acid |
| $E_L$ *(%)* | Leaching efficiency |
| $E_P$ (%) | Precipitation efficiency |
| $E_S$ (%) | Stripping efficiency |
| ESR | Early-stage researcher |
| ETN | European training network |
| EtOH | Ethanol |
| EU | European Union |

| | |
|---|---|
| FTIR | Fourier transform infrared spectroscopy |
| ICP-OES | Inductively coupled plasma−optical emission spectrometry |
| IL | Ionic liquid |
| IX | Ion exchange |
| L/S | Liquid-to-solid ratio |
| LA | Lead-acid battery |
| LD | Lethal dose |
| M | Metal |
| *MC* % | Moisture content |
| $m_F$ | Mass of the residue after drying |
| $m_I$ | Mass of the residue before drying |
| MSA | Methanesulfonic acid |
| MSCA | Marie Sklodowska Curie Actions |
| NMR | Nuclear magnetic resonance |
| NWE | Network-wide event |
| PGMs | Platinum-group metals |
| PLS | Pregnant leach solution |
| Q | Cation of an ionic liquid |
| QPA | Quantitative phase analysis |
| QXRD | Quantitative X-ray diffraction |
| REEs | Rare-earth elements |
| RLE | Roast–leach–electrolysis |
| $R_R$ *(%)* | Recovery rate |
| *S* | Selectivity |
| SEM | Scanning electron microscopy |
| SX | Solvent extraction |
| TBP | Tri-n-butyl phosphate |
| TOA | Tri-*n*-octylamine |

| | |
|---|---|
| TSL | Top Submerged Lancing |
| TXRF | Total-reflection X-ray fluorescence |
| $v_F$ | Final volume |
| $v_I$ | Initial volume |
| $v_{LIX}$ | Volume of lixiviant |
| WP | Work package |
| wt% | Weight percentage |
| XRD | X-ray diffraction |

# Table of contents

# Preface

This PhD dissertation entitled “Organic lixiviants for metal recovery from industrial process residues” consists of four experimental chapters. The first two chapters focus on the selective recovery of lead and zinc from jarosite from the zinc industry, followed by a chapter on the selective recovery of antimony from lead-rich dross of lead smelter, and the last chapter about the selective recovery of lead from matte and slag from lead smelter.

Chapter 1 introduces the background information and the theoretical concepts relevant to this PhD thesis. The concept of circular economy is firstly presented, and the importance of the valorization of industrial process residues is discussed. The production process of zinc via hydrometallurgy and lead via smelting is described, with a special focus on the residues generated during these processes. Solvometallurgy as a tool for recovering metals from industrial process residues is discussed, and the different organic lixiviants for treating the residues are given.

Chapter 2 describes the specific objectives of this PhD thesis.

Chapter 3 discusses the selective recovery of lead and zinc from jarosite using ionic liquids. Different organic lixiviants are screened first, and the ionic liquids Aliquat 336 ([A336][Cl]) and Cyphos IL 101 ([C101][Cl]) equilibrated with 0.5 mol $L^{-1}$ are chosen for selective leaching of lead and zinc. The dissolved metals are recuperated from the pregnant leach solution (PLS) by selective precipitation-stripping with an aqueous ammonia solution. A process flow sheet for solvometallurgical recovery of the valuable metals from jarosite is presented.

Chapter 4 presents the use of pure methanesulfonic acid (MSA) for the selective recovery of lead and zinc from jarosite. Comparison of MSA leaching with that of mineral acids ($H_2S0_4$, $HNO_3$, HCl) in water is made. The remaining MSA in the PLS is recovered by vacuum distillation and successfully reused for three leaching cycles. Finally, a closed-loop process flow sheet which recycles methanesulfonic acid is presented.

Chapter 5 discusses the selective recovery of antimony from lead-rich dross of lead smelter. 2 mol $L^{-1}$ hydrochloric acid in ethanol is used as a lixiviant to achieve selective leaching of antimony. The dissolved antimony is recovered as a high purity antimony oxide chloride ($Sb_4O_5Cl_2$) by hydrolysis precipitation. Finally, a closed-loop process flow sheet is presented.

Chapter 6 discusses the selective recovery of lead from iron-rich matte and slag of lead smelter by using aqueous EDTA solution as a lixiviant. The dissolved metals are recovered by precipitation using ammonium sulfide. Finally, a closed-loop process flow sheet of the selective recovery of valuable metals is presented.

Chapter 7 contains the conclusions and the outlook for future work.

At the end, notes about the safety aspects, list of publications, conferences and trainings are given.

# Chapter 1: Introduction

## 1.1 Circular economy for raw materials

A linear material flow model of 'extract-produce-use-dump' dominates the current economic system.[1] The global consumption of natural resources such as fossil fuels, metals and minerals is expected to double in the next 40 years,[2] while the annual waste generation is forecast to increase by 70% by 2050.[3] The European Commission (EC) is promoting an alternative economic system called the 'Circular Economy' to limit the exploitation of the earth's limited resources. According to the EC, the circular economy is an economic model based on sharing, leasing, reuse, repair, refurbishment and recycling, in an (almost) closed loop, of products, components and materials at all times (Figure 1.1).[4] It must be noted that the circular economy is not the same as the recycling economy. In circular economy, products are designed to last longer via maintain, repair, redistribute, refurbishment and/or re-manufacture loops, so that they rarely end up as a waste. Recycling economy is an energy-intensive approach, which solely focuses on converting waste materials into new materials and products. However, recycling is a necessary component of the circular economy, but it should be considered only when there are no other alternatives for re-use, remanufacture or repair.

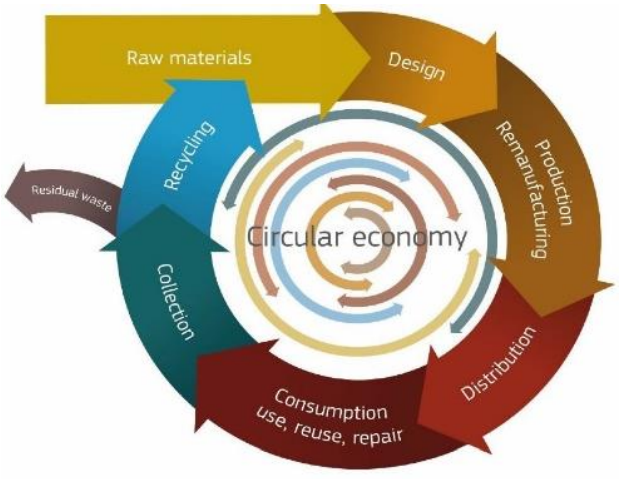


Figure 1.1: Circular Economy according to the European Commission. Reproduced from the EC report on circular economy, 2014.[4]

In 2015, the EC initiated the Circular Economy Action Plan, accompanied by over 10 billion € of funding, to set out 54 ways to "close the loop" of products' lifecycles.[5] This action plan indicates that a diversified and sustainable access to raw materials must involve maximizing the potential domestic resources in the European Union (EU), by improving product durability and reusability, and enabling remanufacturing and high quality recycling. The development and implementation of closed-loop material recycling technologies is crucial to reduce the import dependency on geo-politically unreliable countries and to achieve a genuine circular economy within the EU countries. The EC adopted a new Circular Economy Action Plan in 2020, which builds on the work done since 2015, and further stresses designing and producing products that are easier to reuse, repair and recycle, and incorporate as much as possible recycled material instead of primary raw material.[6] The closed-loop material flow (Figure 1.2) can be achieved by valorization of: 1) mine tailings, 2) industrial process residues, 3) manufacturing scraps, 4) end-of-life products, and 5) urban solid wastes. Implementation of the circular economy measures is estimated to create 600 billion € of economic gain, 450 million tonnes of carbon emissions less and 6 million extra jobs, in the EU by 2030.[5]

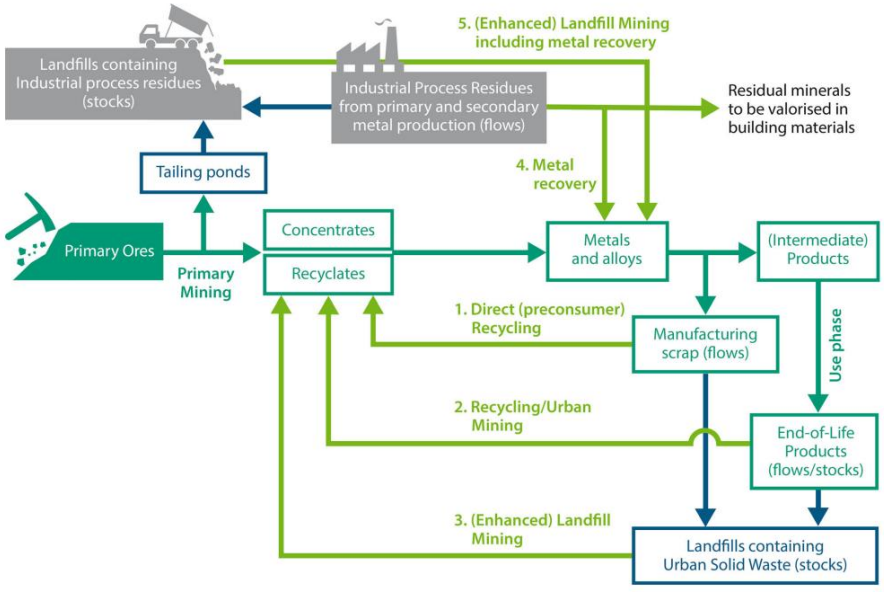


Figure 1.2: Closed-loop material flowsheet of metal-containing waste streams. Reprinted with permission from Binnemans et al.[7] (https://rdcu.be/cdNbo).

The presented PhD thesis is part of the project Horizon2020 MSCA SOCRATES, the European Training Network (ETN) for *the sustainable, (near-) zero waste valorization of valuable-metal-containing industrial process residues* (Figure 1.3).[8] The project aimed to valorize industrial process residues by recovering the toxic and economically important metals, and by using the remaining residues for applications in cementitious binders, geopolymers and catalyst. Although Europe does not have unfettered access to rich ore deposits, it has many interconnected metallurgical and thermal treatment facilities, which generate vast quantities of easily accessible industrial process residues. The SOCRATES project had 15 early-stage researchers (ESRs) to work on four work packages (WPs): WP1: Metal extraction from industrial process residues, WP2: metal recovery from the pregnant leach solutions (PLS), WP3: Residual matrix valorization as cement, inorganic polymers and catalyst, and WP4: integrated assessment of developed flowsheets (Figure 1.3). The investigated industrial-process residues include: 1) flotation tailings from copper industry, 2) iron-rich sludges from zinc production, 3) slags, drosses, dusts and ashes from primary and secondary (non-ferrous) metal production, and 4) thermal treatment residues. As part of the MSCA ETN project SOCRATES, this PhD thesis primarily focusses on the metal extraction (WP1) from the solid residues, but attention is also paid to the metal recovery (WP2) from the pregnant leach solutions.

In this PhD thesis, novel metallurgical processes are developed using organic lixiviants for recovering toxic and valuable metals from the residues of a zinc hydrometallurgy plant and a secondary lead smelter. In the next sections, the current technologies in extractive metallurgy will be discussed and compared, followed by an overview of zinc and lead production processes with a special focus on the generation of process residues. Finally, the importance of using organic lixiviants for recovering valuable metals from the residues of zinc hydrometallurgy plants and lead smelters will be discussed.

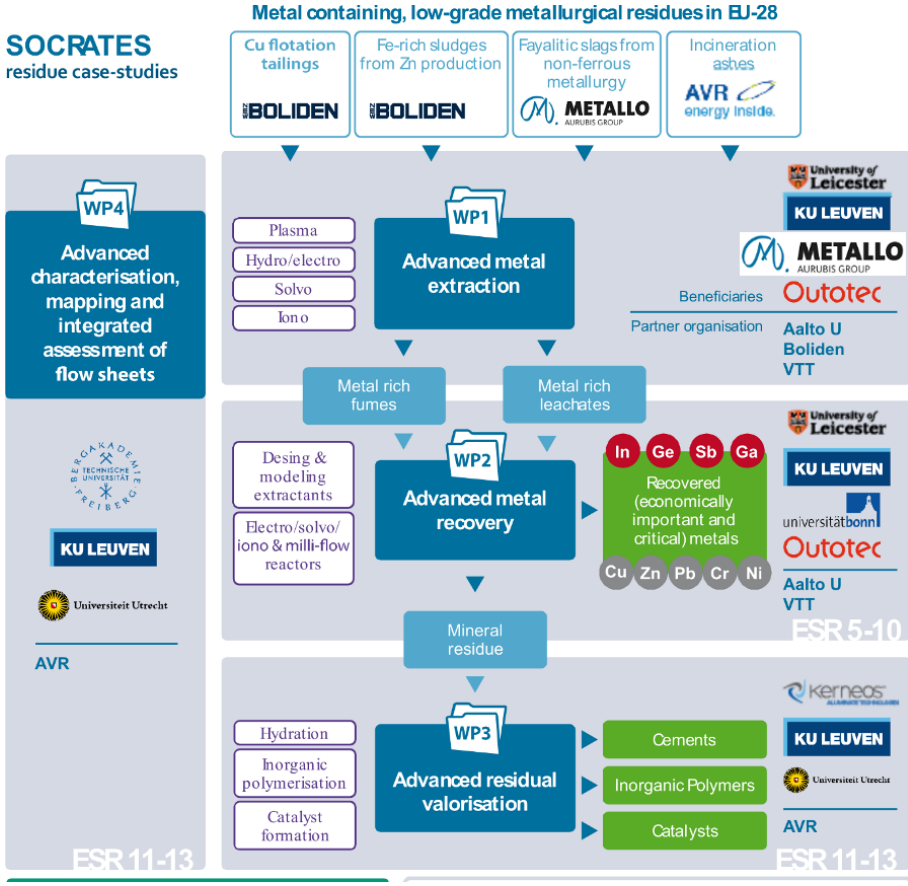


Figure 1.3: Overview of the SOCRATES work packages, and the role of the early-stage researchers (ESRs), beneficiaries and partner institutions.[8]

## 1.2 Industrial process residues

Metallurgical industries generate substantial amounts of residues during the processing of metals. These residues are currently discarded or stockpiled, however they contain toxic and valuable metals that cannot yet be recovered. In this PhD thesis, valorization schemes are developed for the recovery of valuable metals from jarosite of the zinc industry and lead smelter residues.

### 1.2.1 Jarosite of zinc hydrometallurgy plants

Jarosite is a by-product of zinc hydrometallurgy plants. Currently, 75–80% of the annual world's zinc metal production (8 million tons) is produced via hydrometallurgical processes.[9–13] Zinc metal is produced from zinc sulfide (sphalerite) concentrates via the roast–leach–electrolysis (RLE) process (Figure 1.4).[14] The concentrate typically contains 50 wt% zinc, 30 wt% sulfur and 5–12 wt% iron.[9] The dissolved iron in the PLS is commonly removed by precipitation as jarosite.[15–21]

In the RLE process, the zinc sulfide concentrates are firstly roasted in air at about 900 °C in multiple-hearth roasters or fluidized-bed reactors.[14,9] During the roasting, the zinc sulfide minerals are oxidized to zinc oxide with a formation of sulfur dioxide (Equation 1.1), which is converted to sulfuric acid as an essential co-product of the zinc production. Additionally, the iron in the zinc sulfide concentrate combines chemically with zinc to form zinc ferrite (franklinite, $ZnO{\cdot}Fe_2O_3$,) and a small amount of the zinc reacts with silica to form zinc-containing silicates. The roasted concentrate is referred to as 'calcine'. After the roasting, the calcine undergoes two leaching steps.[14,9] The first leaching, named 'neutral leach step', is done by diluted sulfuric acid at 60–80 °C with a final pH >4. During this step, the zinc oxide is readily dissolved as zinc sulfate (Equation 1.2), but the zinc ferrite and zinc-bearing silicates are insoluble, resulting in a zinc-sulfate-rich and almost iron-free solution that is set for purification and electrolysis.

Roasting: $\mathrm{ZnS\ (s) + 1.5O_2\ (g) \rightarrow\ ZnO(s) + SO_2\ (g)}$ (1.1)

Leaching: $\mathrm{ZnO\ (s) + H_2SO_4\ (l) \rightarrow ZnSO_4(l) + H_2O\ (l)}$ (1.2)

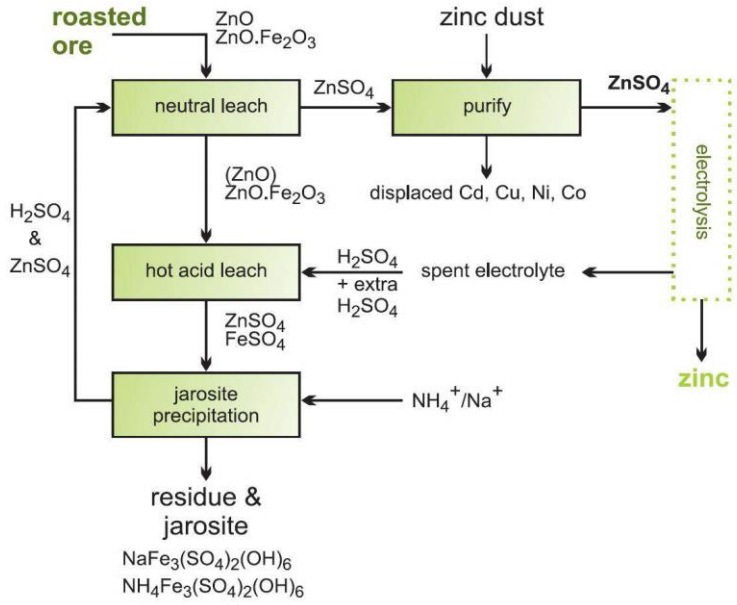


Figure 1.4: Simplified flowsheet showing the jarosite precipitation during the production of zinc in the roast-leach-electrolysis of zinc oxide concentrate. Reproduced with permission from university of York, UK (https://www.essentialchemicalindustry.org/metals/zinc.html).

The second leaching step, named 'hot leach step', is carried out with concentrated sulfuric acid at 95 °C to dissolve the zinc ferrite and zinc-bearing silicates. With this additional leaching step, the leaching efficiency of zinc increases significantly, but a considerable amount of iron is also co-dissolved. The iron is removed from the PLS by precipitating as jarosite, which is a basic ferric sulfate compound.[14,9] The precipitation of jarosite is achieved by adding a source of a monovalent cation (*e.g.* $Na_2SO_4$) at a temperature of about 95 °C and adjusting the pH of the PLS to about 1.5 by the addition of fresh zinc calcine.[14,9] The source of monovalent cation is usually $Na^+$ or $NH_4^+$ in industrial practice, and it leads to the formation of sodium or ammonium jarosite, respectively, but these cations are sometimes substituted in the jarosite structure by other cations (e.g. $NH_4^+$, $K^+$, $½Pb^{2+}$ and $H_3O^+$) that are present in the solution. The precipitation reaction of iron from sulfate solution as jarosite involves the hydrolysis of ferric ions to form the solid compound and with coproduction of a significant amount of sulfuric acid as shown in equation 1.3. The ideal pH for jarosite formation is 1.5. When the pH value is less than 1.5, no or less precipitate is formed because the reaction

equilibrium is shifted to the left, and when the pH value is higher than 1.5, other iron-bearing phases are formed.[14,9] Therefore, the pH during the hot leaching step is maintained at 1.5 by the addition of fresh zinc calcine to consume all the free acid formed during the precipitation reaction. The precipitated jarosite is then easily filtered and washed.

$$3Fe_2(SO_4)_3\ (l) + M_2SO_4\ (l) + \ 12H_2O \rightarrow 2MFe_3(SO_4)_2(OH)_6\ (s) + 6H_2SO_4(l) \qquad (1.3)$$

where M represents any of the ions $Na^+$, $NH_4^+$, $H_3O^+$, $Li^+$, $K^+$ and $½Pb^{2+}$.

In the final step of the RLE process, the resulting zinc sulfate solutions from the neutral leach step and the hot leach step are electrowon to obtain both high zinc metal and sulfuric acid (Equation 1.4). The spent electrolyte rich in sulfuric acid is reused for leaching new concentrates.

Electrowinning: $ZnSO_4(l) + H_2O(l) \rightarrow Zn(s) + \ H_2SO_4(l) + 0.5O_2(g)$ (1.4)

**Comparison of jarosite process with other iron removal processes**

The iron impurities in the leaching solutions are also removed as goethite[9,14,22,23] or hematite[9,14,24] in the zinc industy. The advantage of the jarosite process over the other iron removal processes mainly lies in the property of jarosite itself. Since jarosite is precipitated at relatively acidic conditions, it allows for efficient usage of zinc calcine to control the pH of the solutions.[9,14] It also enables the removal of excess of alkalis and sulfates from the solutions. Moreover, jarosite is very resistant to acid attack and therefore, it can be easily washed with acid to recover the undissolved zinc calcine mixed with it. These properties offer a significant degree of flexibility during the operation and allow for process optimization to meet particular requirements.[9,14] The disadvantages of the process are the additional operational expense for having to add a precipitating agent and the generation of large volumes of jarosite for disposal.

The goethite process involves reduction of ferric iron to the ferrous state at 90 °C, by using unroasted zinc sulfide concentrate as a reducing agent.[9,14]

After the reduction of iron, air is injected to oxidise the ferrous iron, which hydrolyses and precipitates as goethite (FeOOH). Calcine is added during the precipitation to maintain the pH at 3. The goethite process does not have the flexibility of the jarosite process and it requires very careful control of the operational conditions such as pH for efficient operation. The goethite precipitate cannot be washed with acids to recover the undissolved zinc calcine because it would be resolubilized by the acid. As a result, the goethite process usually suffers from lower overall zinc recoveries than the jarosite process.

During the hematite process, the ferritic zinc leach residue from the neutral leaching step is leached with sulphuric acid (spent electrolyte) in the presence of $SO_2$, at 95–110 °C, in an autoclave at total pressure of 0.2 MPa (30 psi).[9,14] The zinc ferrites dissolve readily in the presence of $SO_2$ and iron enters into the solution in the divalent state. First, the leaching solution is neutralised to pH 2 to precipitate gypsum and maintain the sulfate balance in the solution. Then the leaching solution is again neutralised with limestone (with air) to pH 4–5 to precipitate some of the iron and other impurities. Finally, the iron in the neutralised solution is oxidised with oxygen at 200 °C, in a titanium-clad autoclave at a total pressure of 2 MPa (300 psi). Zinc calcine is not required to control the pH in the hematite process, and this reduces the loss of zinc to the iron precipitate. However, the use of pressure equipment in the process leads to high capital and operating costs. The hematite process generates lower volumes of waste compared to the jarosite and goethite processes, due to its high iron content. A zinc hydrometallurgy plant producing 150,000 tons of zinc per year generates about 30,000 tons of hematite, yearly. A similar sized plant using one of the other two processes would produce about 50,000 tons of goethite, or 75,000 tons of jarosite per annum.[14]

**Literature studies on the valorization of jarosite**

Jarosite is generated in large quantities by the zinc hydrometallurgy plants, which causes great disposal difficulties. A plant producing 150,000 tons of metallic zinc annually generates about 125,000 tons of jarosite.[9] India, the European Union and China annually produce about 0.25, 0.60 and 1 million tons of jarosite, respectively.[25–27] Jarosite contains unrecovered base metals (Zn, Pb, Cu), precious metals (Ag), valuable metals (Ni, Co), and toxic metals and metalloids (Cd, As).[28,29] Literature examples of metals present in jarosite generated by different zinc hydrometallurgical plants are shown in Table 1.1.

This residue is classified as a hazardous waste since it contains potentially toxic metal(loid)s above threshold limits, making it unsuitable for direct application.[30] Currently, most of the jarosite produced by the zinc industries is stockpiled in landfills or tailing ponds since it is still allowed in many countries (Figure 1.5).[31] There is an increasing pressure from governments and the general public regarding the environmental concerns of jarosite landfills. As a result, efforts are made to minimize the environmental risk of jarosite landfilling, such as designing dedicated containment facilities like ponds lined with impermeable geomembranes[9] or mixing with lime or cement to make it sufficiently stable.[32,33] Many studies focus on using jarosite as a material for construction[34–36] and ceramic applications, after limiting the leaching of potentially toxic metal(loid)s and soluble salts, in order to comply with the maximum allowable values to be safe.[37,38]

The valuable metals in jarosite can be recovered by pyrometallurgical[10,27] or a combination of pyro- and hydro-metallurgical methods.[27,39–44] The Onsan Refinery of Korea Zinc used Top Submerged Lancing (TSL) Technology to recover zinc, lead, silver and copper,[10] and some plants in China recover zinc, lead and germanium by fuming the residue in a rotary kiln, using coal as heat source.[27] The pyro–hydro processing of jarosite is generally carried out by roasting to convert lead sulfate to lead oxide, which is followed by acidic ($H_2SO_4$), alkaline (NaOH) and salt (NaCl) leaching.[27,39–44] However, there is currently no industrial implementation of metal recovery from jarosite by hydrometallurgical methods.


Figure 1.5: Europe's second largest zinc production plant and the jarosite landfill area of Boliden in Kokkola, Finland. Photo available online by courtesy of Boliden (http://prometia.eu/wp-content/uploads/2014/02/05_Salminen_Boliden.pdf).

Table 1.1: Literature examples of jarosite generated by zinc hydrometallurgical plants and their metal content (wt%).

| | Fe | Pb | Zn | Si | Ca | Al | As | Cu | Cd | Co | Ni | Ag |
|---|---|---|---|---|---|---|---|---|---|---|---|---|
| Hindustan Zinc limited (HZL), India[34] | 22.5 | 1.8 | 7.4 | 3.2 | 4.9 | 3.57 | | | | | | |
| Impala Base Metal Refinery (BMR), South Africa[43] | 41.3 | 1.1 | | 6.8 | 0.06 | 1.8 | 1.4 | | | 0.03 | 3.5 | |
| Mitrovica Industrial Park (MIP), Kosovo[30] | 31.4 | 6.3 | 15 | | | 0.6 | | 0.83 | 0.2 | 0.003 | 0.009 | |
| Zinc plant, EU[45] | 17.4 | 4 | 2.4 | 0.2 | 2.5 | 0.6 | | 0.1 | | | | |
| Beiyin Nonferrous Metals Group, China[27] | 19.9 | 4 | 7 | 4.7 | | | 0.2 | 0.2 | 0.1 | | | 0.01 |

### 1.2.2 Lead smelter residues

About 60% of the world's annual lead consumption is met by recycling of lead-acid (LA) batteries, lead pipes, and other lead-containing wastes.[46,47] The rest is obtained from primary mining of lead sulfide ores (galena, PbS). Lead is produced almost exclusively using pyrometallurgical methods at industrial scale. The primary and secondary lead production processes are very similar: they apply the same processes except for the pretreatment step before smelting (Figure 1.6). During the traditional production of lead from primary sources, the lead(II) sulfide ores are concentrated by floatation followed by a roasting step to convert lead(II) sulfide into lead(II) oxide, and finally a sintering step to form sinter (Equation 1.5).[47] [47] There are also direct smelting processes for lead production (e.g. QSL, KIVCET technology), which combine the oxidation and reduction in a one-stage process, and mitigates the drawbacks of the conventional sinter-smelting processes.[48] Compared to the traditional processes, a direct smelting process significantly reduces the energy consumption, the amount of off-gas to be treated, and the sulfur dioxide emissions. Secondary lead production is almost entirely dependent on the recycling of spent LA batteries.[49] The acids are removed first by draining and the batteries are crushed to separate lead from the plastic, for instance by gravity separation. After the pretreatment of the feed materials, pure lead is produced via a smelting–drossing–refining process.[47] During the smelting process, the primary or secondary feed materials are fed into a blast furnace together with limestone (flux for slag formation) and coke (reducing agent) (Equation 1.6 and 1.7).

Roasting: $\mathrm{PbS\,(s) + 1.5O_2\,(g) \rightarrow\ PbO(s) + SO_2\,(g)}$ (1.5)

Smelting: $\mathrm{PbO(s) + C\,(g) \rightarrow\ Pb\,(l) + CO\,(g)}$ (1.6)

$\mathrm{PbO(s) + CO\,(g) \rightarrow\ Pb\,(l) + CO_2\,(g)}$ (1.7)

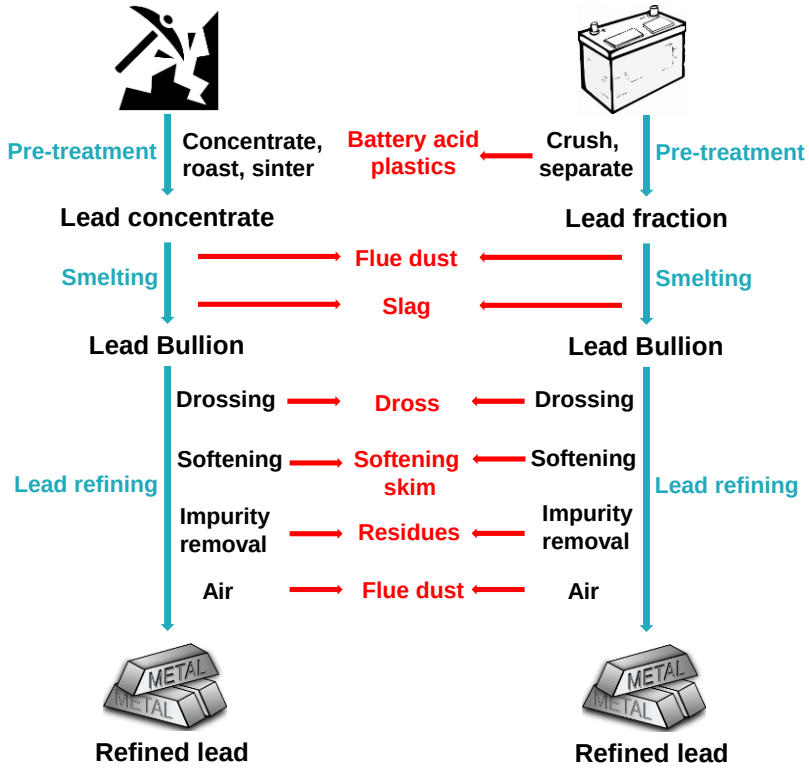


Figure 1.6: Simplified flowsheet showing the primary and secondary production of lead and its metal-containing process residues. Blue arrows are production processes and red arrows are waste streams. Adapted with permission from Dupont *et al.*[47] (https://rdcu.be/cdNhs).

The molten lead sinks to the bottom of the furnace and is tapped separately for further refining. The less dense mineral phases (i.e., the smelting residue) float on the top of molten lead and these are tapped into a separate pot to settle. There, the denser *matte,* consisting mostly of molten sulfides, sinks to the bottom, and the *slag* consisting of molten silicate floats on the top. After cooling, the matte is physically separated from the slag. Matte and slag are rich in iron with varying amounts of other metals such as lead, copper, zinc, silicon and arsenic. The metallic lead bullion coming from the furnace is further purified by a drossing process, where the molten lead is cooled down, and the remaining oxidized impurities called *dross* are formed on the surface.[47] Dross is generally composed mainly of lead and antimony along with small amounts of iron, zinc, tin and arsenic. The dross is then skimmed off from the surface, and the lead is then further refined by a thermal or

electro-refining process. The thermal-refining process further removes metal impurities from the lead and these impurities are referred to as *softening skim*. During the electro-refining, the impurities are collected at the bottom of the electrolysis tank, and these residues are referred to as *anode slime*. *Dust* is also collected during the sintering, smelting and refining steps.[47] The softening skim, anode slide, and the dust contains mostly antimony and lead with minor amounts of arsenic and copper.[30]

**Literature studies on the valorization of lead smelter residues**

The lead smelter residues (matte, slag dross, softening skim, anode slime and dust) contain lead as one of the major components along with iron or antimony (Table 1.2). Some research has focused on the valorization of lead slags as a construction material, but the recovery of the valuable metals prior to their application as construction materials was not considered.[50,51] Kim *et al.* recovered lead and other valuable metals from lead slag and matte using nitric acid, but with low selectivity.[52,53] With regards to antimony containing residues of lead smelter (dross, softening skim, flue dust and anode slime), both hydrometallurgical and pyrometallurgical processes were considered for valorization. In pyrometallurgical processes, antimony is usually recovered via volatization techniques due to the high vapor pressure of antimony(III) oxide ($Sb_2O_3$).[54–57] Hydrometallurgical processing of antimony-containing lead smelter residues either use alkaline sulfide or chloride-based leaching. Anderson used alkaline sulfide leaching followed by electrodeposition to selectively recover antimony over lead from dross, softening skim and flue dust and anode slime.[58] The problem with alkaline sulfide leaching is that it generates waste products ($Na_2SO_4$ and $Na_2S_2O_3$) which are difficult to dispose of.[59] Singh *et al.* and Cao *et al*. used chloride-based hydrometallurgical leaching of dross and anode slimes, but the use of high concentrations of chloride usually leads to corrosion of equipment.[60,61]

Table 1.2: Literature examples of lead processing residues and their metal contents (wt%).

| | Fe | Pb | Sb | Zn | As | Cu | Ag | Sn | Bi | Ni | Si | Cr | Mn |
|---|---|---|---|---|---|---|---|---|---|---|---|---|---|
| Slag[62] | 36.6 | 4 | | 0.5 | | 0.4 | | 0.2 | | | 7.6 | 0.4 | 0.5 |
| Matte[62] | 51.4 | 8.2 | | 0.5 | | 1 | | 0.2 | | 0.2 | 2.6 | 0.2 | 0.3 |
| Dross[63] | | 58.3 | 29.9 | 0.7 | 0.07 | | | 0.2 | | | | | |
| Softening skim[58] | | 52.9 | 31.7 | | 3.3 | | | | | | | | |
| Anode slime[61] | | 12.6 | 63.6 | | 4 | 1.5 | 1.1 | | 3.3 | | | | |
| Sb dust[64] | | 7.5 | 42.4 | | 10.4 | 0.1 | | | 0.6 | | | | |

## 1.3 Solvometallurgy as a tool for metal recovery from industrial process residues

As discussed in section 1.2, industrial process residues such as matte and slag of lead smelters, or jarosite of zinc hydrometallurgy plants contain low concentration of more valuable metals (e.g. Pb and Zn) mixed with high concentration of less valuable metals (e.g. Fe) in the matrix. The extractive metallurgy of these residues can be generally classified into three types: (1) pyrometallurgy, (2) hydrometallurgy, and (3) solvometallurgy.

Pyrometallurgy involves the processing of metal-bearing materials at high temperatures (above 300 °C and often even > 1000 °C) to bring about physical and chemical transformations to recover metals.[65–68] However, pyrometallurgy is not an economically viable process to extract metals from low-grade industrial process residues since it requires too much energy compared to the amount of metal that can be extracted.[7] Likewise, conventional hydrometallurgy suffers from poor selectivity and high chemical consumption when treating low-grade metal sources such as industrial process residues.[7] Hydrometallurgy involves the use of aqueous solutions containing various leaching agents (e.g. acid, base, salts) to bring about physical and chemical transformations of metal-bearing materials for the recovery of metals.[27,69–71] It makes use of water as a solvent, and operates at much lower temperatures (20–200 °C) than pyrometallurgy. Acid leaching (generally HCl, $H_2SO_4$ or $HNO_3$ dissolved in water),[14,72–75] in particular, suffers from poor selectivity as it dissolves not only the metals of interest, but also a large amount of matrix elements, which results in impure PLS, and an excess consumption of acid.[7] Alkaline leaching (e.g. NaOH or $NH_3$ dissolved in water) and salt leaching (e.g. $Na_2CO_3$ dissolved in water) are more selective, but not all metals of interest can be leached by these lixiviants.[70,76,77]

A promising group of chemicals that are rarely explored in extractive metallurgy are organic solvents. The use of organic solvents as a lixiviant has the potential to solve the issues of selectivity and reactivity during the hydrometallurgical processing of industrial process residues.[7] By replacing the aqueous phase in hydrometallurgical processes by organic solvents, it is possible to attain high reactivity and selectivity because non-hydrated anions have a greater affinity to bind to some metal ions and the lack of water's high solvating power makes it impossible for some metals to enter into the solution. When the leaching solution consists mainly of organic solvents instead of an aqueous phase, it is called "solvometallurgy".[7] Solvometallurgy does not imply anhydrous conditions, but the water content must be less than 50 vol%. Solvometallurgical processes using organic lixiviants are a

relatively new field in extractive metallurgy and, currently they are not used for leaching metals at a commercial scale due to their high cost.[7] However, the depletion of high-grade ores and the global movement towards a circular economy has accelerated the research on solvometallurgical leaching processes for metal recovery from low-grade metal sources.

The unit processes of solvometallurgy are largely similar to that of hydrometallurgy, except that the water is replaced by an organic solvent in solvometallurgy. There are three units processes in solvometallurgy: (1) leaching, (2) solution concentration and purification, and (3) metal recovery (Figure 1.7).

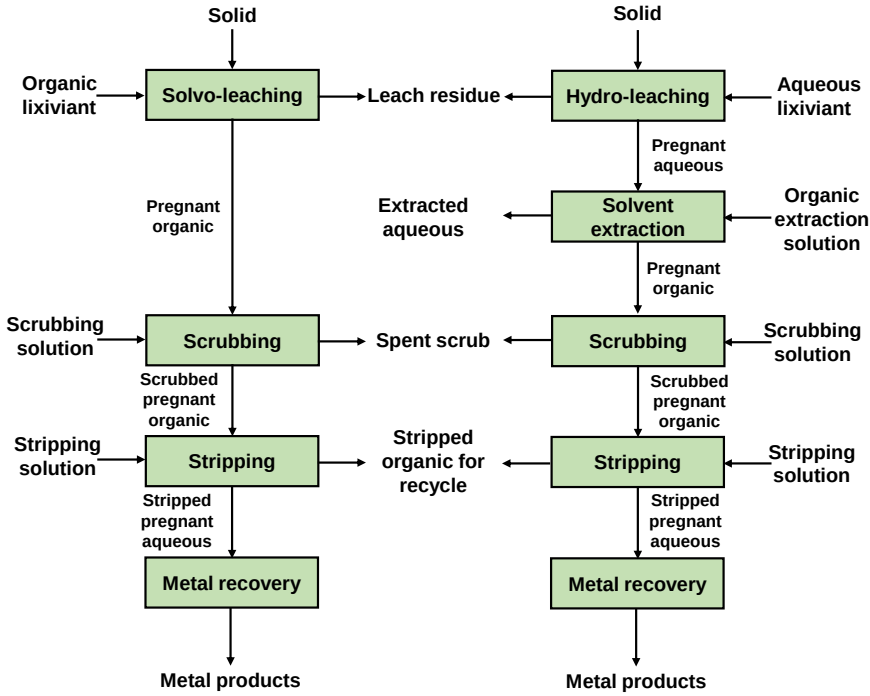


Figure 1.7: Simplified comparison of unit processes in solvo- and hydro-metallurgical leaching. Solvent extraction, scrubbing and stripping are part of the solution concentration and purification unit process.

### 1.3.1 Leaching

Leaching is a process where metals from solid materials are dissolved in a lixiviant, which is usually composed of a leaching agent and a solvent. In hydrometallurgy, the leaching agent is usually an acid (e.g. HCl, $H_2SO_4$,

$HNO_3$),[14,72–75] base (e.g. $NH_3$, NaOH)[76,77] or chelating agent (e.g. EDTA, citric acid),[78–86] and the solvent is water. In solvometallurgy, the lixiviant can solely be an organic acid, acting as both the leaching agent and the solvent, or a composite lixiviant comprised of a leaching agent (e.g. extractants, mineral acids) and an organic solvent.[7] Some solvometallurgical lixiviants contain a small amount of water, but the water content should be less than 50 vol% to be considered as solvometallurgical lixiviants. The solvometallurgical lixiviant will be, hereafter, referred to as organic lixiviant, since the organic phase is its main component. Three main groups of organic lixiviants can be used: (1) organic acids on their own, such as formic acid, acetic acid and methanesulfonic acid (MSA) ,[62,87] (2) mineral acids (often HCl) in water-miscible (polar) organic solvent (e.g. acetone, methanol, ethanol, ethylene glycol),[88,89] and (3) others such as ionic liquids (ILs), deep-eutectic solvents (DESs), and water-immiscible (nonpolar) organic solvents with dissolved extractants (acidic, basic or neutral).[7] All the above mentioned organic lixiviants are discussed in detail in 1.4. In addition to leaching agents, the organic lixiviants can also contain reducing agents to leach minerals with high oxidation states, and oxidizing agents to leach elemental metals and sulfide minerals.[7,88,90] After the leaching with an organic lixiviant, a solid leaching residue and an organic PLS with dissolved metals are generated. The leaching residue can be separated from the PLS by filtration, decantation, or centrifugation.

**General considerations of leaching processes**

Leaching is a result of chemical reactions between the leaching agents and the solids. The chemical reactions during the leaching can be classified into three types: acid-base, oxidation-reduction, and complexation reactions. The feasibility of a chemical reaction in a certain direction is determined by the laws of thermodynamics and kinetics.

Thermodynamic activity is an important parameter that determines the feasibility of a chemical reaction during leaching. It is the amount of effective dissolved ions that is totally free and available for reaction.[91,92] In general, thermodynamic activity depends on any factor that alters the chemical potential. These factors include: concentration, temperature, pressure, interactions between chemical species, and electric fields. Pourbaix diagrams, also known as potential/pH diagrams, are useful guidelines that predict the possible thermodynamically stable phases (at equilibrium) of metal species in aqueous systems.[93,94] Although the Pourbaix diagrams are

only applicable for aqueous systems, they still give a good general information of stability of different metal species at different potential and pH for other systems.

Other important parameters of the leaching process are the overall rate and the variation in rate with leaching time. During leaching, the interaction between a solid and a leaching agent follows three steps: (1) diffusion of the leaching agent through the liquid to the solid-liquid interface, (2) chemical or electrochemical reaction at the interface involving adsorption and desorption, and (3) diffusion of the products from the interface into the bulk solution.[70,71,95] Any of these steps may be rate-controlling depending on its relative velocity with respect to the others. When the rate of chemical reaction (i.e., step 2) is much slower than the rate of diffusion (i.e., step 1 and 3), then the reaction is called *chemically-controlled leaching*.[72,95] A chemically controlled leaching reaction is characterized by independence on the stirring speed since diffusion does not play a crucial role.[71] The process is strongly dependent on temperature because the rate of chemical reaction changes exponentially with temperature. When the rate of diffusion of reactant (i.e., step 1 and 3) is much slower than the rate of chemical reaction (i.e., step 2), then the reaction is called *diffusion-controlled leaching*.[71,95] Such leaching process is characterized by a strong dependence on the stirring speed since stirring decreases the thickness of the boundary layer in contact with the solid surface.[71,95]

### 1.3.2 Solution concentration and purification

Beside the metal(s) of interest, unwanted impurities and other metals are also co-dissolved during the leaching. Therefore, the organic PLS is subjected to various concentration and purification processes to remove the unwanted components, and to obtain a concentrated solution containing mainly the metal(s) of interest. The various processes employed for concentration and purification of the organic PLS include: (1) solvent extraction, (2) precipitation/crystallization, and (3) ion exchange.

*Solvent extraction* (SX) is a liquid-liquid separation and purification process in which metal ions are distributed separately in two immiscible solvents, usually with an aid of an extractant.[121–123] In general, the PLS containing the dissolved metals is put in contact with another immiscible phase comprising of an extractant, a diluent, and sometimes a modifier, and then the two liquid phases are mixed until equilibrium is reached (Figure 1.8). During the mixing, the metal ions are distributed differently between the two phases, due to the

difference in the binding affinity of the metal ions to the organic extractant. After phase disengagement and stripping stages, the phases are finally separated and can be easily recovered again. In conventional solvent extraction processes, the dissolved metals in the PLS (aqueous phase) are transferred to a water-immiscible organic phase, followed by a removal of any impurities in the loaded organic phase by scrubbing with an aqueous solution. Thereafter, the valuable metal ions in the scrubbed organic phase are recovered by stripping using an aqueous stripping solution. If solvometallurgical leaching was carried out using low-polarity organic lixiviant, the loaded organic PLS can undergo a scrubbing step to remove impurities, followed by a stripping step to recover the valuable metals.[99] This is a form of process intensification compared to hydrometallurgical leaching since the leaching and solvent extraction are combined into a single step, whereas the conventional approach (hydrometallurgy) requires two separate steps (Figure 1.7). If the solvometallurgical leaching is performed using polar organic phases, the dissolved metals cannot be recovered by scrubbing or stripping steps, since the polar organic solvent will form one phase with the aqueous solution. However, the liquid-liquid separation is still possible by contacting the loaded polar organic phase with a less-polar organic solvent.[100–104] This approach is also referred to as non-aqueous solvent extraction. The most important requirement for solvent pairs in non-aqueous solvent extraction is the ability to form two immiscible phases and have low mutual solubility between the two solvents. Based on that, the reported miscibility data[105,106], Hildebrand solubility parameter for solvents[107], and mixotropic series[100,108] are useful guidelines for the selection of suitable solvent pairs.

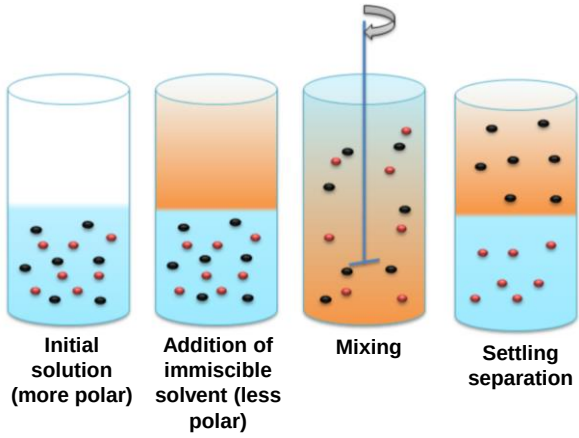


Figure 1.8: General scheme for a solvent extraction process showing the main steps involved. Reproduced with permission from S. Riano.[109]

*Precipitation* and *crystallization* are two alternative approaches to the recovery of dissolved metals from the PLS in which the metals are recovered as a salt. *Precipitation* is a purification process whereby the dissolved metals in the PLS are converted into an insoluble compound, by adding a precipitating agent. The precipitation occurs when the precipitating agent reacts with the dissolved metals in the solution to form a new metal ion pair, and the concentration of that ion pair exceeds the solubility product.[110] This process consists of three stages: (1) nucleation, (2) growth of nucleus, and (3) aggregation or crystallization (figure 1.9).[110,111]

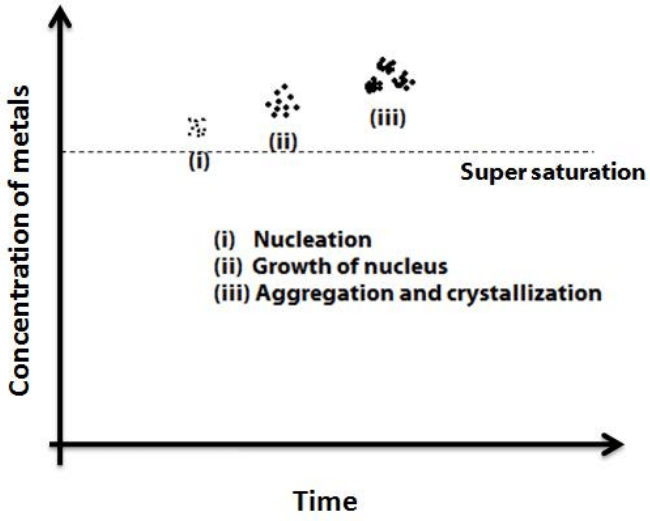


Figure 1.9: Various stages in the recovery of metals by precipitation.[110] (https://tel.archives-ouvertes.fr/tel-01407248/document).[110]

In hydrometallurgy, the dissolved metals are precipitated from aqueous PLSs by increasing the pH or by adding a precipitating agent. Precipitation can be also used for the recovery of metals from organic PLSs, by adding a suitable precipitating agent. For instance, Önal *et al.* leached REE hydroxide using 20 vol% Versatic Acid 10 diluted in an aliphatic diluent, and then recovered the dissolved REE by precipitation using oxalic acid solution.[112] After the precipitation, the organic lixiviant was regenerated with virtually the same composition as the fresh lixiviant, and the rare-earth oxalate precipitates were calcined to produce high-purity rare-earth oxides. *Crystallization* is a process where the metal-loaded PLS is evaporated until the solution becomes saturated and the metal salts start to form crystals. Crystallization can be easily performed on aqueous PLSs from hydrometallurgical processes by heating but it is more complicated on organic lixiviants, since the organic lixiviant can contain more than one component, or decompose with heating. However, organic lixiviants using concentrated organic acids (e.g. acetic acid, MSA) can be evaporated by distillation and the dissolved metals can be recovered. For instance, Forte et al. used concentrated acetic acid to selectively leach lead from lead smelter residues (matte and slag), and the acetic acid was recovered by distillation and subsequently reused for leaching of more residues.[62] Many organic solvents have a lower heat of

vaporization than water, thus it requires less energy to distil. For organic solvents that decompose before reaching their boiling point, the distillation can be carried out under vacuum condition to lower its boiling point.

*Ion exchange* (IX) is another solution purification method often used for the removal of metal ions or metal salts from aqueous solutions. During this process, dissolved ions are removed from the solution and replaced with other ions of the same or similar electrical charge.[7,113] The IX is typically carried out using an IX resin, which is composed of a network of organic polymers with functional groups affixed on it. The functional groups can be positively-charged or negatively-charged ions, which remove ions by cation exchange or anion exchange mechanisms, respectively. Usually, IX is a preferred method over solvent extraction for recovery of metals from dilute aqueous solutions. The resins must swell sufficiently, if the metals ions are to be removed from organic solvent via ion exchange.[7] Metal ions can be removed from organic solvents with a solution of a mineral acid in a polar organic solvent, such as HCl in acetone by using a cation exchanger in the protonated ($H^+$) form.[113] Metal chloride salts in organic solvents (of both low or high polarity) can be removed by using anion exchangers in the chloride form. Ion exchange from organic solvents can lead to stronger adsorption of metal ions by the IX resin and to higher selectivity in separation processes. For instance, more metal ions form anionic complexes with chloride or nitrate ions in organic solvents than in water, which means that more metals can be recovered using an anion exchanger for an organic solution than for an aqueous solution.[7] It must be noted that solvent extraction processes using acidic extractants (e.g. D2EHPA, Cyanex® 272, Versatic Acid 10) or basic extractants (e.g. Aliquat® 336, Cyphos® IL 101) involve ion exchange reactions, and therefore, these processes are sometimes referred to as ion-exchange processes.

### 1.3.3 Metal recovery

Metal recovery is the final process unit in extractive metallurgy where high-purity metals or metal salts are produced. In hydrometallurgy, electrolysis is commonly used to recover metals directly from the aqueous PLS or the stripped aqueous solution.[17] The metals are recovered by deposition of the desired metal from the electrolyte on to the cathode material by electrolytic reduction. This process is also referred to as electrowinning. Similarly in solvometallurgical leaching using organic lixiviant, metals can be directly recovered from the organic PLS (e.g. molten salts) or aqueous stripped

solution via electrolysis. There are a number of studies on the electrowinning of metals from ILs[114–116] and DESs[117–121]. For instance, Abbott *et al.* leached lead and zinc from electric-arc-furnace (EAF) dust using DES, followed by the recovery of the dissolved metals from the organic electrolyte by electrowinning.[117]

The dissolved metals in the organic PLS can be also recovered in their elemental form by *cementation*. In this process, a sacrificial metal with a more negative redox potential than the metal being recovered is immersed in the solution. The metal ions in the liquid are reduced and deposited onto the sacrificial metal, which in turn is oxidized and goes into solution. An example of metal recovery from an organic PLS by cementation is the selective recovery of lead from DES by the addition of zinc metal as the sacrificial metal to produce metallic lead.[117,122]

## 1.4 Organic lixiviants

Organic lixiviants generally contain a leaching agent and a solvent: the former to react with the metal-bearing solids and the later to solubilize the metal ions. However, some organic acids such as acetic acid can be used without requiring any additional solvent because it can act as both the leaching agent and the solvent. Some organic lixiviants can contain small amounts of water as well. The organic lixiviants can be categorized into following types:

- Mineral acids in organic solvents
- Organic acids (e.g. formic acid, acetic acid)
- Extractants (acidic, neutral, basic)
- Ionic liquids and deep eutectic solvents

### 1.4.1 Mineral acids in organic solvents

Mineral acids (HCl, $H_2SO_4$, $HNO_3$) dissolved in organic solvents are promising lixiviants for leaching metals from industrial process residues.[88,89,123–127] HCl is often selected as the acid, and acetone, methanol, ethanol, isopropanol, ethylene glycol, or *n*-octanol are commonly used as the organic solvent (Figure 1.10). The mineral acid reacts with the solid metal minerals to form a metal complex (e.g. metal-chloro complexes), and the dissolved metal complex will either precipitate or remain solubilized, depending on the solubility of the metal complex in that particular (organic) solvent. Kimball *et al.* used HCl–acetone to selectivity leach uranium over calcium from calcite-rich low-grade uranium ores ($U_3O_8$ <1wt%).[89] The high selectivity of uranium

over calcium is due to the high solubility of uranyl chloride, and the low solubility of calcium chloride in acetone. The hydrometallurgical process using HCl in water is not economical due to the large acid consumption, resulting from the co-dissolution of the calcite gangue material. Özdemir *et al.* found that HCl−ethanol or HCl−ethanol-water solutions were better solvents than HCl−water solutions in the leaching of scheelite ($CaWO_4$).[123] The leaching rate of scheelite in HCl−water is very low due to the limited solubility of the reaction product (tungstic acid) in water, which precipitates and covers the undecomposed ore particles, and thus decreases the chemical reaction rate of the process. On the other hand, using HCl−ethanol or HCl−ethanol-water prevented the formation of tungstic acid and thus the complete dissolution of scheelite could be achieved. Jana *et al.* found that less HCl concentration was required to leach metals from sea nodules when water is partially or fully replaced by an organic solvent such as ethanol.[88] This was attributed to the increase in the chloride ion activity when ethanol is added to an aqueous chloride solution, which promotes the metal-chloro complex formation. In fact, the chloride ion activity increases more by incorporating longer-chain alcohols, which would further reduce the requirement of HCl to leach similar amounts of metals. Similarly, Kopkova *et al.* found that resistant ores such as titanomagnetite ($Fe_{3-x}Ti_xO_4$, $0 \leq x \leq 1$) can be leached with five times less activation energy, by replacing HCl−water with HCl−octanol as a lixiviant.[124] In conclusion, using mineral acids in organic solvent as a lixiviant improves selectivity, reduces power consumption, and requires less chloride concentration than using mineral acids in water.

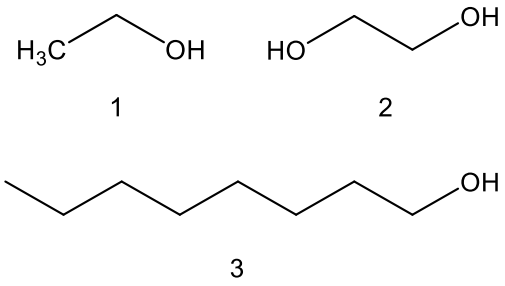


Figure 1.10: Examples of organic solvents used for dissolving hydrochloric acid: 1) ethanol, 2) ethylene glycol and 3) 1-octanol.

### 1.4.2 Organic acids

Organic acids such as formic acid, acetic acid and methanesulfonic acid (MSA)

are attractive organic lixiviant because they are biodegradable and less toxic than the mineral acids (Figure 1.11).[128] They are mild (formic acid $pK_a$ = 3.82, acetic acid $pK_a$ = 4.76) or strong acids (MSA $pK_a$ = −1.19), and they can be used as both the leaching agent and the solvent for metals during leaching.[129] Organic acids are usually more selective than mineral acids mainly because their acid strength is not too strong to leach all metals but sufficient enough to leach the metals of interest. Formic acid has been used to leach magnesium from magnesite ores ($MgCO_3$), and copper from low-grade malachite ores ($Cu_2CO_3(OH)_2$) to avoid co-dissolution of impurities and corrosion issues associated with aqueous mineral acid solutions.[130,131] Acetic acid has been used for selective leaching of lead over iron from iron-rich secondary lead smelter residues.[62] Acetic acid (with oxygen as an oxidizing agent) has been also used for selective leaching of metallic cobalt from tungsten carbide based hard metal scrap.[132] MSA is a strong organic acid that is considered to be a green solvent. Due to its strong acidity, it can easily dissolve metal minerals and form either a soluble or insoluble metal methanesulfonate salts. MSA was used for leaching the rare-earth elements (terbium, cerium and lanthanum) from real lamp phosphor waste residue, and lead and silver from zinc leaching residue.[87,133] In conclusion, organic acids can be directly used as lixiviants without the need of adding mineral acids as leaching agents, and can achieve higher selectivity compared to that of an aqueous solution containing mineral acids.

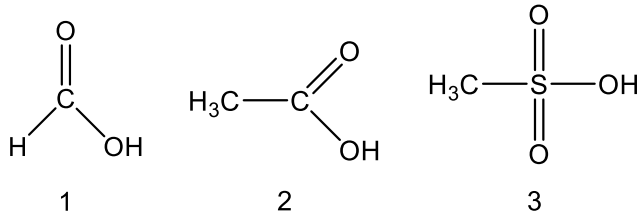


Figure 1.11: Examples of organic acids: 1) formic acid, 2) acetic acid and 3) methanesulfonic acid.

### 1.4.3 Extractants

In solvent extraction processes, extractants dissolved in water-immiscible organic solvents are used for the extraction of metals from aqueous PLSs.[7] In leaching processes, the same extractants can be used as an organic lixiviant to transfer the metals from the solid materials. There are three types of extractants: acidic, basic, and neutral extractants. The chemical structures of

selected acidic and neutral extractants are shown in Figure 1.12. Acidic extractants leach metals minerals by cation exchange mechanisms. They can be directly used for leaching in diluted or undiluted form, using either water or organic solvents as a diluent. Some examples are organophosphorus acids (e.g. D2EHPA, Cyanex® 272), carboxylic acid (e.g. Versatic acid 10), α-hydroxyoximes (e.g. LIX® 63), β-hydroxyaryloximes (e.g. LIX® 65 N), β-diketones (e.g. LIX® 54), and 8-hydroxyquinolines (e.g. Kelex® 100). Versatic Acid 10 is already known to be effective in leaching zinc from chloride-containing solid zinc waste residues.[134] Neutral extractants (e.g. tributyl phosphate (TBP), Cyanex® 923) are poorer lixiviants because they leach and dissolve metal minerals by solvation mechanisms. However, powerful lixiviants can be obtained by equilibrating TBP with concentrated mineral acid solutions (e.g. $HNO_3$).[135,136] Basic extractants such as quaternary ammonium salts (e.g. Aliquat® 336) and quaternary phosphonium salts (e.g. Cyphos® IL101) leach metal minerals by anion exchange mechanisms. These are chemically classified as ionic liquids (ILs), and will be discussed separately in the next section.

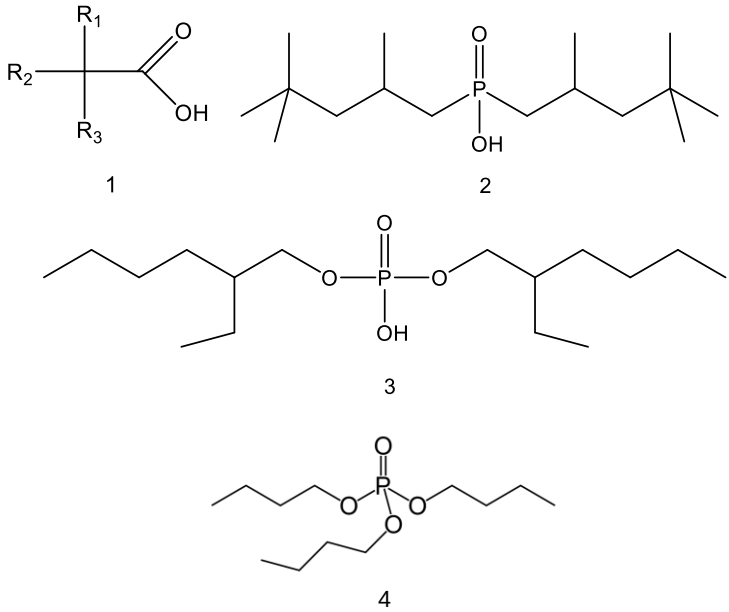


Figure 1.12: Examples of acid and neutral extractant: 1) Versatic acid, 2) Cyanex 272, 3) D2EHPA and 4) TBP.

### 1.4.4 Ionic liquids and deep-eutectic solvents

Ionic liquids (ILs) are solvents that consist entirely of ions.[7] Some of the most important characteristics of ILs are their chemical and thermal stability, wide electrochemical potential window, low flammability and negligible vapor pressure. Ionic liquids such as quaternary ammonium salts (e.g. Aliquat® 336) and quaternary phosphonium salts (e.g. Cyphos® IL101) combined with mineral acids (e.g. HCl) have shown to be good lixiviants (Figure 1.13).[137] The mineral acids react with metal minerals to form metal-chloro anionic complexes, which are accommodated by the IL cationic counter ions.[137] A good example of selective leaching by IL is the use of the functionalised IL betainium bistriflimide, [Hbet][$Tf_2N$], to recover rare earths from fluorescent lamp phosphor waste and end-of-life permanent magnets.[138] [Hbet][$Tf_2N$] selectively dissolved the red phosphor $Y_2O_3$:$Eu^{3+}$ (YOX) without affecting the other components in the waste fraction. A drawback of ILs is their high price and high viscosity, which has hindered the commercialization of IL processes.

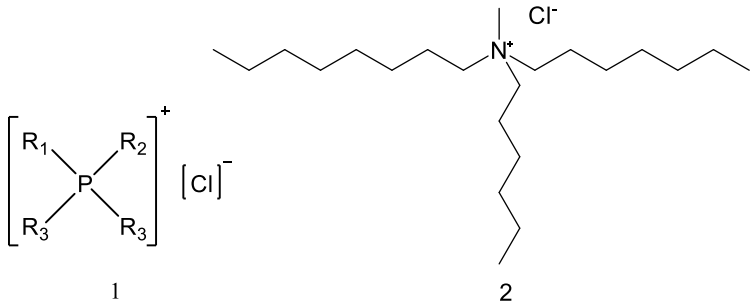


Figure 1.13: Examples of ionic liquids/basic extractants: 1) Cyphos® IL 101 and 2) Aliquat® 336.

A cheap alternative to ILs are the deep-eutectic solvents (DESs). DESs are formed from an eutectic mixture of Lewis or Brønsted acids and bases which can contain a variety of anionic and/or cationic species.[139] Most of them are mixtures of choline chloride and a hydrogen-bond donor (urea, ethylene glycol, malonic acid) or mixtures of choline chloride with a hydrated metal salt (Figure 1.14). DESs have been used for: selective leaching of zinc from goethite residue of zinc industry,[140] yttrium and europium from spent fluorescent lamps,[141] cobalt from lithium-ion battery cathode materials,[102] and complete dissolution of NdFeB magnets.[142]

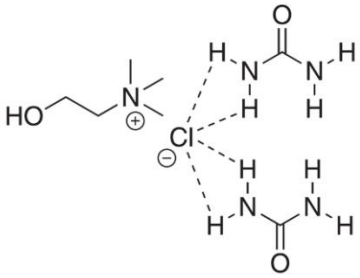

Figure 1.14: Example of a deep-eutectic solvent (DES): Choline chloride/urea.[143]

## 1.5 Chelating agents

Chelating agents such as ethylenediaminetetraacetic acid (EDTA) and citric acid can be used for leaching metals (Figure 1.15). These organic chelating agents are not considered organic lixiviants because they are usually dissolved in a higher volume of water. However, the use of chelating agents in metal recovery is discussed here because they are also suitable for the recovery of metals from low-grade industrial process residues due to their higher selectivity towards certain metals, compared to inorganic acids, bases and salts in hydrometallurgy. The chelating agents dissolve metals from solid minerals via chelation by forming a metal–EDTA and metal–citrate complexes. EDTA has been widely used as an effective reagent for decontamination of lead and other potentially toxic metal(loid)s from soil because of its high lead extraction efficiency, enabled by the high thermodynamic stability of the lead–EDTA complexes.[78–81] The stability constant (log $K_S$, 25 °C and $\mu$ = 0.1) of some metal–EDTA complexes in water are as high as: Fe(III) = 25.1, Fe(II) = 14.3, Pb(II) = 18.04, Cu(II) = 18.7 , Zn(II) =

16.44.[78] Moreover, EDTA can be recuperated and recycled which is economically and environmentally important since EDTA is expensive and poorly biodegradable.[82,144] Aqueous EDTA solution has been used to recover lead from recycled lead–acid battery slag and spent lead glass.[83,84] Another chelating agent is citric acid, a weak acid ($pK_{a1}$ = 3.09) [129] that can dissolve metals via two mechanisms, i.e.: direct displacement of metal ions by hydrogen ions and the formation of soluble metal complexes by chelation. Aqueous citric acid solution (with oxidizing or reducing agents) have been used to leach nickel, cobalt, lithium and manganese from spent lithium ion batteries;[85,86] rare-earth elements from neodymium magnet waste;[145] and potentially toxic metal(loid)s from sewage sludge, smelter slag and smelter soil.[146–148]

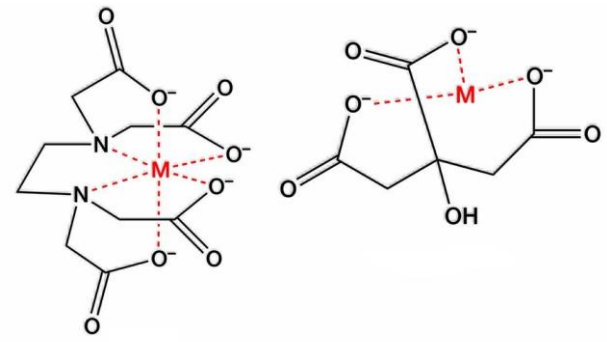


Figure 1.15: Metal chelation by EDTA and citric acid.

## 1.6 Advantages and challenges of using organic lixiviants for leaching industrial process residues

### 1.6.1 Advantages of using organic lixiviants

Recent studies have shown that using a suitable organic lixiviant can achieve higher selectivity than using aqueous lixiviant.[62,112,138,140,141,149–151] Selective leaching of only metal(s) of interest is an important requirement when treating low-grade metal sources such as industrial process residues. The mineral acids used in conventional hydrometallurgical leaching are so strong that they co-dissolve unwanted metals. This results in an excess consumption of acids in the leaching process, and of energy and chemicals in the further separation processes of the impurities in the resulting PLS. On the contrary,

using organic lixiviants can be selective towards the target metals, which allows for efficient consumption of chemicals during the leaching and downstream separation processes.

Another problem during acidic or alkaline aqueous leaching is the silica gel formation from silicate-containing residues, which causes serious difficulties during the solid-liquid filtration and the downstream solvent extraction process.[7] The mineral acids or bases dissolve the silica as silicic acid, which gradually polymerizes to form a gel. This silica gel formation can be avoided or reduced using a water-lean organic lixiviant because silicic acid cannot be formed without water.[7] In fact, Marin Rivera *et al.* showed that the formation of gel phases in leaching processes increases as the concentration of mineral acids increases, but decreases when the overall water content in the system decreases.[152] Moreover, organic lixiviants contain no or very little water, which means that less waste-water is required. This can be very practical in metal recovery in arid areas, where the water supply is limited. Lastly, using organic lixiviants can allow for process intensification, since the leaching and solvent extraction are combined in one step, where hydrometallurgical leaching requires two separate steps.

### 1.6.2 Challenges of using organic lixiviants

Currently, the organic lixiviants are not used at a commercial scale for leaching metals from high-grade ores or low-grade secondary sources. The main reasons may be due to the economical, engineering and environmental challenges associated with organic lixiviants.

The components of organic lixiviants (extractants and solvents) are much more expensive than the hydrometallurgical lixiviants (mineral acids or bases or salts and water).[7] The low concentration of valuable metals in industrial process residues make it even more difficult to convince the metallurgical industries to commercialize a leaching process using organic lixiviants. Therefore, it is crucial to consider the recyclability of the organic solvents when developing a leaching process using organic solvents. This PhD thesis pays special attention on the recyclability and reusability of the organic solvents used in the developed process. In addition, the organic lixiviants such as ILs and DESs are highly viscous, which hampers the mass transport and slows down the chemical reactions occurring during the leaching and metal recovery.[7] To reduce the viscosity, heating or water addition can be applied. Therefore, engineering an appropriate leaching set-up and equipment is critical for viscous organic lixiviants to achieve a comparable

leaching efficiency to that of lab-scale tests. Lastly, some organic lixiviants are not environmentally friendly. For instance, some ILs are non-biodegradable and have a large environmental impact because they are produced after multi-step synthesis and purifications processes.[153,154] Moreover, IL substituted with longer alkyl chains are found to be toxic to the aquatic microorganisms. However, these environmental issues are of little concern when the organic lixiviants can be recycled and reused. Nevertheless, choosing more environmentally friendly organic lixiviants will certainly help in adoption of its use in industries.

## 1.7 Why does lead metallurgy matter?

This PhD thesis focusses on the removal/recovery of lead from jarosite of zinc industry and lead smelter residues. Lead is a soft, ductile, highly malleable and bluish-white metal. It has high density and high coefficient for thermal expansion,[46,49,155] in contrast to low tensile strength and low electrical conductivity. Lead is easily combined with many other metals to make low melting-point alloys, which can be cast into many shapes. Today, about 11 million tons of lead are produced globally each year.[156] About 85% of the lead is used in lead-acid (LA) batteries, while the rest is used in pigment, cable sheathing, lead sheet, alloys, and ammunition (Figure 1.16). However lead is a toxic metal.[46] Lead interferes with biochemical processes in the human body by inhibiting or mimicking the actions of calcium and interact with proteins.[157] The release of high concentrations of lead by human activities, such as fossil fuels burning, mining, and manufacturing, has led to environmental contamination and the subsequent human exposure to lead.[157] As a result, almost all countries made stringent environmental regulations to limit the amount of lead in air and water, and prohibited the use of lead in many traditional objects (such as pigments, anti-knocking agents, solder alloys, plumbing, gunshot).

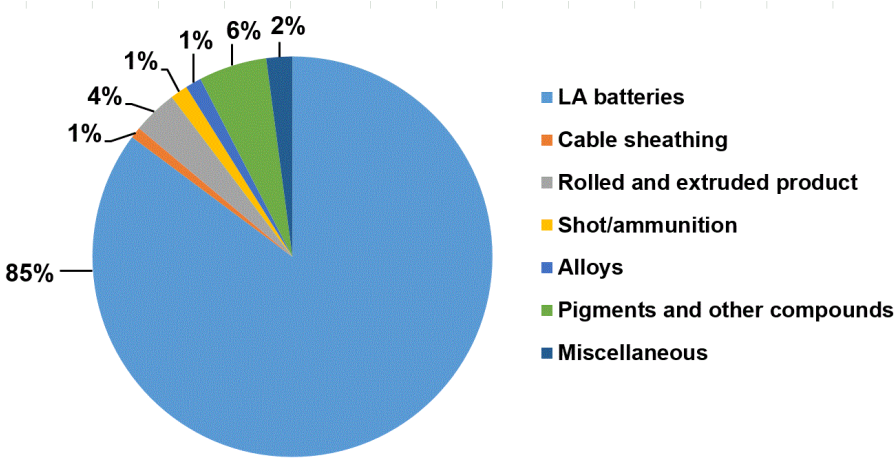


Figure 1.16: Distribution of lead applications. (https://www.ila-lead.org/lead-facts/lead-uses--statistics).[156]

However, completely phasing out the lead metallurgy due to its toxicity would have a detrimental impact, not only on the lead industry itself and the other linked industries, but also on the circular economy. Lead is a key enabler in the circular economy.[158] It is a carrier metal for many important metals (antimony, gold, tin, bismuth, indium, gallium, tellurium and silver), that are indispensable component in today's technologies (solar cells, LED lighting, LCD screen, phones, flame retardant) (Figure 1.17).[159,160] Primary lead ores always carry minerals of these metals, which are separated from lead during the refining process.[159] Lead also acts as liquid metal solvent where the abovementioned metals are dissolved during the pyrometallurgical processing of both ores and residues. Therefore, lead metallurgy should be further innovated and developed, while carefully managing its associated risks.

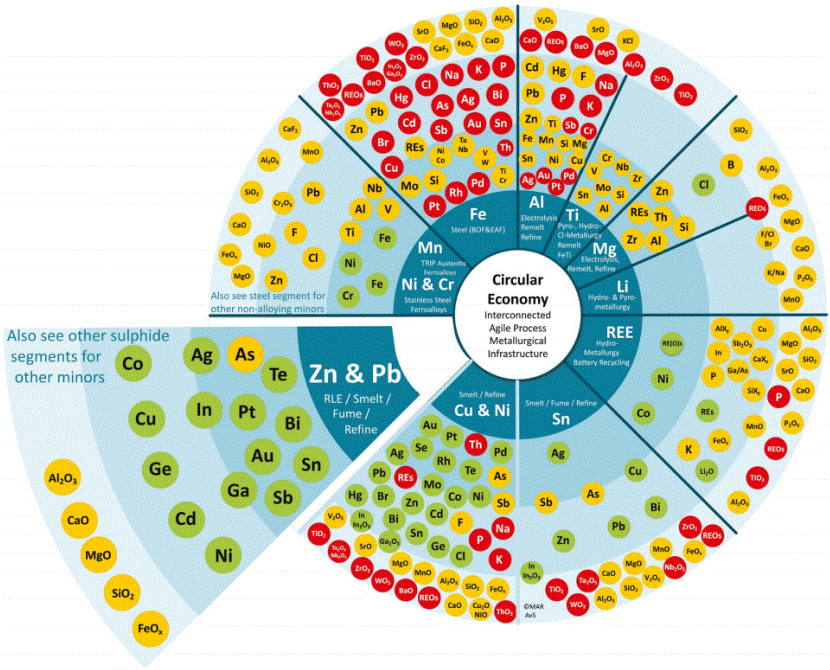


Figure 1.17: The Metal Wheel, showing the close symbiosis between the base metals and technology metals. The metals for which the base metal of that segment can act as a carrier metal are indicated with green circles. (https://kuleuven.sim2.be/wp-content/uploads/2019/02/SOCRATES-Policy-Brief-2019-Lead.pdf).[158]

# Chapter 2: Objectives

The overarching objective of this PhD thesis is to investigate the potential of organic lixivants for the metal recovery from low-grade industrial process residues. Jarosite from zinc hydrometallurgy plants, and lead smelter residues (matte, slag and dross) have been selected as the model industrial process residues for this research. These residues contain significant concentrations of toxic metals such as lead and economically important metals such as zinc and antimony. These residues are currently landfilled, but there is an increasing pressure from governments and the general public regarding the environmental concerns of landfills. The challenge with these residues is to selectively recover the target metals (e.g. Pb and Zn) with minimum co-dissolution of the matrix elements (e.g. Fe). The desired selectivity can be, in theory, achieved by choosing a suitable organic lixiviant for a specific residue. A screening test will be carried out to choose a suitable organic lixiviant for a particular residue, based on the maximum leaching of target metals and minimal co-dissolution of matrix elements. The composition and mineralogy of the fresh residues and leaching residues will be determined to understand the possible chemical reactions taking place during the leaching process. The operative leaching parameters (concentration of lixiviant, pH, liquid−to−solid ratio, temperature) will be optimized. A harsh operative condition will be only chosen if it is justifiable by a significant improvement in the leaching efficiency of the target metals. The leaching results by the chosen organic lixiviant will be compared with that of hydrometallurgical methods. The leaching at optimized conditions will be upscaled from few milliliters to one liter to check the scalability of the process.

Another important objective is to recover the organic lixiviant and reuse it for leaching fresh residue as many times as possible. This will significantly reduce the cost of the process, and justify the use of more expensive organic compounds over water, which is important for commercialization of the process. The recovery of the organic lixiviant will be carried out by precipitation/stripping of the dissolved metals, or by distillation of the organic components.

# Chapter 3: Selective metal recovery from jarosite residue by leaching with acid-equilibrated ionic liquids and precipitation-stripping

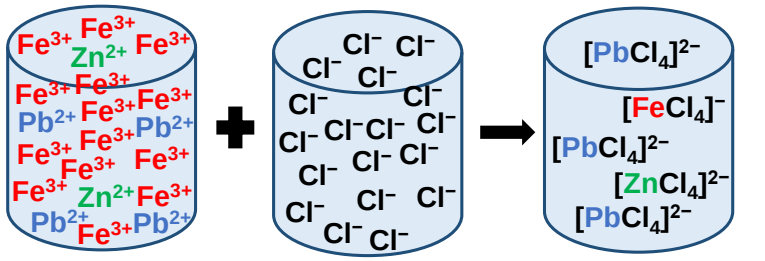


This chapter is based on the published paper:

**Palden, T.**; Regadío, M.; Onghena, B.; Binnemans, K. Selective Metal Recovery from Jarosite Residue by Leaching with Acid-Equilibrated Ionic Liquids and Precipitation-Stripping. *ACS Sustain. Chem. Eng.* **2019**, *7*, 4239–4246. https://doi.org/10.1021/acssuschemeng.8b05938.

The text may contain slight adjustments compared to the original publication.

*Author contributions:*

K.B., M.R. and T.P. conceived the original research idea. T.P. designed and executed the experiments, treated the data, drew the conclusions, and wrote the article. K.B. and M.R. contributed to the discussion of the results. All authors helped in the correction of the manuscript.

## Abstract

Recovery of valuable metals from industrial process residues is complex because those metals are often present in very low concentrations and often locked in complex matrices. Hence it is important to develop a process that selectively recovers the metal(s) of interest, while the undesired metals remain in the solid residue. Conventional pyrometallurgical and hydrometallurgical routes suffer from high cost and poor selectivity. In this work, a solvometallurgical approach was investigated for the selective leaching of lead and zinc from iron-rich jarosite of the zinc industry. Solvometallurgy uses organic solvents rather than water in order to reduce energy, acid and water consumption and to improve selectivity and reactivity. The screening of different solvometallurgical lixiviants showed that the presence of chloride anions in the lixiviant was crucial for leaching of lead. The ionic liquids Aliquat 336 ([A336][Cl]) and Cyphos IL 101 ([C101][Cl]), after equilibration with HCl, leached more lead and zinc compared to the other lixiviants. [A336][Cl] and [C101][Cl] equilibrated with 0.5 mol $L^{-1}$ HCl, were selected for the optimization study due to their higher selectivity towards lead and zinc and lower co-dissolution of iron, compared to the same ionic liquids equilibrated with a higher concentration of HCl. At optimized leaching conditions, the metal/iron mass ratio increased from 1/4 for Pb/Fe, and from 1/7 for Zn/Fe in the initial jarosite, to over 2/1 and 1/2, in the leachate, respectively. The dissolved metals were recovered by selective precipitation-stripping with an aqueous ammonia solution. Finally, the corresponding flowsheets were developed for the recovery of zinc and lead for both [A336][Cl] and [C101][Cl].

Keywords: basic extractants; iron-rich sludges; lead leaching; zinc leaching; solvometallurgy

## 3.1 Introduction

Currently, 75–80% of the world's zinc metal production is produced via hydrometallurgical processes.[9,11–13] This is about 8 million tons annually. Pure zinc metal is produced via a process combining roasting of sphalerite (ZnS) ore to an impure zinc oxide (ZnO) called "zinc calcine" followed by leaching of the calcine in different steps by sulfuric acid and electrowinning.[18] After the leaching process, a precipitation step is applied to remove the co-dissolved iron impurities from the solution. In the "jarosite" process, iron is removed from the leach liquor by precipitation as jarosite, which is a basic iron(III) sulfate complex $MFe_3(SO_4)_2(OH)_6$.[161,162] However, some amounts of lead, zinc, and valuable metals such as indium and germanium are co-precipitated along with iron upon the formation of jarosite. A plant producing 150,000 tons of metallic zinc annually generates about 125,000 tons of jarosite.[9] India, the European Union and China annually produce about 0.25, 0.60 and 1 million tons of jarosite, respectively.[25–27] Due to the high production rate and large generated volume, jarosite not only requires a lot of space for storage, but a large amount of valuable metals are lost with it and thus never return back to the value chain.

Much research has focused on the valorization of industrial process residues including jarosite as a material for construction and ceramic applications.[34–38] However, recovery of the valuable metals prior to their application as construction and ceramic materials was not considered. Hence these approaches result in a great loss of valuable metals. The recovery of metals from jarosite, like other industrial process residue, is complex because the relevant metals are present in low concentrations and often locked in complex matrices (sulphides, oxides, phosphates or silicates).[7] There are few examples of metal recovery from jarosite on a commercial scale. The Onsan Refinery of Korea Zinc used Top Submerged Lancing (TSL) Technology to recover 82% Zn, 92% Pb, 86% Ag and 61% Cu.[10] In China, some factories recovered about 75% Zn, 68% Pb, and 80% Ge by fuming the residue in a rotary kiln, using a mass of coal as heat source.[27] However, these pyrometallurgical processes applied to industrial residues with low concentration of valuable metals cause air pollution during fuming, and have high fixed investment and operation costs. Other studies applied hydrometallurgical routes to recover valuable metals from jarosite.[39–44] Rusen et al. (2008) recovered 71.9% Zn and 98.9% Pb using acid leaching ($H_2SO_4$) followed by brine (NaCl) leaching.[39] Turan et al. (2004) extracted 86% of Zn and 89% of Pb from the residue via $H_2SO_4$ blending and roasting, followed by water leaching and NaCl leaching.[40] Ju et al. (2011) developed a

roasting–$NH_4Cl$–alkali leaching process where more than 95% of the Zn, Pb, Cu, Cd, and Ag can be recovered from jarosite.[27] These hydrometallurgical routes are cheaper and considered to be cleaner compared to the pyrometallurgical routes, but they still have disadvantages. The most important disadvantage is their poor selectivity towards the target metals over iron. The co-dissolution of iron during the leaching process should be limited as much as possible to avoid high consumption of chemicals and to simplify the downstream purification processes.

However, by replacing the aqueous phase in hydrometallurgical processes by organic solvents, it is possible to attain high reactivity and selectivity because non-hydrated anions have a greater affinity to bind to some metal ions and the lack of water's high solvating power makes it impossible for some metals to enter into the solution, if they do not have sufficient affinity for the anions in the organic solution. This new approach to extractive metallurgy, based on the use of organic solvents instead of an aqueous phase, is called "solvometallurgy".[7]

This work presents the development of a novel solvometallurgical process to selectively recover lead and zinc from jarosite of the zinc industry. A suitable lixiviant was chosen after an initial screening test, based on the leaching efficiencies of lead and zinc and the selectivity towards these metals over iron. Finally, the recovery of the dissolved metals from the organic leachate (stripping) was studied.

## 3.2 Experimental

### 3.2.1 Chemicals

Jarosite was kindly provided by a European zinc producing company. Acetic acid (AnalR NORMAPUR, 100%), ammonia solution (≥25 wt% $NH_3$ in water, AnalR NORMAPUR) and hydrochloric acid (37 wt% HCl in water) were purchased from VWR Chemicals (Leuven, Belgium). Formic acid (99–100% pure), nitric acid (65 wt% $HNO_3$ in water), tri-*n*-butyl phosphate (TBP, >99wt%) and praseodymium standard (1000 mg $L^{-1}$, 2–5 wt% $HNO_3$) were purchased from Chem-Lab NV (Zedelgem, Belgium). Versatic Acid 10 was obtained from Resolution Europe B.V. (Hoogvliet, The Netherlands). Trihexyl(tetradecyl)phosphonium chloride (Cyphos® IL 101, >97%) and bis(2,4,4-dimethylpentyl) phosphinic acid (Cyanex® 272, >85%) were obtained from Cytec Industries (Niagara Falls, Ontario, Canada). Aliquat® 336 (trialkylmethylammonium chloride-based commercial mixture with trioctylmethylammonium chloride as the main component, 88.2–90.6%) was

purchased from Sigma-Aldrich (Diegem, Belgium). Di-(2-ethylhexyl)phosphoric acid (D2EHPA, >95%) and 1-octanol (99%) and Triton X-100 were supplied by Acros Organics (Geel, Belgium). Absolute ethanol was obtained from Fisher Scientific (Loughborough, United Kingdom). The silicone solution in isopropanol for the treatment of the TXRF quartz glass carriers was obtained from SERVA Electrophoresis GmbH (Heidelberg, Germany). All chemicals were used as received without any further purification.

### 3.2.2 Instrumentation

The jarosite sludge (as received) was dried in an oven at 110 °C for 24 h. The dried material was crushed and milled using a vibratory ring mill (Retsch RS200) for 30 s at 1000 rpm. Since the obtained powder sample may collect some moisture from the environment during the milling and sample handling prior to leaching experiment, the moisture content (MC%) of the final residue after milling was determined on the basis of its mass loss after drying in an oven at 110 °C for 48 h. The drying time was doubled compared to the first drying process to make sure that all the free water adsorbed on the surface of the powders was evaporated. The MC% was calculated according to equation (3.1).

$$MC(\%) = \frac{m_I - m_F}{m_F} \times 100 \qquad (3.1)$$

where $m_F$ is the mass of the residue (g) after drying and $m_I$ is the mass of the residue (g) before drying.

The morphology of the finely-milled powder was examined by scanning electron microscopy (SEM) using a Philips XL30 model (Philips, Amsterdam, The Netherlands) at an accelerating voltage of 10 keV. The powder sample was coated with a 10 nm platinum layer to avoid charging issues related to insulating sample.[163] The mineralogy was determined by powder X-ray diffraction (XRD) analysis using a Bruker D2 Phaser diffractometer (Bruker, Billerica, MA, USA). Diffractograms were recorded in the measurement range of 10 – 80° 2θ using $CuK_\alpha$ radiation and applying an acceleration voltage of 45 kV, a current of 30 mA, a step size of 0.020° and a counting time of 2.5 s per step. The raw data were processed with the X'pert HighScore Plus PANalytical software. The metal content of the jarosite was determined after

fully dissolving 10 mg of the milled sample in 10 mL of a 2/3 (v/v) mixture of 37 wt% HCl and 65 wt% $HNO_3$ solution using microwave-assisted acid digestion (Speedwave Xpert, Berghof, Germany). Nitric acid is a preferred mineral acid for microwave digestion because of its safe manipulation, facility of purification and oxidative characteristics.[164] The acid mixture of HCl and $HNO_3$ was necessary for complete dissolution of the residue. The sample dissolution via microwave digestion was done in triplicates to check the reproducibility of the composition. The metal concentrations in each of the digested acid solutions were measured in triplicate by Inductively Coupled Plasma-Optical Emission Spectrometry (ICP-OES, Optima 8300, Perkin Elmer, Waltham, MA, USA) for comparison. The particle size distribution of the milled jarosite was determined by dispersing the residue in water and measuring with a laser particle size analyzer (Mastersizer 3000, Malvern, Worcestershire, UK) in liquid mode. The leaching experiments were carried out in duplicate by shaking and heating using a laboratory shaker (Thermoshaker TMS-300, Nemus Life AB, Lund, Sweden). The concentration of the metals in the PLS was determined by Total-Reflection X-ray Fluorescence (TXRF, Bruker S2 Picofox, Bruker, Billerica, MA, USA).

### 3.2.3 Methodology

In the initial screening experiments, the hydrochloric acid containing organic lixiviants Cyphos IL 101, Aliquat 336, 1-octanol, and TBP were prepared by equilibrating with a 12 mol $L^{-1}$ hydrochloric acid solution. The equilibration was performed by mixing the lixiviant and the hydrochloric acid solution in a glass vial, forming a biphasic mixture with a volume phase ratio of 1:1, and stirring at 60 °C for 1 h at 2000 rpm in a laboratory shaker. The intensive shaking at 2000 rpm was done to ensure that equilibrium was attained.[165] After the equilibration, the separation of the organic and aqueous phases was accelerated by centrifugation at 5000 rpm for 20 min in a Heraeus Labofuge 200 centrifuge. The organic and aqueous phases were removed from the vial separately with a micropipette and kept in different vials. The nitrate analogues ([C101][$NO_3$] and [A336][$NO_3$]) of Cyphos IL 101 ([C101][Cl]) or Aliquat 336 ([A336][Cl]) were prepared by a metathesis reaction between the ionic liquid and a 2.5 mol $L^{-1}$ $KNO_3$ solution in three equilibration contacts with a volume phase ratio of 1:1, followed by three washes with aqueous $HNO_3$ solution of pH 3–4. The [C101][$NO_3$] and [A336][$NO_3$] were then equilibrated with 5 mol $L^{-1}$ nitric acid solution by using the same equilibration procedure as the abovementioned lixiviants. The lixiviants 1.2 mol $L^{-1}$ hydrochloric acid in ethanol were prepared by mixing 12

mol $L^{-1}$ hydrochloric acid in ethanol with a volume ratio of 1:9 followed by stirring at room temperature for 10 min at 600 rpm. The rest of the lixiviants were used without prior treatment.

For the leaching experiments, the solid material and lixiviant were mixed in 4 mL glass vials and agitated in the laboratory thermoshaker. The initial screening of lixiviants was performed using the following operation conditions: a liquid-to-solid ratio (L/S) of 10 mL $g^{-1}$, a temperature of 60 °C, a contact time of 2 h and a shaking speed of 2000 rpm. Once the most suitable lixiviants were selected, these operation conditions were further optimized. Finally, the leaching system was scaled up using a 250 mL separatory funnel and stirred by placing it sideways on a heating plate (IKA RCT classic). The leachate was separated from the solid residue through centrifugation (5300 rpm, 30 min). The finer particles suspended in the leachate were further separated by a syringe filter made of a polyester membrane (Chromafil® PET, 0.45 µm pore size).

For TXRF analysis, the sample was 10 times diluted with ethanol to minimize the matrix effects and a known amount of praseodymium internal standard (1000 mg $L^{-1}$) was added for quantification.[166] A quartz glass carrier was made hydrophobic by drying a 30 µL of a silicon solution in isopropanol (SERVA) on its surface and, finally, 2.5 µL of the diluted sample was pipetted on a quartz glass carrier and dried in oven for 30 minute at 60°C for analysis. The leaching efficiency $E_L$ *(%)* was calculated according to equation (3.2):

$$E_L(\%) = \frac{c_{M.L} \times v_{LIX}}{m_I \times c_{M.I}} \times 100 \qquad (3.2)$$

where $c_{M.L}$ is the metal concentration in the leachate after leaching (mg $L^{-1}$), $v_{LIX}$ is the volume of lixiviant used for leaching (L), $m_I$ is the mass of the solid material used for leaching (kg), and $C_{M.I}$ is the concentration of the metal in the jarosite before leaching (mg $kg^{-1}$).

The selectivity *S* of the process towards lead or zinc over iron was calculated according to equation (3.3):

$$S = \frac{c_{M.L} / c_{Fe.L}}{c_{M.I} / c_{Fe.I}} \quad (3.3)$$

where $c_{M.L}$ is the concentration of lead or zinc in the leachate (mg $kg^{-1}$), $c_{Fe.L}$ is the concentration of iron in the leachate (mg $kg^{-1}$), $c_{M.I}$ is the concentration of lead or zinc in the initial jarosite (mg $kg^{-1}$), and $c_{Fe.I}$ is the concentration of iron in the initial jarosite (mg $kg^{-1}$). The preferred case is $S > 1$ because then, the selectivity towards lead or zinc has improved after leaching, as compared to the initial jarosite residue. If the $S = 1$, the selectivity has not changed, and a low value of $S$ (less than 1) is unwanted as it means that the selectivity has declined in the leachate.

For the stripping experiments, the metal-loaded leachate was contacted with an aqueous ammonia solution (0.025 or 2 mol $L^{-1}$) in a glass vial using a volume phase ratio of 1:1 (commonly written as phase ratio $\Theta = 1$ ) and stirred in a thermoshaker at 60 °C at 1500 rpm for 1 h. The phase separation was aided by centrifugation and the precipitates were filtered using polyester syringe filters. The metal concentrations in the organic phase were analyzed by TXRF using the same methodology as described above. Similarly, the metal concentrations in the aqueous phase were analyzed via TXRF, but the liquid was diluted with 5 vol% Triton X-100 in water instead of ethanol.[166] The stripping efficiency $E_S$ (%) and the precipitation efficiency $E_P$ (%) were calculated according to equations (3.4) and (3.5):

$$E_S(\%) = \frac{c_S}{c_L} \times 100 \quad (3.4)$$

$$E_P(\%) = \frac{c_L - c_{S.L} - c_S}{c_L} \times 100 \quad (3.5)$$

where $c_L$ is the concentration of the metal in the leachate before stripping, expressed in mg $L^{-1}$, $c_S$ is the concentration of the stripped metal in the aqueous phase after stripping, expressed in mg $L^{-1}$, and $c_{S.L}$ is the concentration of the metal remaining in the stripped leachate, expressed in mg $L^{-1}$.

## 3.3 Results and discussion

### 3.3.1 Characterization of jarosite

The jarosite, which was provided as a sludge, was characterized after drying and milling into a fine powder (Figure 3.1). The moisture content of the dried and milled residue was 1.22% of the dried mass. The particle size ranged from 0.3 to 20 µm, although 90% of the particles were smaller than 1.95 µm. The elemental composition of the residue is shown in the Table 3.1. The elemental composition studied in triplicate varied by less than 5% from the mean, which indicates that the elements are well-dispersed throughout the sample and the composition is representative. The XRD pattern of the jarosite sample revealed that the main metal phases were natrojarosite ($NaFe_3(SO_4)_2(OH)_6$), anglesite ($PbSO_4$) and sphalerite (ZnS) (Figure 3.2). It must be noted that the jarosite studied here is a mixture of jarosite residue of the roast-leach-electrolysis process and the sulfur residue of the direct zinc leaching process. During the direct leaching process, zinc sulfide concentrates are directly leached in sulfuric acid solution in oxidizing conditions ($Fe_2SO_4$ as oxidizing agent) in atmospheric conditions.[167] This explains the presence of elemental sulfur and zinc sulfide in the residue since the former is a byproduct of the oxidation reaction and the latter is the undissolved feed which remained with the residue. Regarding the presence of lead sulfate in the residue, lead is present as an impurity in zinc sulfide concentrate and it easily precipitates in acidic solutions due its poor solubility. The phases of the other metals were not detected in the XRD pattern. It is most likely because of their low concentration and good dispersion in the sample, which result in no or very little X-ray diffraction.

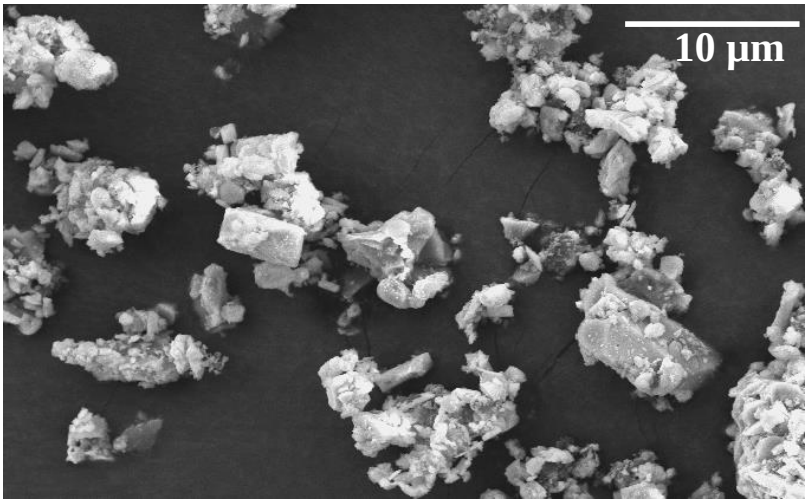


Figure 3.1: SEM micrograph of jarosite after drying (110 °C, 24 h) and milling (30 s, 1000 rpm).

Table 3.1: Elemental composition of milled jarosite residue.

| Metal | [g/kg] |
|---|---|
| $S^0+S^{2-}$ (a) | 187.00 |
| S as $SO_4^{2-}$ (a) | 92.00 |
| Fe | 173.53 ± 5.64 |
| Pb | 40.29 ± 0.35 |
| Zn | 24.04 ± 0.34 |
| Ca | 25.13 ± 1.71 |
| Na | 18.47 ± 0.83 |
| Al | 5.67 ± 0.33 |
| Mg | 3.04 ± 0.13 |
| K | 2.51 ± 0.14 |
| Si | 1.52 ± 0.08 |
| Cu | 0.90 ± 0.04 |
| Other (b) | 2.44 |

(a) The values were provided by the European zinc producing company,
(b) Others include Ba, Sr, Sn, P and B.

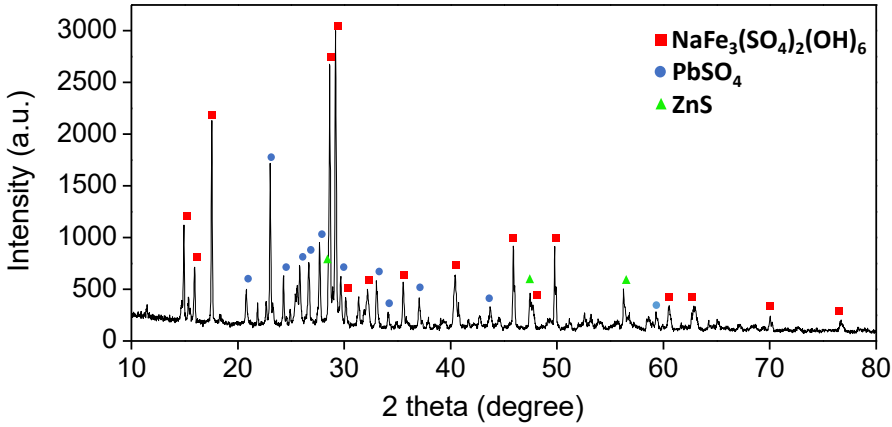


Figure 3.2: XRD pattern of jarosite after drying (110 °C, 24 h) and milling (30 s, 1000 rpm).

### 3.3.2 Comparison of solvometallurgical lixiviants

Various solvometallurgical lixiviants were compared in order to determine their suitability for the leaching of lead and zinc from jarosite. The tested lixiviants include organic acids with carboxylic and phosphoric acid functional groups, alcohols containing dissolved mineral acids and acidic, basic and neutral extractants equilibrated with mineral acids. Leaching with solutions of mineral acids (HCl, $H_2SO_4$, $HNO_3$) in alcohols such as ethanol is reported to be an effective solvometallurgical approach.[88,123] A promising system of *n*-octanol equilibrated with HCl has been developed to chemically attack resistant ores such as titanomagnetite.[124] Organic acids and acidic extractants, such as formic acid, acetic acid, D2EHPA, Versatic Acid 10 and Cyanex 272, can be applied directly for solvent leaching of a solid material, without the need of adding a mineral acid.[7] For example, Versatic Acid 10 is already known to be effective in recovering zinc from chloride-containing solid zinc waste residues.[134] Neutral extractants such as tri-*n*-butylphosphate (TBP) are poor lixiviants, but TBP equilibrated with mineral acids has been found to be a powerful lixiviant.[135,136] Similarly, basic extractants such as [C101][Cl] and [A336][Cl] combined with mineral acids have shown to be good lixiviants.[137] It should be noted that [C101][Cl] and [A336][Cl] can also be considered as ionic liquids. Therefore, [C101][Cl] and [A336][Cl] will be hereafter referred to as ionic liquids.

The ideal lixiviant should achieve a high recovery of zinc and lead and a limited co-dissolution of iron. The experimental results showed that the organic acids, namely formic acid, acetic acid and Versatic Acid 10, and the

acidic extractants D2EHPA, Cyanex 272 (unequilibrated) and Cyanex 272 (equilibrated with water) all leached a small amount of zinc (<6%), but no lead (Table 3.2). Similarly, the ionic liquids [A336][$NO_3$] and [C101][$NO_3$] equilibrated with 5 mol $L^{-1}$ $HNO_3$ leached a small amount of zinc (<7%) but no lead. The poor leaching of zinc and lead by these lixiviants could be due to the fact that zinc is present in jarosite as ZnS and lead as $PbSO_4$, whereas the lixiviants were previously used for leaching metals in oxide phases. On the other hand, the neutral extractant TBP equilibrated with 12 mol $L^{-1}$ HCl leached both lead (4%) and zinc (40%). Likewise, ethanol containing 1.2 mol $L^{-1}$ HCl and 1-octanol equilibrated with 12 mol $L^{-1}$ HCl also leached both lead (3%) and zinc (28%) but pure ethanol without dissolved HCl did not leach any lead (Table 3.2). Since the lixiviants that leached lead were the ones that contained chloride anions, it is obvious that the presence of this anion is crucial. Lead(II) forms the insoluble $PbCl_2$ at low chloride concentrations in water, while it forms the soluble $[PbCl_4]^{2-}$ complex in concentrated chloride solutions, according to the equations (3.6), (3.7), and (3.8).[40,168,169] The exact chloride concentration for forming insoluble $PbCl_2$ or soluble $[PbCl_4]^{2-}$ can vary from one system to another, depending on conditions such as the type of chloride sources (NaCl, $CaCl_2$, HCl), complexity of the solution (single-metal or multi-metal), mineral type of lead ($PbSO_4$, PbO, $PbCO_3$, etc.), temperature and kinetics.[170] A high chloride concentration is crucial for the dissolution of lead, zinc and iron.

$$Pb^{2+}(aq) + 2Cl^{-}(aq) \rightleftharpoons PbCl_2(s) \quad (3.6)$$

$$PbCl_2(aq) + Cl^{-}(aq) \rightleftharpoons [PbCl_3]^{-}(aq) \quad (3.7)$$

$$[PbCl_3]^{-}(aq) + Cl^{-}(aq) \rightleftharpoons [PbCl_4]^{2-}(aq) \quad (3.8)$$

The ionic liquids [C101][Cl] and [A336][Cl] equilibrated with 12 mol $L^{-1}$ HCl leached more lead (51% and 66%, respectively) than any of the other tested chloride-containing lixiviants, which could be explained by the higher chloride concentration in the ionic liquids. Furthermore, these ionic liquids contain cationic counter-ions, which means that they can more easily accommodate anionic species such as $[PbCl_4]^{2-}$ than molecular solvents such as 1-octanol. Based on the results in Table 3.2, TBP, [A336][Cl] and [C101][Cl] equilibrated with HCl were selected as the most promising lixiviants. The leaching of lead and zinc by [A336][Cl] and [C101][Cl] equilibrated with HCl can be expressed with equations (3.9) and that of iron by equations (3.9) and (3.10).[137]

$$2[Q][Cl] + 2HCl + M^{2+} \rightarrow [Q]_2[MCl_4] + 2\ H^+ \quad (3.9)$$

$$[Q][Cl] + 3HCl + M^{3+} \rightarrow [Q][MCl_4] + 3\ H^+ \quad (3.10)$$

where Q is the cation of the ionic liquid and M is Pb, Zn or Fe.

Table 3.2: Leaching efficiency ($E_L$ %) of lead, zinc and iron from jarosite by various lixiviants.[§]

| Lixiviant | Pb ($E_L$%) | Zn ($E_L$%) | Fe ($E_L$%) |
|---|---|---|---|
| Formic acid (undiluted) | 0 | 4.70 | 11.98 |
| Acetic acid (undiluted) | 0 | 0.65 | 5.33 |
| Versatic Acid 10 (undiluted) | 0 | 0.02 | 0.04 |
| Di-(2-ethylhexyl)phosphoric acid (D2EHPA) (undiluted) | 0 | 1.26 | 3.30 |
| Cyanex 272 (equilibrated with water) | 0 | 5.74 | 0.85 |
| Cyanex 272 (non-equilibrated) | 0 | 1.59 | 0.5 |
| [A336][$NO_3$] (equilibrated with 5 mol $L^{-1}$ $HNO_3$) | 0 | 6.70 | 1.18 |
| [C101][NO3] (equilibrated with 5 mol $L^{-1}$ $HNO_3$) | 0 | 1.04 | 0.01 |
| Ethanol (undiluted) | 0 | 2.85 | 3.64 |
| 1.2 mol $L^{-1}$ HCl in ethanol | 0.29 | 29.27 | 19.67 |
| 1-octanol (equilibrated with 12 mol $L^{-1}$ HCl) | 2.96 | 28.10 | 62.81 |
| TBP (equilibrated with 12 mol $L^{-1}$ HCl) | 4.22 | 39.48 | 89.85 |
| [A336][Cl] (equilibrated with 12 mol $L^{-1}$ HCl ) | 66.11 | 56.00 | 81.38 |
| [C101][Cl] (equilibrated with 12 mol $L^{-1}$ HCl ) | 51.06 | 66.14 | 87.42 |

[§]Leaching parameters: leaching time 2 h, 60 °C, 2000 rpm, L/S ratio 10 mL $g^{-1}$.

### 3.3.3 Effect of HCl concentration used for equilibration

The selected lixiviants [A336][Cl], [C101][Cl] and TBP were equilibrated with different concentrations of HCl to study their subsequent effect on the dissolution of metals from jarosite. For [A336][Cl] and [C101][Cl], the effect of HCl concentration used for equilibration was very similar (Figure 3.3 a, b). The leaching efficiency of lead, zinc and iron generally increased with increasing HCl concentration except for lead which reached a peak at 6 mol $L^{-1}$ and then decreased with increasing HCl concentration. The decrease in the leaching efficiency of lead at a HCl concentration higher than 6 mol $L^{-1}$ was not expected as high concentrations of $Cl^-$ normally increases its leaching efficiency by forming $[PbCl_4]^{2-}$ complexes. This could be explained by the fact that jarosite is not a single-metal residue and there could be competition for $Cl^-$ anions from iron and zinc in the residue. The existence of competition for $Cl^-$ ion can be further supported by the fact that the leaching efficiency for iron and zinc continuously increased after 6 mol $L^{-1}$ HCl concentration, showing higher affinities for these metals than for lead. For [A336][Cl] and [C101][Cl], the highest leaching efficiency of lead was achieved at 6 mol $L^{-1}$ with 74% and 88%, and the highest leaching efficiency for zinc was achieved at 12 mol $L^{-1}$ with 56 and 66%, respectively. The leaching efficiency of iron increased more than that of lead and zinc with increasing HCl concentration. It has to be noted that since the iron content in jarosite is much higher than the zinc or lead content, the same percentage increase in the leaching efficiencies of iron, zinc and lead results in a larger amount of iron being leached compared to zinc and lead. At 0.5 mol $L^{-1}$ HCl concentration, [A336][Cl] and [C101][Cl] leached more lead than zinc and iron. Hence the selectivity for lead was high compared to zinc and iron. When the HCl concentration was increased, the leaching of iron increased much more than that of lead and zinc. Hence, the selectivity towards lead and zinc over iron was significantly reduced at high HCl concentration due to greater co-dissolution of iron. Figure 3.4 clearly shows the decrease in the selectivity towards lead and zinc over iron when the HCl concentration was increased. Regarding TBP, the leaching of lead was very low at all HCl concentrations compared to that of [A336][Cl] and [C101][Cl] (Figure 3.3 c). This is most likely because the cations in the ionic liquids enhanced the leaching of insoluble lead sulfate since they can accommodate large anionic complexes like $[PbCl_4]^{2-}$ and keep them solubilized in the solution. TBP, being a neutral extractant, does not comprise cations, and therefore, the insoluble lead sulfate may have remained either fully or partially undissolved, and the dissolved lead may have precipitated as $PbCl_2$. The high leaching efficiency of

iron at different HCl concentrations in TBP is most likely due to the high solubility of jarosite in HCl-containing solutions.

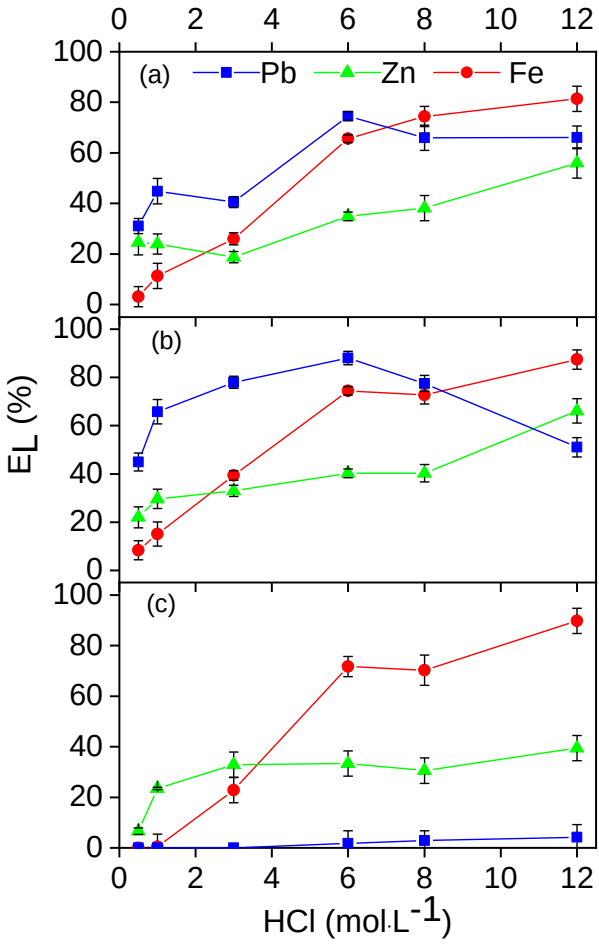


Figure 3.3: Leaching efficiency $E_L$ (%) of Pb (■), Zn(▲) and Fe(●) from jarosite by (a) [A336][Cl], (b) [C101][Cl] and (c) TBP equilibrated with different HCl concentrations. Leaching parameters: L/S ratio 10 mL $g^{-1}$, leaching time 2 h, 60 °C, 2000 rpm.

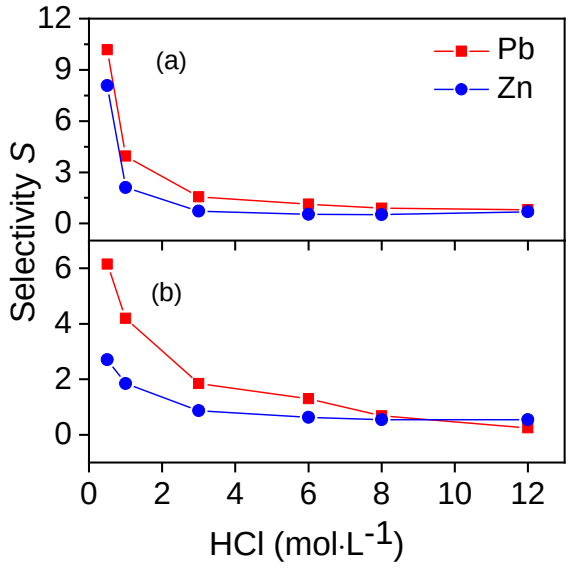


Figure 3.4: The selectivity S towards Pb (■) and Zn(●) over Fe, after leaching jarosite using (a) [A336][Cl] and (b) [C101][Cl] equilibrated with different HCl concentrations.

Although equilibrating [C101][Cl] and [A336][Cl] with a higher HCl concentration leached more lead and zinc, it also decreased their selectivity against iron. The co-dissolution of iron would interfere in the downstream processes of the metal recovery. Therefore, the ionic liquids equilibrated with 0.5 mol $L^{-1}$ HCl were chosen as the most suitable lixiviants due to their better selectivity against iron. TBP equilibrated with HCl was a poor lixiviant for lead and thus, it was not studied further.

### 3.3.4 Optimization and upscaling

The leaching parameters such as temperature, liquid-to-solid ratio, residence time were optimized for [C101][Cl] and [A336][Cl] equilibrated with 0.5 mol $L^{-1}$ HCl (Figure 3.5 a–c). The increase in temperature and L/S ratio did not have significant effect on the leaching efficiencies of lead, zinc and iron. However, as the contact time increased, the leaching efficiencies of the metals first increased and then decreased after reaching a plateau. The decreasing trend in the leaching as a function of the contact time could be due to the precipitation of metal ions due to chemical changes (e.g. pH, concentration of ions) in the solution medium over time.[171,172] Some studies also attribute a similar trend to the adsorption of dissolved species on the

surface of the residual solids.[171,173] The best leaching and selectivity values (Table 3.3) were achieved at L/S of 15 mL $g^{-1}$, 45 °C, 2 h leaching time and a stirring speed of 1500 rpm. After solvometallurgical leaching under these conditions, the relative concentration of lead over iron in the PLS compared to that of the original residue has improved by about eight times ($S \approx 8$), and that of zinc over iron by about three times ($S \approx 3.5$).

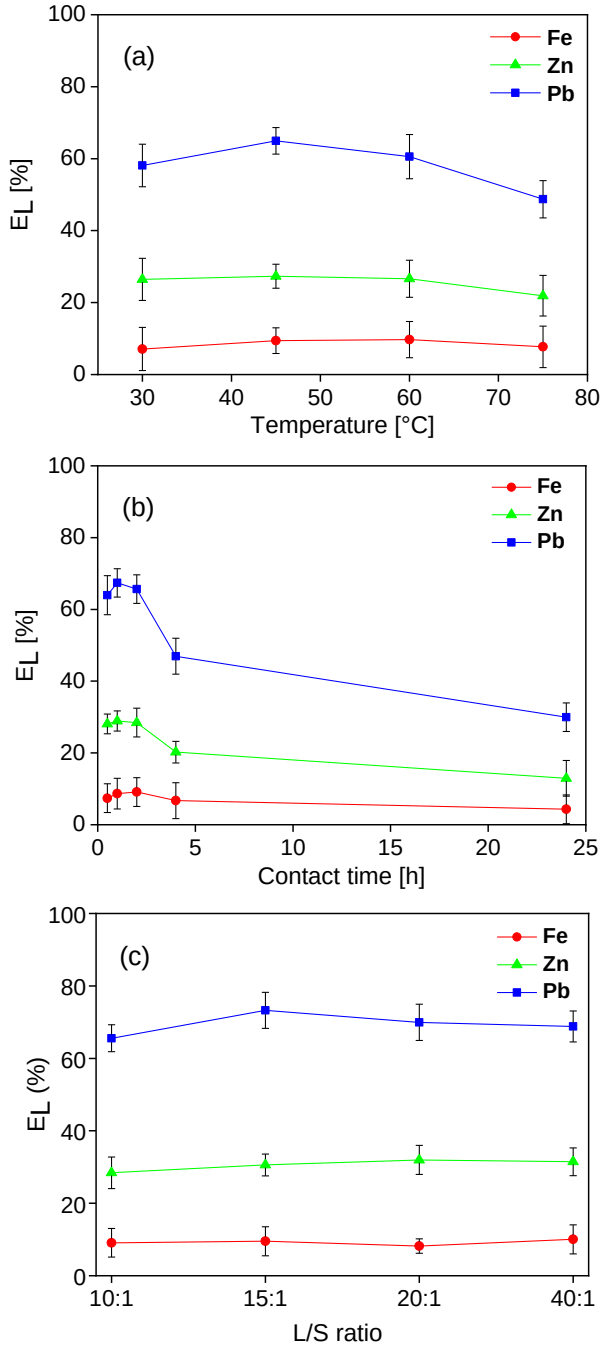


Figure 3.5: Effect of (a) temperature, (b) contact time and (c) liquid to solid ratio on leaching efficiency $E_L$ (%) of Pb, Zn and Fe from jarosite by [C101][Cl] equilibrated with 0.5 mol $L^{-1}$ HCl. (Stirring speed 1500 rpm)

Table 3.3: Leaching efficiencies and selectivity of lead, zinc and iron for jarosite at the optimized conditions[§].

| Lixiviants | Pb | | Zn | | Fe |
|---|---|---|---|---|---|
| | $E_L$ (%) | $S$ | $E_L$ (%) | $S$ | $E_L$(%) |
| [A336][Cl] (eq. with 0.5 mol $L^{-1}$ HCl) | 62 | 8.86 | 27 | 3.86 | 7 |
| [C101][Cl] (eq. with 0.5 mol $L^{-1}$ HCl) | 73 | 7.30 | 31 | 3.10 | 10 |

[§] Leaching parameters: L/S ratio 15 mL $g^{-1}$, 2 h, 45 °C, 1500 rpm

The scalability of the leaching results by [A336][Cl] and [C101][Cl] equilibrated with 0.5 mol $L^{-1}$ HCl was investigated by increasing the mass of the jarosite used for leaching from 0.1 to 10 g and by increasing the lixiviant volume from 1 to 100 mL. Upscaling the experiments resulted in a slight decrease of the leaching efficiency of lead by [A336][Cl] and [C101][Cl] equilibrated with 0.5 mol $L^{-1}$ HCl which is most likely because the L/S ratio was decreased from 15 to 10 (Table 3.4). A lower L/S of 10 was preferred because it reduces the cost of the process from an industrial perspective. Besides the slight decrease in the leaching efficiency of lead, the leaching efficiencies and selectivity of the other metals remained similar. The leaching of jarosite by [A336][Cl] and [C101][Cl] equilibrated with 0.5 mol $L^{-1}$ HCl can therefore be upscaled.

Table 3.4: Leaching efficiencies and selectivity of lead, zinc and iron after upscaling from 0.1g to 10 g of jarosite[§]

| Lixiviants | Pb | | Zn | | Fe |
|---|---|---|---|---|---|
| | $E_L$ (%) | $S$ | $E_L$ (%) | $S$ | $E_L$ (%) |
| [A336][Cl] (eq. with 0.5 mol $L^{-1}$ HCl) | 46 | 1.85 | 32 | 0.75 | 6 |
| [C101][Cl] (eq. with 0.5 mol $L^{-1}$ HCl) | 58 | 1.68 | 25 | 0.42 | 8 |

[§]L/S ratio 10 mL $g^{-1}$, contact time 2 hr, 45 °C, and magnetic stirring with temperature control

### 3.3.5 Metal recovery by selective precipitation-stripping

Wellens *et al.* successfully stripped zinc and iron from a [C101][Cl] leachate by using 2.67 mol $L^{-1}$ $NH_3$ solution.[137] Therefore, the recovery of dissolved metals from the [C101][Cl] leachate produced during the upscaling test was investigated by stripping with different concentrations of $NH_3$ in water. Three distinct phases were present after the stripping process: 1) a liquid organic phase, 2) a liquid aqueous phase and 3) a solid precipitate. At low range of $NH_3$ concentrations, from 0.0015 to 0.025 mol $L^{-1}$ $NH_3$, only about 30% of iron remained in the organic phase. The rest was either precipitated (30%) or stripped to the aqueous phase (40%) (Figure 3.6 a–c). Lead and zinc were neither stripped nor precipitated at those $NH_3$ concentrations. The iron in the organic and aqueous liquid phases continued to precipitate when the $NH_3$ concentration was increased from 0.025 mol $L^{-1}$, until complete precipitation of iron occurred at ≥1 mol $L^{-1}$ $NH_3$ concentration. Similarly, lead started to precipitate at $NH_3$ concentrations above 0.025 mol $L^{-1}$ and nearly 100% was precipitated by using 0.48 mol $L^{-1}$ $NH_3$. Interestingly, lead was never present in the aqueous liquor, denoting the preference to precipitate or remain dissolved in the organic phase. The pH of the aqueous phase was monitored during the stripping (Table 3.5). The poor solubility of Pb(II) in aqueous solution at acidic pH could be explained by the fact that it is, in general, hardly soluble in solutions with a low chloride concentration. Moreover, the solubility of Pb(II) in HCl solution is lower than in $CaCl_2$ or NaCl solution.[170] The very limited solubility in basic pH range is due to the formation of insoluble $Pb(OH)_2$.[174] On the other hand, zinc began to strip to the aqueous phase when the $NH_3$ concentration was increased above 0.32 mol $L^{-1}$, reaching 100% stripping at 2 mol $L^{-1}$ $NH_3$ concentration. A certain amount of zinc also precipitated at 0.32 to 1 mol $L^{-1}$ $NH_3$ concentration but it solubilised back in the aqueous solution at higher $NH_3$ concentrations. This odd behavior of zinc occurs because the Zn(II) ion forms insoluble $Zn(OH)_2$ in alkaline conditions, but it readily dissolves in excess of $NH_3$ owing to the formation of $[Zn(NH_3)_4]^{2+}$ ion.[175] In general, when contacting the HCl-containing ionic liquid with an aqueous solution, HCl was stripped to the aqueous phase. The strip solutions with a low $NH_3$ concentration (≤0.05 mol $L^{-1}$) became acidic after stripping because the protons from the stripped HCl were present in excess and fully neutralized all the $OH^-$ ions in the $NH_3$ solution (Table 3.5). On the other hand, stripping with $NH_3$ concentrations higher than 1 mol $L^{-1}$ resulted in a decrease of the pH but the solution remained basic since the $OH^-$ concentration in these $NH_3$ solutions was higher than the concentration of protons from the stripped HCl solution.

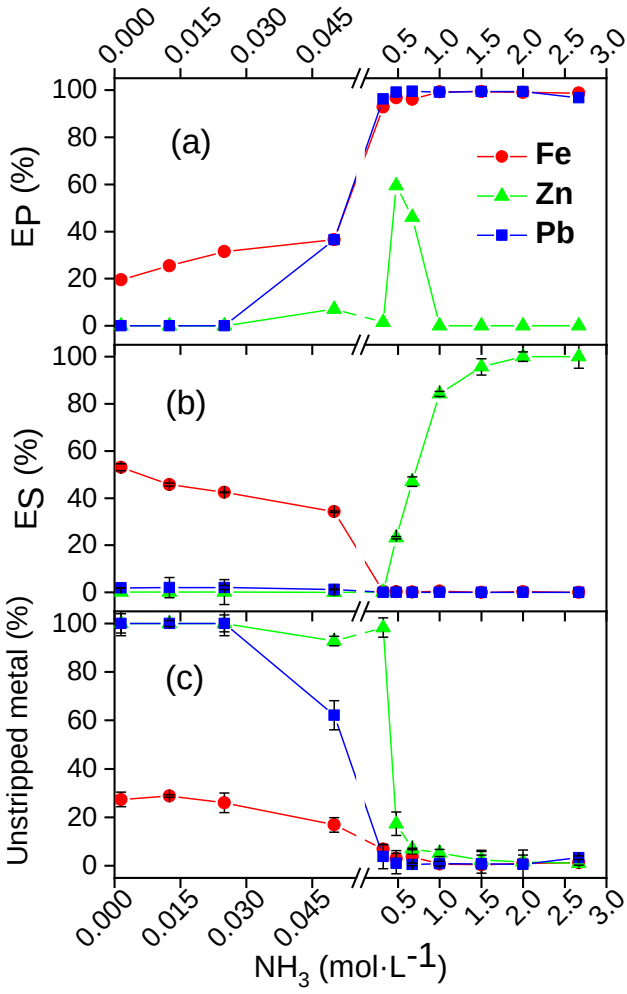


Figure 3.6: (a) The precipitating efficiency $E_P$ (%), (b) the stripping efficiency $E_S$ (%) and (c) the metals remaining in the stripped leachate (%) of Pb (■), Zn(▲) and Fe(●) from [C101][Cl] leachate to the aqueous phase when contacted with solutions with varying $NH_3$ concentration. Stripping parameters: volume phase ratio $\Theta$ = 1 (mL/mL), 1 h, 60 °C, 1500 rpm.

Table 3.5: pH of the different $NH_3$ solutions before and after contacting with the [C101][Cl] leachate.

| $NH_3$ [mol $L^{-1}$] | pH (before) | pH (after) |
|---|---|---|
| 0.0015 | 8.86 | 1.63 |
| 0.0125 | 10.17 | 1.76 |
| 0.025 | 10.58 | 1.86 |
| 0.05 | 10.86 | 2.08 |
| 1 | 11.73 | 9.74 |
| 1.5 | 11.77 | 10.20 |
| 2 | 11.87 | 10.30 |
| 2.67 | 11.94 | 10.61 |

Based on the results above, a two-step cumulative stripping process was proposed to selectively recover lead and zinc from [C101][Cl] leachate. This process consisted of stripping with 0.025 mol $L^{-1}$ $NH_3$ solution and then with a 2 mol $L^{-1}$ $NH_3$ solution. The first step with 0.025 mol $L^{-1}$ $NH_3$, to separate iron apart from the lead and zinc in the organic phase, stripped 34% of iron to the aqueous phase while 31% of iron precipitated (Table 3.6). The second stripping step was done with a 2 mol $L^{-1}$ $NH_3$ solution to strip 100% of zinc to the aqueous solution and to precipitate 100% of the lead along with the remaining 35% of the unstripped iron. Unlike what happened with the [C101][Cl] leachate, contacting the [A336][Cl] leachate with a 0.025 mol $L^{-1}$ $NH_3$ solution precipitated both iron and lead together. Since selective recovery of lead was not possible for the [A336][Cl] leachate, one-step stripping with a 2 mol $L^{-1}$ $NH_3$ solution was carried out where 100% of the lead and 100% of the iron were precipitated together, and 100% of the zinc was stripped selectively to the aqueous solution (Table 3.7).

Table 3.6: The stripping efficiency ($E_S$, %) and precipitating efficiency ($E_P$, %) of lead, zinc and iron during a two-step cumulative stripping of [C101][Cl] leachate [§]

| Step | Stripping agent | Phase | Pb | Zn | Fe |
|---|---|---|---|---|---|
| 1 | 0.025 mol $L^{-1}$ $NH_3$ | Precipitate ($E_P$, %) | 0 | 0 | 31 |
| | | Aq. Solution ($E_S$, %) | 0 | 0 | 34 |
| 2 | 2 mol $L^{-1}$ $NH_3$ | Precipitate ($E_P$, %) | 100 | 0 | 35 |
| | | Aq. Solution ($E_S$, %) | 0 | 100 | 0 |

[§] Stripping parameters: volume phase ratio $\Theta$ = 1 (mL/mL), contact time 1h, 60 °C, 1500 rpm

Table 3.7: The stripping efficiency ($E_S$, %) and precipitating efficiency ($E_P$, %) of lead, zinc and iron from [A336][Cl] leachate[§]

| Step | Stripping agent | Phase | Pb | Zn | Fe |
|---|---|---|---|---|---|
| 1 | 2 mol $L^{-1}$ $NH_3$ | Precipitate ($E_P$, %) | 100 | 0 | 100 |
| | | Aq. Solution ($E_S$, %) | 0 | 100 | 0 |

[§]Stripping parameters: volume phase ratio $\Theta$ = 1 (mL/mL), contact time 1h, 60 °C, 1500 rpm

After recovering lead, zinc and iron, the ionic liquid can be used for leaching a new batch of jarosite. A schematic representation of the leaching and subsequent recovery of the metal ions from the [C101][Cl] and [A336][Cl] leachate is shown in Figure 3.7.

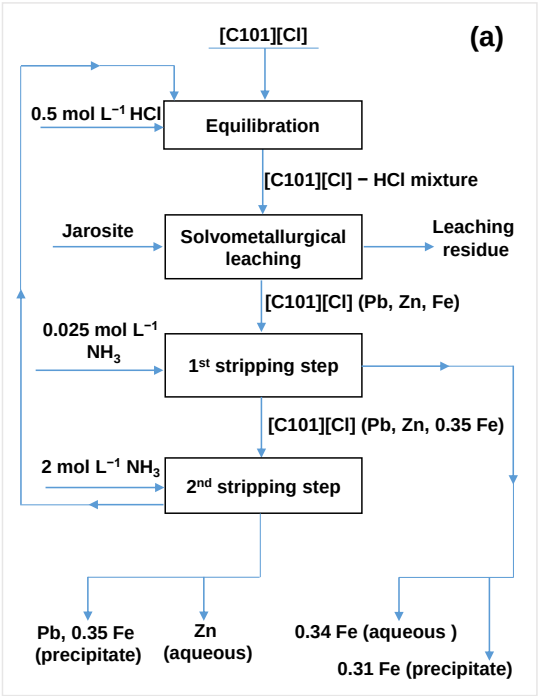


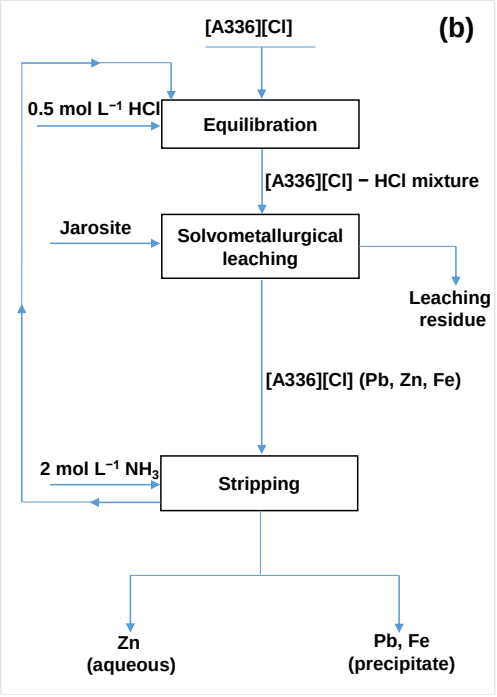


Figure 3.7: Flow chart for the recovery of lead and zinc from jarosite by using (a) [C101][Cl] and (b) [A336][Cl] equilibrated with 0.5 mol $L^{-1}$ HCl.

## 3.4 Conclusions

Solvometallurgical leaching was applied on a real jarosite residue from the zinc industry to selectively recover lead and zinc over iron. The presence of chloride in the lixiviant was crucial for the leaching of lead. The ionic liquids [A336][Cl] and [C101][Cl] equilibrated with HCl leached the highest amount of lead and zinc. This is due to the presence of high chloride concentration which resulted in the formation of the $[PbCl_4]^{2-}$ complexes and the presence of cations to counterbalance the dissolved anionic metal complexes. The selectivity towards lead and zinc over iron was strongly influenced by the concentration of HCl used for equilibrating the ionic liquids. The leaching efficiency of lead, zinc and iron generally increased with increasing HCl concentration but the selectivity decreased with increasing HCl concentration. The most selective leaching of lead and zinc over iron took place when the [A336][Cl] and [C101][Cl] were equilibrated with 0.5 mol $L^{-1}$ HCl. The leaching system could be upscaled from 0.1 to 10 g with minimal change in leaching efficiency and selectivity. The selective recovery of the dissolved metals from the [A336][Cl] and [C101][Cl] leachates was done by precipitation-stripping with aqueous $NH_3$ solutions. A two-step stripping with a 0.025 mol $L^{-1}$ $NH_3$ solution and a 2 mol $L^{-1}$ $NH_3$ solution was performed to recover the metals from the [C101][Cl] leachate. In this way, the majority of iron was separated from lead and zinc in the first step. In the second stripping step, lead and the remaining iron were precipitated, while zinc was fully separated from lead and iron by stripping to the aqueous phase. A one-step stripping with a 2 mol $L^{-1}$ $NH_3$ solution was carried out for the [A336][Cl] leachate. In this case, a precipitate containing lead and iron and an aqueous strip solution containing zinc were immediately obtained.

# Chapter 4: Methanesulfonic acid: a sustainable acidic solvent for recovering metals from jarosite residue of the zinc industry

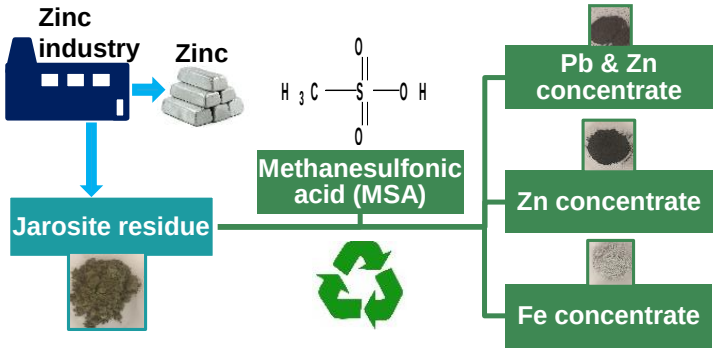


This chapter is based on the published paper:

**Palden, T**.; Onghena, B.; Regadío, M.; Binnemans, K. Methanesulfonic Acid: A Sustainable Acidic Solvent for Recovering Metals from the Jarosite Residue of the Zinc Industry. *Green Chem.* **2019**, *21*, 5394–5404. https://doi.org/10.1039/C9GC02238D.

The text may contain slight adjustments compared to the original publication.

*Author contributions:*

K.B., B.O. and T.P. conceived the original research idea. T.P. designed and executed the experiments, treated the data, drew the conclusions, and wrote the article. K.B. and B.O. contributed to the discussion of the results. All authors helped in the correction of the manuscript.

## Abstract

Methanesulfonic acid (MSA) is a green acid with a remarkably high solubility for several speciality and base metals including lead, making it an interesting leaching agent for metals. MSA is safer and less toxic than the mineral acids (HCl, $H_2SO_4$, $HNO_3$) currently employed for leaching metals from primary and secondary sources. In this study, MSA was tested for the leaching of lead and zinc from iron-rich jarosite residue of the zinc industry. The leaching of lead, zinc and iron increased as a function of the MSA concentration in water up to 90 vol% MSA. Higher MSA concentrations resulted in precipitate formation due to the limited solubility of the iron and zinc methanesulfonate salts in water-lean MSA. Leaching with pure MSA resulted in a pregnant leach solution (PLS) comprising most of the lead and zinc, and a precipitate comprising the majority of the iron and a fraction of the zinc originally present in the jarosite. The optimization of the leaching conditions showed that increasing the liquid-to-solid ratio or temperature increased the leaching efficiencies of the metals, especially of lead. The leaching at optimized conditions was successfully performed on a larger scale using a temperature-controlled batch leaching reactor. The metal/iron mass ratio increased from 1/4 for Pb/Fe, and from 1/7 for Zn/Fe in the initial jarosite, to over 2.66/1 and 1/2, in the PLS, respectively. The remaining MSA in the PLS was recovered by vacuum distillation and successfully reused for three leaching cycles.

Keywords: jarosite; metal recovery; methanesulfonic acid; selective leaching; solvometallurgy

## 4.1 Introduction

Methanesulfonic acid (MSA) is considered to be a green solvent.[128,176] The combination of its favorable physical and chemical properties makes MSA a suitable solvent for development of sustainable processes. It has a very low vapor pressure and high boiling point, and no dangerous volatile compounds evolve from the liquid under normal operational conditions.[128,176,177] The toxicity of MSA is relatively low compared to many commercially available acids. For instance, the $LD_{50}$ (oral, cat) of MSA is reported to be 1158 mg $kg^{-1}$ compared to 238−277 mg $kg^{-1}$ for hydrochloric acid.[178] It is readily biodegradable with a sulfate and carbon dioxide as the degradation products.[128,176] MSA is considered to be a natural product, and it is part of the natural sulfur cycle.[179] MSA is a strong acid with a $pK_a$ of −1.19 which is close to that of nitric acid ($pK_a$ = −1.3) and sulfuric acid ($pK_{a1}$ = −3) and higher than that of other organic acids such as formic acid ($pK_a$ = 3.82), acetic acid ($pK_a$ = 4.76) and citric acid ($pK_{a1}$ = 3.09).[129] The application of this strong acid as a commercial chemical is based on the fact that it is a non-oxidizing, highly conductive acid and that metal methanesulfonate salts are highly soluble in water.[128,176,180] As a result it has become the electrolyte of choice for many electrochemical processes, especially for electrodeposition of tin and lead.[128] Moreover, MSA has many prospective applications in catalysis[128,181–185] and as solvent for polymer synthesis and depolymerization.[186,187] With its beneficial physical and chemical properties, MSA is also a valuable candidate as reagent in extractive metallurgy, but it has been very little explored to date. MSA's high acidity and its ability to dissolve metal salts make it promising for the leaching of metals from primary and secondary metal sources.

Wu *et al.* achieved quantitative dissolution of lead from galena concentrate using a ferric methanesulfonate solution.[188] Feng *et al.* fully leached copper from malachite and zinc from smithsonite concentrates by using an MSA solution.[189,190] Hidalgo *et al.* leached copper from chalcopyrite using MSA solution containing ferric chloride as an oxidant.[191] Zhang *et al.* studied the dissolution kinetics of the zinc ore mineral hemimorphite in MSA.[192] These studies are largely of fundamental nature, targeting the leaching of one specific metal from an ore concentrate, which does not necessarily represent the complex composition of ores treated by the metallurgical industries. These studies also lack the downstream processing of the pregnant leach solutions (PLS). Gijsemans *et al.* used concentrated MSA to leach rare-earth elements terbium, cerium and lanthanum from real lamp phosphor waste residue where yttrium and europium were previously removed.[133] This is the

first and only study where concentrated MSA was applied as a leaching agent for the recycling of metals from real waste streams. However, the authors diluted the PLS containing unreacted MSA by 40 times with water to recover the dissolved metals via solvent extraction, and this makes recovery of MSA very difficult.

In this paper, we describe the development of a novel solvometallurgical process to recover lead and zinc from iron-rich jarosite residue using MSA as a leaching agent.[7] Jarosite is a solid residue generated by the zinc metallurgical industry.[9,18,45,161] The residue contains iron as the main component and some lead, zinc, and low concentrations of valuable metals such as indium, germanium and silver. Storage of jarosite in tailings ponds has some environmental issues and it is becoming increasingly difficult to get a license to open new jarosite tailing ponds. These issues could be prevented by valorizing jarosite, by recovering valuable metals and using the remaining residue in, for instance, building materials.[193,194]

## 4.2 Experimental

### 4.2.1 Chemicals

Jarosite was kindly provided by a European zinc producing company. Acetic Methanesulfonic acid (99.5%) was purchased from Carl Roth (Karlsruhe, Germany). Hydrochloric acid (37%) was purchased from VWR Chemicals (Haasrode, Belgium). Elemental iron (≥99%, reduced fine powder), elemental lead (≥99%, 325 mesh), elemental zinc (≥98%, <10 µm, dust), iron(II,III) oxide(95%, <5 µm ), lead(II) oxide (+99%) and zinc(II) oxide (>99% pure) were purchased from Sigma-Aldrich (Diegem, Belgium). Tri-*n*-octylamine (TOA, 98%), di-(2-ethylhexyl)phosphoric acid (D2EHPA, >95%) and Triton X-100 were supplied by Acros Organics (Geel, Belgium). Absolute ethanol and sulfuric acid (>95%) was obtained from Fisher Scientific (Loughborough, United Kingdom). Nitric acid (65%), tri-*n*-butyl phosphate (TBP, >99 wt%) and praseodymium standard (1000 mg $L^{-1}$, 2−5 wt% $HNO_3$) were purchased from Chem-Lab NV (Zedelgem, Belgium). Cyanex 923 was provided by Cytec Industries (Ontario, Canada). The silicone solution in isopropanol for the treatment of the total-reflection X-ray fluorescence spectroscopy (TXRF) quartz glass carriers was obtained from SERVA Electrophoresis GmbH (Heidelberg, Germany). All chemicals were used as received without any further purification. Jarosite was kindly provided by a European zinc producing company.

### 4.2.2 Instrumentation

The characterization techniques used for the milled jarosite were reported in a previous article by the same authors.[45] The leaching was carried on a RCT classic heating plate (IKA). The phase disengagement between the solid and liquid after leaching was carried out by centrifugation using a Heraeus Labofuge 200. The metal concentrations in the liquid phases were measured in duplicate by TXRF spectroscopy using a Bruker S2 Picofox spectrometer. The error associated with the measurements was ±5%. The MSA in the pregnant leach solution (PLS) was recovered by vacuum distillation using a standard set-up equipped with an Adixen pump (Pascal 2015SD) and a manometer (TPG 201 Pfeiffer Vacuum). The mineralogy of the solid materials was determined by powder X-ray diffraction (XRD) analysis using a Bruker D2 Phaser diffractometer. Diffractograms were recorded in the measurement range of 10 – 80° 2θ using $CuK_{\alpha}$ radiation and applying an acceleration voltage of 45 kV, a current of 30 mA, a step size of 0.020° and a counting time of 2.5 s per step. The raw data were processed with the X'pert HighScore Plus PANalytical software. The carbon and hydrogen content in the solid materials was measured in triplicate using an elemental CHN analyzer (FLASH2000, Thermo Scientific). The structural changes in distilled MSA were studied with Fourier Transform Infrared Spectroscopy (FTIR) spectroscopy and $^{1}H$ nuclear magnetic resonance ($^{1}H$ NMR). FTIR spectra were recorded in attenuated total reflectance (ATR) mode on a Bruker Vertex 70 spectrometer equipped with a Bruker Platinum ATR module with a diamond crystal. For $^{1}H$ NMR spectroscopy, the samples were dissolved in deuterated water and the spectra were recorded on Bruker Avance 400 spectrometer operating at 400 MHz. The scalability of the leaching at optimized conditions was studied using a customized 1 L jacketed laboratory reactor, linked to an automatic filtration unit (LabKit 36167) constructed by HiTec Zang GmbH, Germany.

### 4.2.3 Methodology

All the experiments hereon were carried out in duplicates and relative standard deviations were within ±5%. The jarosite sludge (as received) was dried in an oven at 110 °C for 24 h. The dried material was crushed and milled using a vibratory ring mill for 30 s at 1000 rpm. The moisture content (MC%) of the final residue (after initial drying and milling) was determined on the basis of its mass loss after drying again in an oven at 110 °C for 48 h, according to equation (4.1):

$$MC(\%) = \frac{m_I - m_F}{m_F} \times 100 \quad (4.1)$$

where $m_F$ is the mass of the residue (g) after drying and $m_I$ is the mass of the residue (g) before drying.

The initial leaching experiments were carried out by adding jarosite and MSA in a 4 mL glass vial and stirring on a heating plate. The following leaching conditions were applied: a liquid-to-solid ratio (L/S) of 10 mL $g^{-1}$, a temperature of 60 °C, a contact time of 2 h and a stirring speed of 600 rpm. The scalability of the leaching system was tested using two different set ups. The first one used a 500 mL round bottom flask which was fixed on a customized aluminum heating block and then stirred on a heating plate. The second one used the 1 L batch reactor.

During leaching, the solids in the vials turned from green to grey. The vials containing the PLS and solids were immediately centrifuged (5300 rpm, 30 min) after leaching. Two solid phases (dark green and white) and one liquid phase were distinctly separated after centrifugation due to difference in their density. The PLS was pipetted out from the vial and the finer particles suspended in the PLS were further separated by a syringe filter made of a polyester membrane (Chromafil PET, 0.45 µm pore size). The MSA in the PLS was recovered by vacuum distillation and the reusability of the distilled MSA in leaching jarosite was tested using the same set-up as in the leaching experiments described above.

The metal concentration in the PLS was measured using TXRF. The samples were 50 times diluted with ethanol to minimize the matrix effects and a known amount of a 1000 mg $L^{-1}$ praseodymium internal standard was added for quantification. The sample preparation and the measurement procedure were carried out following the recommendation by Regadío *et al.*[166] The *leaching efficiency* $E_L$ *(%)* was calculated according to equation (4.2). Precipitated metals are not taken into account in the *leaching efficiency*.

$$E_L(\%) = \frac{c_M \times v_{LIX}}{m_I \times c_I} \times 100 \quad (4.2)$$

where $c_M$ is the metal concentration in the PLS after leaching (mg $L^{-1}$), $v_{LIX}$ is the volume of leaching agent used for leaching (L), $m_I$ is the mass of the solid

material used for leaching (kg), and $c_I$ is the concentration of the metal in the jarosite before leaching (mg $kg^{-1}$).

Two solid phases (color: dark grey and white) were present after leaching and they were clearly separated by centrifugation due to difference in their densities. The two solids were physically separated by scooping the white solid from the top using a spatula. The white solid was water soluble and therefore, it was dissolved in water and elemental analysis was performed using TXRF. The samples for TXRF analysis were prepared by diluting the solution of the white solid with a solution of 5 vol% Triton X-100 in water.[166] For XRD measurements, the solids were dried to remove traces of MSA in a vacuum oven at 130 °C and a pressure of <1 mbar for 24 h. A detailed investigation of the solid phases showed that the grey solid corresponds to the leaching residue and the white solid to a precipitate. The results are discussed more in detail later in the article. The *precipitation efficiency* $E_P$ (%) was calculated according to equations (4.3):

$$E_{\mathrm{P}}(\%) = \frac{c_{\mathrm{M}} \times v_{AQ}}{m_{\mathrm{I}} \times c_{\mathrm{I}}} \times 100 \qquad (4.3)$$

where $c_M$ is the concentration of metals in water after dissolving the white precipitate (mg $L^{-1}$), $v_{AQ}$ is the volume of water used for dissolving the white precipitate (L), $m_I$ is the mass of the solid material used for leaching (kg), and $c_I$ is the concentration of the metal in the jarosite before leaching (mg $kg^{-1}$).

The *selectivity S* of the process towards lead or zinc over iron was calculated according to equation (4.4):

$$S = \frac{c_{\mathrm{M.L}}/c_{\mathrm{Fe.L}}}{c_{\mathrm{M.I}}/c_{\mathrm{Fe.I}}} \qquad (4.4)$$

where $c_{M.L}$ is the concentration of lead or zinc in the leachate (mg $kg^{-1}$), $c_{Fe.L}$ is the concentration of iron in the leachate (mg $kg^{-1}$), $c_{M.I}$ is the concentration of lead or zinc in the initial jarosite (mg $kg^{-1}$), and $c_{Fe.I}$ is the concentration of iron in the initial jarosite (mg $kg^{-1}$). The preferred case is $S > 1$ because then, the selectivity towards lead or zinc has improved after leaching, as compared to the initial jarosite residue. If the $S = 1$, the selectivity has not changed, and

a low value of *S* (less than 1) is unwanted as it means that the selectivity has declined in the leachate.

The *recovery rate $R_R$ (%)* of the MSA was defined as the amount of MSA recovered after vacuum distillation with respect to the total MSA initially used for leaching (equation 4.5).

$$R_R(\%) = \frac{V_F}{v_I} \times 100 \quad (4.5)$$

where $v_I$ is the volume of the MSA initially used for leaching jarosite (L) and $v_F$ is the final volume of MSA recovered after leaching and vacuum distillation (L).

The concentration of sulfate in the white precipitate was determined by gravimetric analysis. The white precipitate was first dissolved in a 6 M HCl solution and then an excess of $BaCl_2$ 0.5 M standard aqueous solution was added. The solution was stirred for 30 min at 60 °C. The solution turned cloudy due to the formation of $BaSO_4$ precipitate, which was separated by centrifugation. Excess amount of the standard $BaCl_2$ solution was added again to the centrifuged solution without the precipitate, and stirred for another 30 min to check for any remaining sulfate. The $BaSO_4$ precipitate was washed three times with water and dried in an oven at 100 °C for 12 h. The amount of sulfate in the original precipitate was determined from the amount of $BaSO_4$ precipitated.

The solubility studies were carried by adding a variable mass of pure metals and metal oxides to a glass vial containing 2 mL of pure MSA. Then the vial was stirred and heated on a heating plate at a temperature of 60 °C, for a contact time of 2 h and at a stirring speed of 600 rpm.

## 4.3 Results and discussion

### 4.3.1 Characterization of jarosite

The moisture content of the dried and milled residue was 1.22% of the dried mass. The particle size ranged from 0.3 to 20 µm, although 90% of the particles were smaller than 1.95 µm. The elemental composition of the residue is shown in the Table 4.1. The main metal phases were natrojarosite ($NaFe_3(SO_4)_2(OH)_6$), anglesite ($PbSO_4$) and sphalerite (ZnS).

Table 4.1: Elemental composition of milled jarosite residue.[45]

| Metal | [g/kg] |
|---|---|
| $S^0+S^{2-}$ (a) | 187.00 |
| S as $SO_4^{2-}$ (a) | 92.00 |
| Fe | 173.53 ± 5.64 |
| Pb | 40.29 ± 0.35 |
| Zn | 24.04 ± 0.34 |
| Ca | 25.13 ± 1.71 |
| Na | 18.47 ± 0.83 |
| Al | 5.67 ± 0.33 |
| Mg | 3.04 ± 0.13 |
| K | 2.51 ± 0.14 |
| Si | 1.52 ± 0.08 |
| Cu | 0.90 ± 0.04 |
| Other* | 2.44 |

(a) The values were provided by the European zinc producing company,

(b) Others include Ba, Sr, Sn, P and B.

### 4.3.2 Effect of the MSA concentration

The leaching of lead, zinc and iron from jarosite was studied as a function of the MSA concentration. All three metals were affected differently by the increasing MSA concentration (Figure 4.1). The decrease in the leaching efficiency of zinc at 50 vol% MSA is most likely because the optimal leaching of zinc requires a high activity of water. The leaching efficiency of lead and iron increased exponentially with increasing MSA concentration, which is likely due to the higher concentration of MSA acting as a strong acid. However, between 90 and 100 vol% MSA, the leaching efficiency of iron and zinc drastically decreased. This could be explained by the poor solubility of their corresponding methanesulfonate salts in pure MSA, due to the weak solvating properties of the concentrated MSA solution towards these metal cations. The high leaching efficiency of lead at 100 vol% of MSA, in contrast to that of zinc and iron, indicates a higher solubility of lead(II) in pure MSA acid than zinc(II) and iron(III). The difference in the solubility of the metal ions in MSA could be explained by the difference in the size of the cations.[195] The solubility increases with increasing cation size. The largest ionic radius is that of lead ($Pb^{2+}$ = 119 pm), followed by zinc ($Zn^{2+}$ = 74 pm) and then iron ($Fe^{3+}$ = 60 pm). Larger cations such as the $Pb^{2+}$ ion have smaller ionic potential

(charge/radius), and thus they have weaker attraction and weaker bonds toward the methanesulfonate anions. Conversely, smaller cations such as iron and zinc have larger ionic potential, and their attraction to anions is stronger, thereby increasing the formation of the methanesulfonate salts.

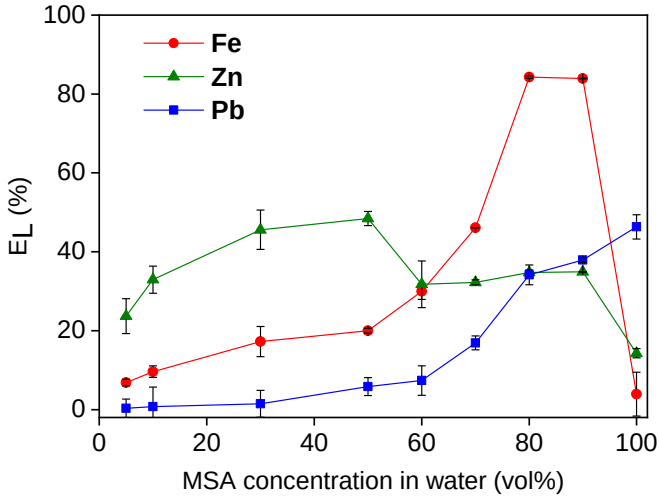


Figure 4.1: Effect of the MSA concentration on the leaching efficiency $E_L$ (%) of Pb (■), Zn (▲) and Fe (●) from jarosite. Leaching parameters: L/S ratio 10 mL $g^{-1}$, contact time 2 h, 60 °C, stirring speed 600 rpm.

At MSA concentrations of more than 90 vol%, the formation of a white precipitate was observed (Figure 4.2). This white precipitate could be separated from the pregnant leach solution (PLS) and the residue by centrifugation and appeared to be soluble in water. To get more insight into the formation of the white precipitate, the leaching efficiency and precipitation efficiency of lead, zinc and iron were studied in more detail at MSA concentrations above 90 vol% (Figure 4.3). Elemental analysis by TXRF showed that the white precipitate is composed of iron and zinc, without the presence of any lead. Upon increasing the MSA concentration above 90 vol%, the leaching efficiency of iron and zinc decreased gradually, while their precipitating efficiencies of the white precipitate increased gradually (Figure 4.3).

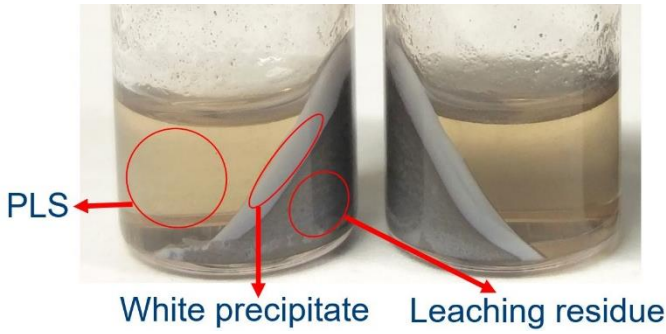


Figure 4.2: One liquid (PLS) and two solid phases (leaching residue and white precipitate) after leaching of jarosite by pure MSA. Leaching parameters: L/S ratio 10 mL $g^{-1}$, contact time 2 h, 60 °C, stirring speed 600 rpm.

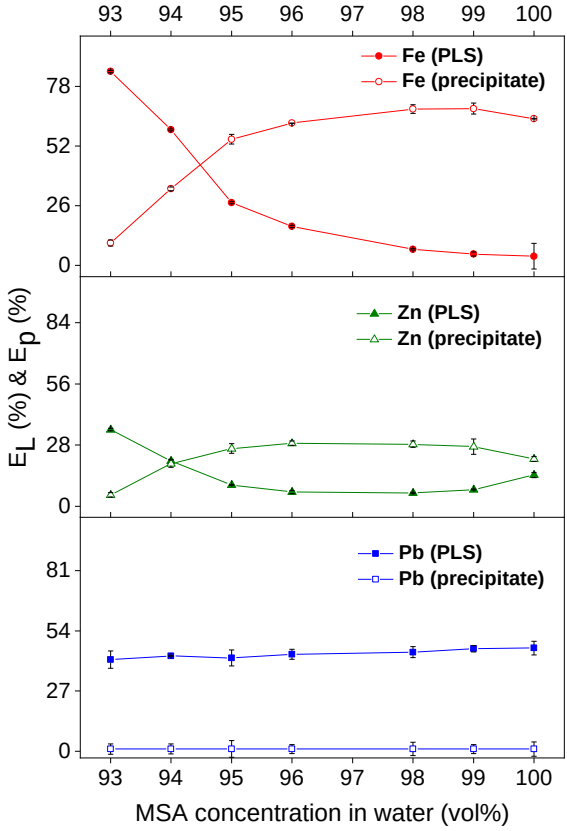


Figure 4.3: Effect of MSA concentration (90-100 vol%) on the leaching efficiency $E_L$ (%) and precipitating efficiency $E_P$ (%) of Pb (■), Zn (▲) and Fe (●) from jarosite. Leaching parameters: L/S ratio 10 mL $g^{-1}$, contact time 2 h, 60 °C, stirring speed 600 rpm.

This might be caused by the low solubility of iron and zinc in pure MSA and shows that these metals require a distinct amount of water to remain in solution. The strongly acidic MSA solution reacts with the iron and zinc minerals in the jarosite, forming well-solvated iron and zinc methanesulfonate in the solution containing distinct amounts of water. In the case of water-lean MSA solutions or pure MSA, the iron and zinc precipitate due to the low solubility of their methanesulfonate salts in pure MSA solution. The high concentration of lead in the PLS and its absence in the precipitate confirms a higher solubility of lead(II) methanesulfonate in pure MSA. The role of water in leaching jarosite is minimal and most likely limited to solvation; water does not act as a proton donor. The fact that water is a weak proton donor together with the high stability of the minerals in the jarosite residue (jarosite, anglesite and sphalerite), makes reactivity of the water towards them low.

The leaching of lead, zinc and iron by MSA can be expressed by equations (4.6), (4.7) and (4.8):[189–191]

$$PbSO_4(s) + 2CH_3SO_3H(l) \rightleftharpoons Pb(CH_3SO_3)_2(l) + H_2SO_4(l) \quad (4.6)$$

$$ZnS(s) + 2CH_3SO_3H(l) \rightleftharpoons Zn(CH_3SO_3)_2(l) + H_2S\,(g) \quad (4.7)$$

$$2NaFe_3(OH)_6(SO_4)_2(s) + 18CH_3SO_3H(l) \rightleftharpoons 6Fe(CH_3SO_3)_3(l) + Na_2SO_4\,(l) + 3H_2SO_4\,(l) + 12H_2O(l) \quad (4.8)$$

### 4.3.3 Leaching jarosite with mineral acids ($H_2SO_4$, $HNO_3$ and HCl)

Jarosite was leached with solutions of different concentrations of common mineral acids ($H_2SO_4$, $HNO_3$ and HCl) in water to compare their leaching results with those of MSA. The leaching results (Figure 4.4) showed comparable trends to those of MSA (Figure 4.1, 4.3). The leaching efficiencies of lead, zinc and iron initially increased due to higher amount of acids available to react with the metal-containing minerals, and sufficient water molecules to keep the metals dissolved. When the concentration of acid was further increased and thus the concentration of water correspondingly decreased, some metals precipitated due to their low solubility in water-lean acid solutions. This explains the decrease in the leaching efficiency of iron and lead after leaching with concentrated nitric acid (14.6 mol $L^{-1}$), and that of lead, zinc and iron when sulfuric acid concentration was higher than 4 mol $L^{-1}$. A white precipitate was formed during leaching at these concentrations.

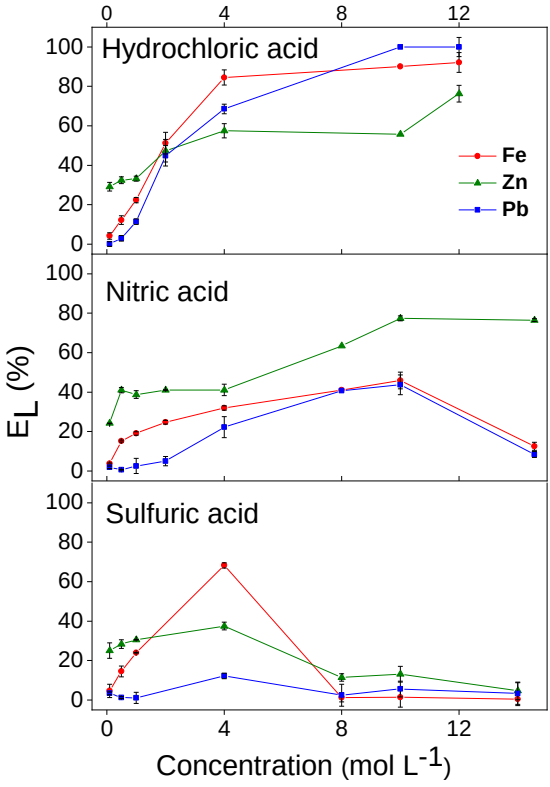


Figure 4.4: Effect of the mineral acid ($H_2SO_4$, $HNO_3$ and HCl) concentration on the leaching efficiency $E_L$ (%) of Pb (■), Zn (▲) and Fe (●) from jarosite. Leaching parameters: L/S ratio 10 mL $g^{-1}$, contact time 2 h, 60 °C, stirring speed 600 rpm.

This is an indication of the low solubility of some metal salts at high acid concentration and low water content. The leaching efficiency of the metals did not decrease with concentrated hydrochloric acid (12.2 mol $L^{-1}$) and that is most likely because there is still a sufficient amount of water available to dissolve the metal chloro complexes. MSA showed superior results compared to the investigated mineral acids in selective leaching of lead and zinc from iron-rich jarosite residue. The leaching with HCl, $HNO_3$ and $H_2SO_4$ resulted in poor selectivity towards lead and zinc due to high co-dissolution of iron in the PLS. During the MSA leaching of lead and iron from jarosite, sulfuric acid and water was released as a by-product (Equations 4.6 and 4.8). Sulfuric acid has high reactivity towards iron and zinc, but it has a negative impact on lead leaching due to the low solubility of lead sulfate. On the other hand, the water molecules will increase the solubility of iron and zinc in the

PLS, and therefore, it would reduce the selectivity towards lead and zinc. Nevertheless, the influence of the by-products on the leaching would be minimal since their concentration in the PLS is very low ($H_2SO_4 \approx 0.05$ mol $L^{-1}$, $H_2O \approx 0.2$ mol $L^{-1}$).

### 4.3.4 Effect of liquid-to-solid ratio and temperature

Pure MSA was selected as the most suitable leaching agent for further optimization studies because it resulted in maximum leaching of lead with minimum co-dissolution of iron in the PLS. The effect of the liquid-to-solid (L/S) ratio and the temperature on the leaching of jarosite with MSA was studied by varying the L/S ratio from 15 to 40 mL $g^{-1}$ and the temperature from 60 to 160 °C (Figure 4.5). Increasing the L/S ratio and the temperature significantly increased the leaching efficiency of lead, which indicates that both parameters have a strong influence on the leaching of lead from the residue. The increase in the leaching efficiency of lead was especially large when the L/S ratio was increased from 15 to 20 mL $g^{-1}$. The influence of L/S ratio is much smaller for the leaching of zinc and iron, which is likely due to the low solubility of the methanesulfonate salts of iron and zinc in pure MSA. Increasing the temperature increased the leaching efficiency of zinc and iron, likely because the maximum solubility is positively correlated to the temperature. It is especially influential for leaching zinc as the leaching efficiency reached >70% at 160 °C. However, when the PLS was cooled overnight from 160 °C to room temperature, part of the dissolved zinc and iron precipitated.

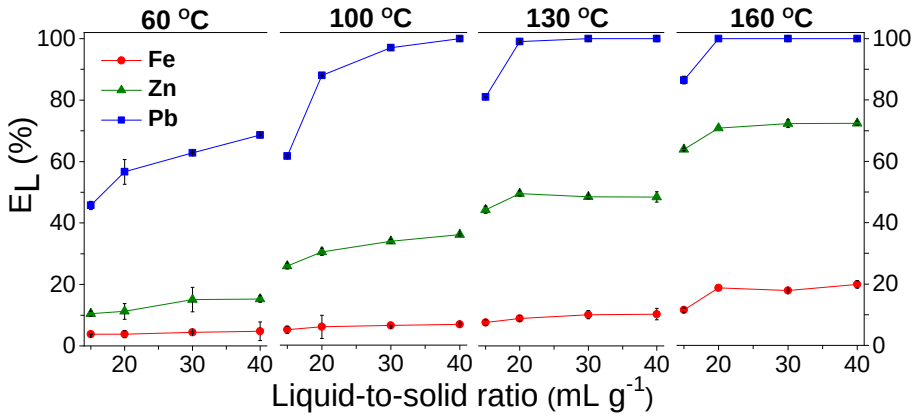


Figure 4.5: Effect of liquid-to-solid ratio and temperature on the leaching efficiency $E_L$ (%) of Pb (■), Zn (▲) and Fe (●) from jarosite by pure MSA. Leaching parameters: contact time 2 h, stirring speed 600 rpm.

The high temperature during leaching resulted in oversaturation of zinc and iron in pure MSA and therefore, these metals partially precipitated when the PLS was cooled. Although 160 °C resulted in more zinc leaching (~72%), it also resulted in more iron leaching (~19%) compared to leaching at lower temperature (Figure 4.5). Additionally, the partial precipitation of zinc and iron upon cooling down of the PLS from 160 °C to ambient temperature further complicates the process for downstream processing. Therefore, leaching at a L/S ratio of 20 mL $g^{-1}$ and a temperature of 130 °C was chosen to be the most suitable conditions for further investigation. At these condition, while the leaching efficiency of lead is 100%, the leaching efficiency of zinc is still high at 50% and that of iron is low at 9%, resulting in a good selectivity towards zinc and lead.

### 4.3.5 Effect of leaching time

The dissolution was faster for lead and iron than for zinc (Figure 4.6). The leaching efficiency of lead was already 85% after 5 min and then it increased slowly to 100% after 120 min. In the case of zinc, the leaching efficiency after 5 min is 28% and it increased to 56% after 360 min. The leaching efficiency of iron was 5% after 0.5 min and then it reached a maximum of 9% after 120 min. Although the leaching efficiency of zinc was higher with longer leaching times (> 2 h), there was a partial precipitation of zinc and iron when the pregnant leach solution (PLS) was cooled down overnight. The optimum

leaching time was kept at 2 h since the leaching efficiency of lead reached its peak of 100% and there was no partial precipitation of zinc and iron when the PLS was cooled down.

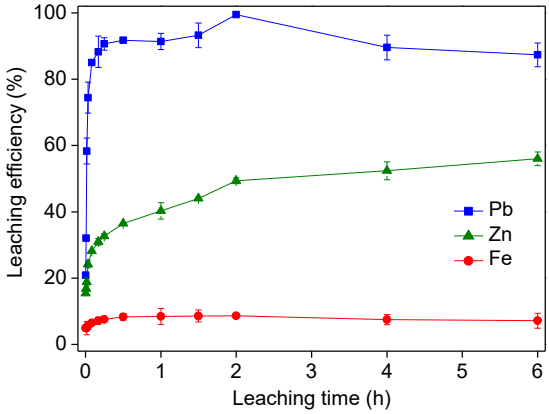


Figure 4.6: Effect of the leaching time on the leaching efficiency $E_L$ (%) of Pb (■), Zn (▲) and Fe (●) from jarosite by pure MSA. Leaching parameters: L/S ratio 20 mL $g^{-1}$, 130 °C, stirring speed 600 rpm.

### 4.3.6 Recovery of MSA by vacuum distillation

To allow the recyclability of the leaching agent, the unreacted MSA in the PLS was recovered by vacuum distillation at a pressure of 0.04 mbar and a vapor temperature of 110 °C. The reduced pressure during distillation was necessary because MSA decomposes (>225 °C) into sulfur dioxide and methanol before boiling at normal atmospheric pressure.[196] Due to the decrease in volume of the solvent, the dissolved metal salts in the PLS precipitated during distillation. The recovery rate of the MSA after leaching and distillation was about 88±2 vol.%, which means that 12±2 vol.% of MSA was not recovered and thus not available for reuse. It must be noted that about 8 vol.% of the total MSA loss is on account of the metal methanesulfonate precipitates and the MSA from the precipitate could be recovered by electrowinning.[128] The mineral phases of the metals in the precipitates are discussed further in this article. The reusability of the distilled MSA was tested by applying it again to leaching of a fresh jarosite sample. The process of leaching and distillation was repeated up to three cycles and the leaching results were compared to that of fresh MSA (Figure 4.7). The metal concentrations in the reused MSA were rather similar to the results of the fresh MSA, indicating that the distilled MSA could be reused

successfully. The leaching efficiency of iron slightly increased with the increasing number of cycles and the leaching efficiency of lead slightly dropped after the third cycle, but these are close to the error margins of the experiment. The distilled MSA was studied with $^{1}$H NMR and FTIR to link the minor difference in the leaching efficiency with possible structural and compositional changes in MSA after each cycle. However, the FTIR and $^{1}$H NMR spectra do not show any difference between the fresh MSA and distilled MSA (Figure 4.8 a,b). The concentration of the impurities was most likely too low to be detected by FTIR and $^{1}$H NMR. The minor difference in leaching efficiency might be due to the formation of a small amount of water and methanesulfonic anhydride impurities during distillation.[197] The presence of water as an impurity could explain the increase in the leaching efficiency of iron since water helps to solvate more iron in the MSA solution. In that case, any formed water and methanesulfonic anhydride impurities can be removed from MSA by equilibrating it with methanesulfonic anhydride for 4 to 6 h at 70 °C and then distilling it under reduced pressure (boiling point = 165 °C at 2 mm Hg).[198]

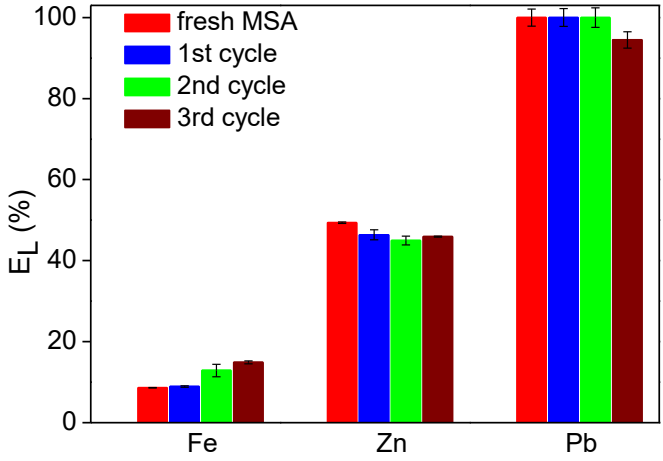


Figure 4.7: Comparative leaching efficiencies of lead, zinc and iron from jarosite by fresh MSA and vacuum-distilled MSA. Leaching parameters: L/S ratio 20 mL g−1, contact time 2 h, 130 °C, stirring speed 600 rpm.

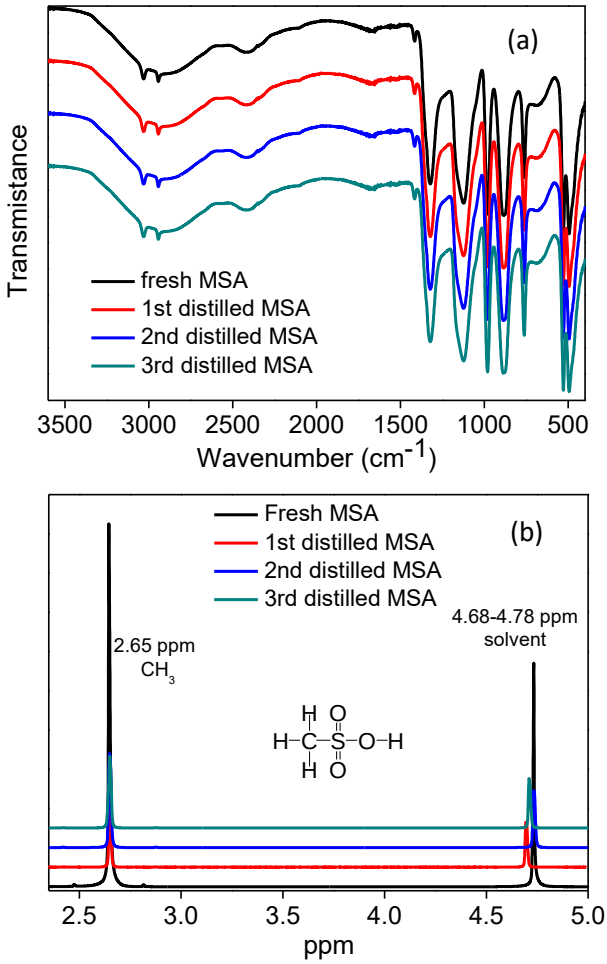


Figure 4.8: (a) FTIR and (b) $^{1}H$ NMR spectra of fresh MSA and distilled MSA in $D_2O$.

### 4.3.7 Solubility studies and characterization of the residues

The difference in solubility of iron, zinc and lead methanesulfonates in pure MSA, was confirmed by studying the dissolution of the elemental form (metallic Fe, Zn and Pb powder) and the oxide forms of iron(III), zinc(II) and lead(II) in pure MSA under the leaching conditions of 60 °C, 2 h, 600 rpm. An excess of the metal powder and the oxides was leached in a constant volume of pure MSA and the concentration of the metals in the MSA was analytically determined and compared to the leaching of jarosite under the same conditions (Table 4.2). Less iron and zinc were leached from the oxides of iron(III) and zinc(II) compared to their corresponding elemental forms and

jarosite, indicating that the oxides are harder to dissolve in pure MSA. High concentration of lead was leached from both lead(II) oxide and elemental lead and it remain dissolved in the pure MSA, which shows its high solubility in pure MSA, and much higher than that of iron and zinc. This is in agreement with the higher solubility of lead compared to iron and zinc when leaching jarosite. Similarly as during the leaching of jarosite, a white precipitate was formed in the experiments with lead(II) oxide and elemental iron, zinc and lead. Most likely, this is because the maximum solubility of the methanesulfonate salts in MSA was exceeded. Unlike iron and zinc, lead was not precipitated from jarosite because it did not reach the maximum solubility in the PLS. It must be stressed that the white precipitate already formed during the leaching at elevated temperatures and not as a result of the cooling of the PLS.

Table 4.2: Solubility of iron, zinc and lead methanesulfonates in pure MSA, from metal oxide, elemental metal and comparison with the leaching of the metals from jarosite using MSA§

| Concentration (mg $L^{-1}$) | Metal oxide | Elemental metal | Jarosite |
|---|---|---|---|
| Fe | 160 | 3000 | 767 |
| Zn | 470 | 3524 | 373 |
| Pb | 50100 | 75668 | 2038 |

§Leaching parameters: 60 °C, 2 h, 600 rpm.

Three solid materials were produced as an output from leaching jarosite using pure MSA, namely, the leaching residue, the white precipitate and the distillation residue. (Figure 4.9) The main mineralogical composition of the leaching residue and distillation residue were analyzed by powder XRD and compared with that of jarosite (Figure 4.10).

XRD measurement was not carried out on the white precipitate because it was hygroscopic. The leaching residue consisted mainly of elemental sulfur and zinc sulfide, which were already present in the jarosite residue. The jarosite mineral and lead sulfate were not present in the leaching residue as they were fully leached. The residue can be sent back to the zinc hydrometallurgical plant and added to their zinc sulfide ore for re-leaching. The distillation residue was mainly composed of lead(II) sulfate ($PbSO_4$) and zinc oxide sulfate ($2ZnO{\cdot}3ZnSO_4$) This was expected as the PLS contained a

significant concentration of sulfate due to the dissolution of jarosite. When MSA was distilled under vacuum, the sulfates precipitated with the metal ions. This lead and zinc-rich precipitates can be of interest for secondary lead and zinc producers.

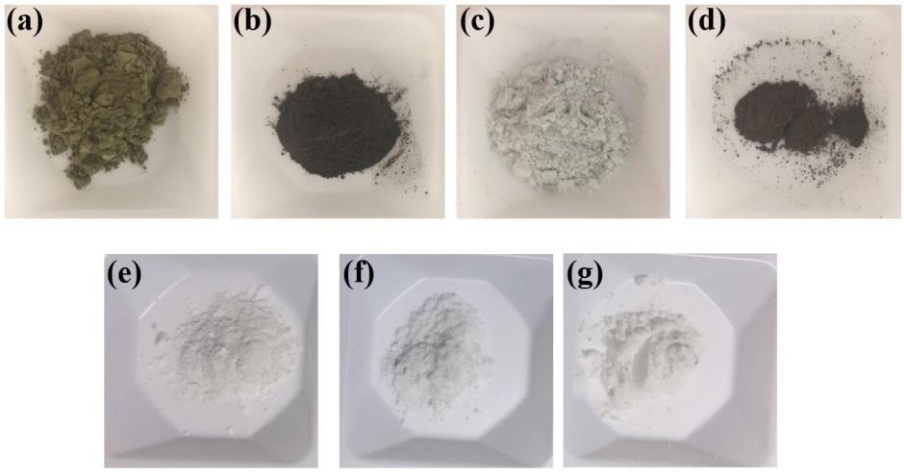


Figure 4.9: Photographs of the starting material (a) jarosite, and (b) leaching residue, (c) white precipitates and (d) distillation residue from MSA leaching of jarosite, and precipitates from MSA leaching of metallic (e) iron, (f) zinc and (g) lead.

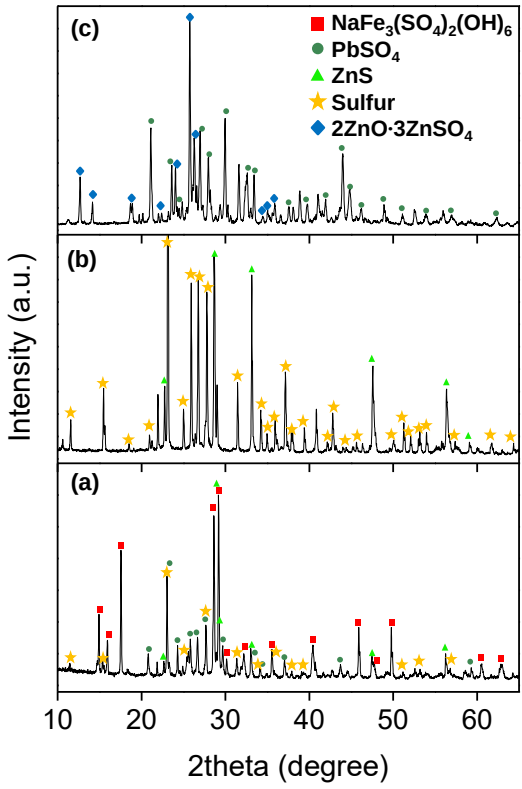


Figure 4.10: XRD pattern of a) jarosite, b) leaching residue and the c) distillation residue.

CHN analysis was carried out on the three solid outputs from the MSA leaching of jarosite, as well as on the synthetic white precipitates formed during the leaching of metallic lead, zinc and iron in pure MSA, as described earlier in the text. The carbon and hydrogen content of the precipitates and the residues were compared with theoretical values of metal methanesulfonate salts (Table 4.3). The composition of the white precipitates formed during MSA leaching of jarosite corresponded well to the theoretical composition of the methanesulfonate salts of iron(II), iron(III) and zinc(II). The presence of iron(II) methanesulfonate salts can be ruled out based on the color of the material: iron(II) methanesulfonate is known to be yellow, whereas the precipitate formed during leaching was white.[199] Since jarosite contains large amounts of sulfate, it is likely that the white precipitate also contains metal sulfate salts. In order to determine the concentration of sulfate in the material, a gravimetric analysis was performed. The precipitate was dissolved in acidic aqueous solution and a

standard solution of 0.5 M $BaCl_2$ was added to it. The amount of sulfate was determined from the amount of $BaSO_4$ precipitated. The analysis result confirmed that the sulfur in sulfate form in the white precipitate was only 0.83 wt.%. This indicates that there was barely any metal sulfate salts in the white precipitates formed during the MSA leaching of jarosite. Therefore, it can be concluded that the white precipitate mostly consists of zinc(II) and iron(III) methanesulfonate.

It was calculated that about 8 mol% of the MSA used for leaching was lost in the white precipitate as metal methanesulfonate salts. Gernon *et al.* described a process to recover pure alkanesulfonic acid (e.g. MSA) from corresponding metal alkanesulfonate salts by electrowinning using an anion-exchange membrane divided cell.[128] Therefore, the MSA in the white precipitate can be recovered by electrowinning and it can be reused in leaching jarosite.

Table 4.3: Percentage of C and H, in the precipitate and residues from MSA leaching of jarosite and metallic iron, zinc and lead.

| Source | Fraction | C (wt. %) | H (wt.%) |
|---|---|---|---|
| Jarosite | Leaching residue | 0.14 | 0.49 |
| | Distillation residue | 0.34 | 1.02 |
| | White precipitate | 9.88 | 3.04 |
| Elemental metals | Fe precipitate | 9.82 | 3.6 |
| | Zn precipitate | 9.46 | 3.45 |
| | Pb precipitate | 5.91 | 1.62 |
| Theoretical values | $Fe(CH_3SO_3)_2$ | 9.75 | 2.44 |
| | $Fe(CH_3SO_3)_3$ | 10.55 | 2.64 |
| | $Zn(CH_3SO_3)_2$ | 9.39 | 2.35 |
| | $Pb(CH_3SO_3)_2$ | 6.04 | 1.51 |

### 4.3.8 Upscaling

The MSA leaching of jarosite at optimal conditions was tested on a larger scale (Figure 4.11). First, the leaching was performed in a 500 mL round-

bottom flask with 10 g jarosite and 200 mL of MSA, which corresponds to 100 times upscaling compared to the screening experiments described above. Next, the leaching was tested in a 1 L temperature-controlled leaching reactor (Figure 4.12) with overhead stirring and automatic filtration starting from 25 g of jarosite and 500 mL of MSA, which corresponds to 250 times upscaling compared to the screening experiments. The results show that the leaching efficiency of lead, zinc and iron using the two larger set-ups corresponds well to the results of the initial small-scale experiments (Figure 4.11). Hence, the MSA leaching of jarosite is stable and shows potential for upscaling to a larger scale. The selectivity S towards lead or zinc over iron in the PLS also significantly improved after leaching jarosite with pure MSA. Iron is the main component of jarosite with a concentration much higher than that of lead and zinc. After leaching with pure MSA, the lead concentration in the PLS surpassed the iron concentration (S ≈9). Furthermore, although zinc was still less concentrated than iron, the difference decreased compared to the original concentration in the jarosite, leading to an enrichment of zinc in the PLS (S ≈5). Finally, a conceptual flowsheet of the leaching of jarosite by MSA and subsequent recovery of the MSA by vacuum distillation is shown in Figure 4.13.

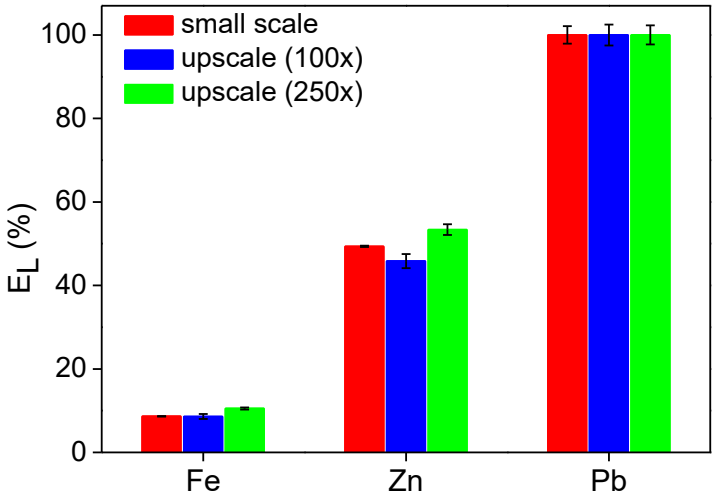


Figure 4.11: Comparative leaching efficiencies of lead, zinc and iron from jarosite by pure MSA at small scale (red) and at a larger scale in a roundbottom flask (blue) and in leaching reactor (green). Leaching parameters: L/S ratio 20 mL $g^{-1}$, contact time 2 h, 130 °C, stirring speed 600 rpm.

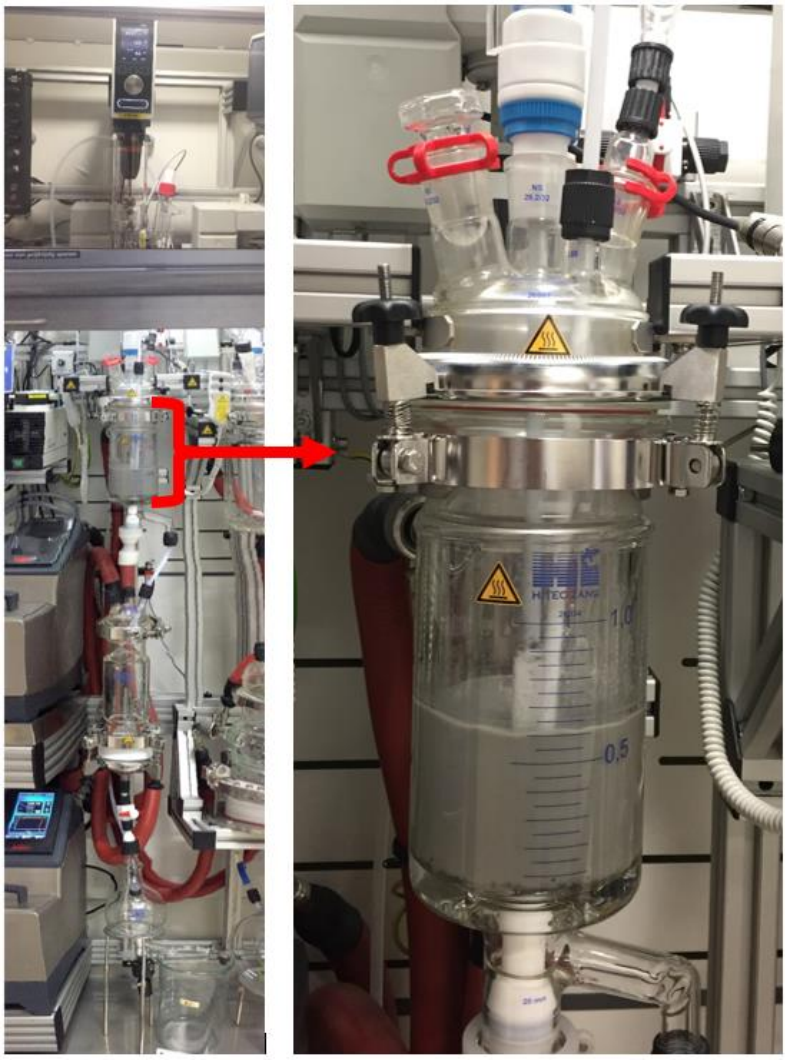

Figure 4.12: 1 L temperature-controlled leaching reactor used for upscaling MSA leaching of jarosite.

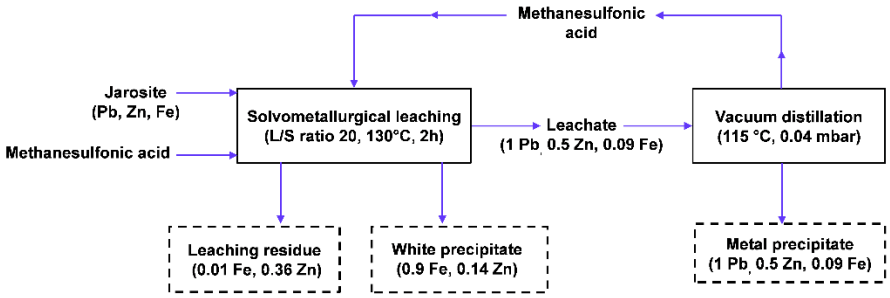


Figure 4.13: Flow chart for the selective leaching of lead and zinc from jarosite by pure MSA. The numbers denote the ratio of extracted metal to the metals in the initial jarosite sample.

## 4.4 Conclusions

Methanesulfonic acid (MSA) is a promising leaching agent for recovering metals from iron-rich jarosite residue. MSA reacts readily with lead, zinc and iron present in the jarosite due to its high acid strength. However, iron and zinc have a low solubility in pure MSA, resulting in a precipitation of the two metals (90% Fe, 14% Zn) as their methanesulfonate salts. The presence of ≥10 vol% of water in the MSA solution avoided these precipitate formations, as the high hydration energy of the metal ions kept them well-solvated in the aqueous MSA solution. Lead, on the contrary, has a significantly higher solubility in pure MSA than iron and zinc. As a result, lead did not precipitate along with iron and zinc. This difference in solubility of the metals in pure MSA resulted in solid-liquid separation of lead and zinc from iron. The pregnant leach solution (PLS) obtained after carrying out the optimized leaching procedure contained 100% of the lead, 50% of the zinc and 9% of the iron from the original jarosite residue. The leaching residue contained only zinc since both lead and iron were fully leached either in the PLS or the precipitate. A conceptual flowsheet was designed, which was tested in a 1L leaching reactor. The MSA in the PLS was recovered by vacuum distillation and successfully reused up to three cycles, resulting in a minimization of the consumption of chemicals by the process.

# Chapter 5: Antimony recovery from lead-rich dross of lead smelter and conversion into antimony oxide chloride ($Sb_4O_5Cl_2$)

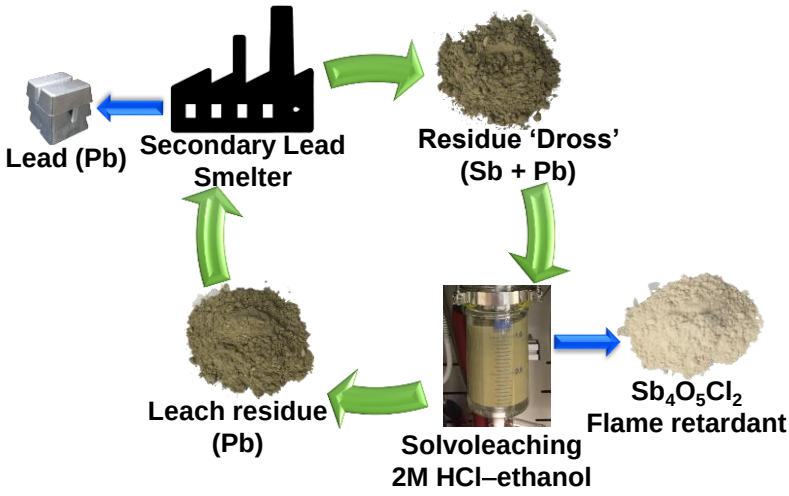


This chapter is based on the published paper:

**Palden, T**.; Machiels, L.; Regadío, M.; Binnemans, K. Antimony recovery from lead-rich dross of lead smelter and conversion into antimony oxide chloride ($Sb_4O_5Cl_2$). *ACS Sustain. Chem. Eng.* **2021**, 9, 5074–5084. https://doi.org/10.1021/acssuschemeng.0c09073.

The text may contain slight adjustments compared to the original publication.

*Author contributions:*

K.B. and T.P. conceived the original research idea. T.P. designed and executed the experiments, treated the data, drew the conclusions, and wrote the article. K.B. and L.M. contributed to the discussion of the results. All authors helped in the correction of the manuscript.

## Abstract

Antimony was selectively leached from a lead-rich industrial process residue called 'dross', and recovered as an antimony oxide chloride ($Sb_4O_5Cl_2$), which can be used as a component in flame retardants or as an anode material in aqueous chloride batteries. The dross is a residue generated by a lead smelter and it contained about 30 wt% of lead and about the same concentration of antimony, along with some minor metals such as zinc, iron and tin. Solutions of hydrochloric acid dissolved in organic solvents such as ethanol, 1-octanol, ethylene glycol and Aliquat 336 chloride were compared for selective leaching of antimony. All investigated lixiviants leached comparable amounts of antimony (60–76%), but the lowest co-dissolution of lead (~0.1%) was achieved by hydrochloric acid in ethanol or in 1-octanol. Only ethanol was chosen for further investigation since it is significantly cheaper than 1-octanol. Moreover, ethanol is classified as an environmentally preferable green solvent. Hydrochloric acid in ethanol leached much less lead than using water, and the former also required lower chloride concentration to get high leaching yields of antimony. Leaching under optimized conditions was successfully upscaled in a 1 L batch leaching reactor, achieving an antimony leaching efficiency of 90% (28000 mg $L^{-1}$) and a lead leaching efficiency of only 0.4% (100 mg $L^{-1}$). The dissolved antimony in the pregnant leach solution (PLS) was fully recovered by hydrolysis precipitation whereby high-purity antimony oxide chloride ($Sb_4O_5Cl_2$) was obtained, by adding to the PLS an equivalent volume of water. The ethanol in the remaining PLS was distilled to be reused for more leaching. The valorization of an industrial process residue and the use of ethanol contribute to the sustainability and the greenness of the process.

Keywords: critical raw materials; green solvents; industrial process residues; recycling; solvometallurgy

## 5.1 Introduction

Lead-acid (LA) batteries for use in cars are one of the main applications of lead. Lead in such batteries contains significant amounts of antimony to harden the lead.[47] End-of-life LA batteries have high collection and recycling rates and, the lead in these spent batteries is typically recycled via pyrometallurgical processes.[49] Lead recycling companies (secondary lead smelters) produce pure lead from LA batteries and other lead-containing waste materials via a melting–drossing–refining process.[47,49,200] In this process, lead alloys in the spent LA battery and other waste materials are first melted in a furnace (e.g. rotary furnaces or Isasmelt furnaces) to reduce lead oxide to metals. The metallic lead bullion coming from the furnace is further purified by a drossing process, where the molten lead is cooled down, and the remaining oxidized impurities called '*dross*' are formed on the surface. The dross is then skimmed off from the surface, and the lead is then further refined by a thermal or electro-refining process. The dross contains large amounts of lead, but also the antimony present in the LA batteries reports to the dross. Given the fact that antimony is considered as a critical raw material, dross could be a valuable secondary antimony source.[47] At present, the drosses are used in reduction processes to create antimonial lead. Since the use is expected to decrease, there is a risk for this material to become obsolete in the future. The challenge is to develop an efficient and sustainable process for the separation of antimony from the dross, so that the rest of the residue could be further processed for lead recovery.

In recent years, considerably research activities have been devoted to the recovery of lead from industrial process residues by hydrometallurgical and solvometallurgical methods.[45,62,87,122,201–203] Solvometallurgy is a new branch of extractive metallurgy that uses non-aqueous solvents instead of aqueous solutions.[7] Much less research attention has been paid to the recovery of antimony from industrial process residue.[47] At this moment, mainly pyrometallurgical processes[64,204–208] are used for recovering antimony from ores or residues, but hydrometallurgical processes are gaining more attention. The two main hydrometallurgical processing routes for antimony recovery are alkaline sulfide leaching[200,58,209–212] and acidic chloride leaching systems,[200,58,213–215] which are both followed by electrowinning step to obtain pure antimony metal. The alkaline sulfide leaching system has been implemented in industry, but it generates waste products which are difficult to dispose ($Na_2SO_4$ and $Na_2S_2O_3$).[59]

Studies have shown that chloride-based solvometallurgical lixiviants improved the leaching efficiency and/or selectivity compared to the chloride-based aqueous lixiviant.[45,88,123,124] Özdemir *et al.* found that hydrochloric acid−ethanol solutions (HCl−EtOH) or hydrochloric acid−ethanol−water (HCl−EtOH−$H_2O$) solutions were better solvents than hydrochloric acid−water (HCl−$H_2O$) solution in the decomposition of scheelite.[123] Kopkova *et al.* developed a promising system of *n*-octanol equilibrated with HCl to chemically attack resistant ores such as titanomagnetite.[124] Similarly, Palden *et al*. have shown that basic extractants such as [C101][Cl] and [A336][Cl] combined with HCl can selectively leach lead from iron-rich jarosite residue.[45] These studies found that complete or partial replacement of water by organic solvents changes, firstly, the reactivity of the lixiviant towards solid metal phases and secondly, the solubility of the resulting dissolved metal complexes. As a result, solvometallurgy promotes or prevents the formation of soluble metal compounds, which subsequently affects the leaching efficiency and selectivity of different metals.

In this paper, we describe a novel solvometallurgical process to selectively recover antimony from lead-rich dross using lixiviants based on hydrochloric acid dissolved in an organic solvent. By replacing the aqueous phase by organic solvents, it is possible to attain higher reactivity and selectivity.[7] Moreover, inclusion of an organic solvent in the lixiviant increases the chloride ion activity, which could mitigate the requirement of high chloride concentrations to achieve maximum antimony leaching. Antimony is recovered as an oxide chloride ($Sb_4O_5Cl_2$), which can be used as a component in flame retardants.[216] $Sb_4O_5Cl_2$ is shown to have excellent flame retardant properties when used in conjunction with a halogenated organic compound.[217,218] It reduces the dosage of the coloring matter and improves the transparency of plastic products compared with other flame retardants such as antimony oxide ($Sb_2O_3$) and sodium antimonate ($NaSb(OH)_6$). $Sb_4O_5Cl_2$ could also find applications as anode material in lithium-ion batteries or aqueous chloride batteries.[219–221]

## 5.2 Experimental

### 5.2.1 Chemicals

Two dross samples (labelled dross1 and dross2) were kindly provided by a European lead recycler. Hydrochloric acid (37 wt% HCl in water) and boric acid (99.5%, $H_3BO_4$ in water) were purchased from VWR Chemicals (Leuven, Belgium). Nitric acid (65 wt% $HNO_3$ in water) and rhodium standard aqueous

solutions (1000 mg $L^{-1}$) were purchased from Chem-Lab NV (Zedelgem, Belgium). Hydrofluoric acid (48 wt%, HF in water) and Aliquat® 336 (trialkylmethylammonium chloride-based commercial mixture with trioctylmethylammonium chloride as the main component, 88.2–90.6%) were purchased from Sigma-Aldrich (Diegem, Belgium). Absolute ethanol (99.8 wt%), ethylene glycol (99.5 wt%), 1-octanol (99 wt%), potassium carbonate (>99 wt%, anhydrous) and sodium sulfide (>90 wt%) were obtained from Fisher Scientific (Geel, Belgium). All chemicals were used as received without any further purification.

### 5.2.2 Instrumentation

The drosses were ground and sieved using a mortar grinder (Pulverisette 2, Fritsch, Germany) and a vibratory sieve shaker (Analysette 3, Fritsch,Germany). The materials were digested using a microwave digester (Mars 6, CEM, USA). The metal content in solution was measured by inductively coupled plasma optical emission spectroscopy (ICP−OES, Optima 8300, Perkin Elmer, USA) from PerkinElmer. The mineral phases in the solid materials were identified by powder X−ray diffraction (XRD) analysis using a Bruker D2 Phaser diffractometer (Bruker, USA). Diffractograms were recorded in the measurement range of 10 – 80° 2θ using $CuK_{\alpha}$ radiation and applying an acceleration voltage of 45 kV, a current of 30 mA, a step size of 0.020° and a counting time of 2.5 s per step. The morphology and elemental composition of the solid materials were analyzed by scanning electron microscopy (SEM, XL-30 FEG, Phillips, Netherlands) and energy-dispersive X-ray spectroscopy (EDS; Octane elite super silicon drift detector, Ametek EDAX, Netherlands). The powder sample was coated with a 5 nm platinum layer to avoid charging issues related to insulating samples. The leaching was carried out on a RCT classic heating plate (IKA, Germany). The phase disengagement between the solid and liquid after leaching was carried out by centrifugation using a Heraeus Labofuge 200 (Thermo Scientific, US) for <10 mL and Eppendorf centrifuge 5804 (Eppendorf, Belgium) for >10 mL of liquid volume. The scalability of the leaching at optimized conditions was studied using a customized 1 L jacketed laboratory reactor, linked to an automatic filtration unit (LabKit 36167) constructed by HiTec Zang GmbH (Herzogenrath, Germany).

### 5.2.3 Methodology

All the experiments hereon were carried out in duplicates and relative standard deviations were within ± 5%. The drosses (as received) were dried in an oven at 110 °C for 24 h to remove any trace of moisture. The materials were ground using a mortar grinder and sieved below 250 µm in particle size using a vibratory sieve shaker. The metal content of the materials was determined after fully dissolving 100 mg of the milled sample in an acid mixture of 7 mL of 37 wt% HCl, 2 mL of 65 wt% $HNO_3$ and 1mL of 48 wt% HF using microwave−assisted acid digestion. The samples were digested using a one stage program where the samples were heated from room temperature to 180 °C in 5.5 min and held for 9.5 min at 1000 W. After the digestion, the excess HF was rendered safe by complexation with 10 mL of 4 wt% of $H_3BO_3$ in the microwave digester where the samples were heated up to 170 °C in 15 min and held for 10 min. After the HF complexation, the digestion vessels were cooled and the digested solutions were transferred to volumetric flasks and filled up to 100 mL with ultrapure water for analysis. The sample dissolution via microwave digestion was done in triplicate to check the reproducibility of the composition. The metal concentrations in each of the digested acid solution was measured by ICP-OES with ±5% of error associated with the measurements.

The lixiviants 2 mol $L^{-1}$ HCl in ethanol, ethylene glycol and 1-octanol were prepared by mixing 37 wt% HCl in each alcohol with a volume ratio of 1:5 followed by stirring at room temperature for 10 min at 600 rpm. The lixiviant Aliquat 336 was equilibrated with aqueous 37 wt% HCl solution by mixing both in a volume phase ratio of 1:1, and stirring the biphasic mixture for 1 h at 2000 rpm in a glass vial in a laboratory shaker. The intensive shaking for 1 h at 2000 rpm was done to ensure that equilibration is reached. After the equilibration, the separation between the organic and aqueous phases was accelerated by centrifugation at 4000 rpm for 20 min in an Eppendorf centrifuge 5804. The organic and aqueous phases were taken out separately with a micropipette and kept in different vials.

The initial leaching experiments were carried out by adding 200 mg of dross and 2 mL of lixiviant solution in a 4 mL glass vial and magnetically stirred on a heating plate using a heating block. The following leaching conditions were applied: a liquid−to−solid ratio (L/S) of 10 mL $g^{-1}$, a temperature of 50 °C, a contact time of 2 h and a stirring speed of 800 rpm. The upscaling of the leaching system was tested for 1 L of lixiviant solution in a 1 L temperature-

controlled leaching reactor with overhead stirring and automatic filtration, at room temperature and 300 rpm.

The *pregnant leach solution* (PLS) obtained after leaching the dross was separated from the solid residue through centrifugation (5300 rpm, 10 min). The finer particles suspended in the PLS were further separated by a syringe filter made of a polyester membrane (Chromafil PET, 0.45 µm pore size). The metal concentration in the PLS was measured using ICP−OES and the *leaching efficiency* $E_L$ *(%),* was calculated according to equation (5.1):

$$E_L(\%) = \frac{c_M \times v_{LIX}}{m_I \times c_I} \times 100 \quad (5.1)$$

where $c_M$ is the metal concentration in the PLS after leaching (mg $L^{-1}$), $v_{LIX}$ is the volume of leaching agent used for leaching (L), $m_I$ is the mass of the solid material used for leaching (kg), and $c_I$ is the concentration of the metal in the dross before leaching (mg $kg^{-1}$).

The dissolved metals in the PLS were recovered by precipitation using potassium carbonate, sodium sulfide and water. The PLS was separated from precipitate through centrifugation (5300 rpm, 10 min) and filtration (Chromafil PET, 0.45 µm pore size). The *precipitation efficiency* $E_P$ (%) was calculated by mass balance according to the equation (5.2):

$$E_P(\%) = 100 - \left(\frac{c_P}{c_M} \times 100\right) \quad (5.2)$$

where $c_P$ is the concentration of metals in PLS after precipitation (mg $L^{-1}$) and $c_M$ is the concentration of metals in PLS before precipitation (mg $L^{-1}$).

The leaching residue and precipitates were dried in an oven (110 °C for 24 h) for later characterization. After recovering the metals by precipitation using water, the ethanol in the PLS was regenerated by distillation using rotary evaporator at 130 mbar and 55 °C.

## 5.3 Results and discussion

### 5.3.1 Characterization of drosses

Two drosses (dross1 and dross2) were characterized after drying and milling into a fine powder (Figure 5.1). The elemental composition of the two drosses was similar, containing about 30 wt% of lead and 30 wt% of antimony (Table 5.1). Other metals such as zinc, iron, tin, silicon and aluminium were present in minor amount (10−13 wt%). The mineralogy of these metals in the two dross samples was slightly different (Figure 5.2). Both drosses contained bindheimite ($2PbO{\cdot}Sb_2O_5$) and valentinite ($Sb_2O_3$). Additionally, dross1 also contained lead antimony oxide ($PbO{\cdot}Sb_2O_3$) and magnesium/zinc antimony oxide ($Mg/ZnO{\cdot}Sb_2O_3$) whereas dross2 contained lead silicate hydrate ($PbSi_2O_5{\cdot}1.6H_2O$) and elemental lead (Pb). The phases of the other metals were not detected in the XRD pattern, most likely because of their low concentration in the sample, which resulted in no or very little X-ray diffraction. Within the performed experiments, only the data for lead and antimony were compared and further discussed. The data for minor metals such as zinc, iron and tin were presented but not discussed, in order to avoid complications in discussing a very large array of data.

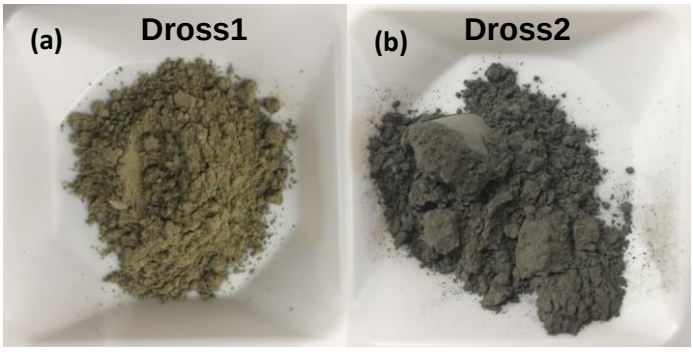


Figure 5.1: Photograph of dried and milled (a) dross1 and (b) dross2.

Table 5.1: Elemental composition of dross1 and dross2

| Metal | Dross1 (wt%) | Dross2 (wt%) |
|---|---|---|
| Sb | 31.50 ± 1.67 | 29.23 ± 0.58 |
| Pb | 28.12 ± 1.91 | 27.37 ± 0.61 |
| Zn | 5.29 ± 0.37 | 1.74 ± 0.06 |
| Fe | 2.14 ± 0.08 | 0.98 ± 0.05 |
| Sn | 1.14 ± 0.06 | 5.25 ± 0.12 |
| Mg | 1.69 ± 0.06 | 0.48 ± 0.02 |
| Si | 1.28 ± 0.03 | 1.42 ± 0.03 |
| As | 0.67 ± 0.02 | 0.54 ± 0.02 |
| Al | 0.43 ± 0.02 | 1.40 ± 0.07 |
| Ni | 0.054 ± 0.003 | 0.00 ± 0.00 |
| Cr | 0.033 ± 0.002 | 0.125 ± 0.006 |

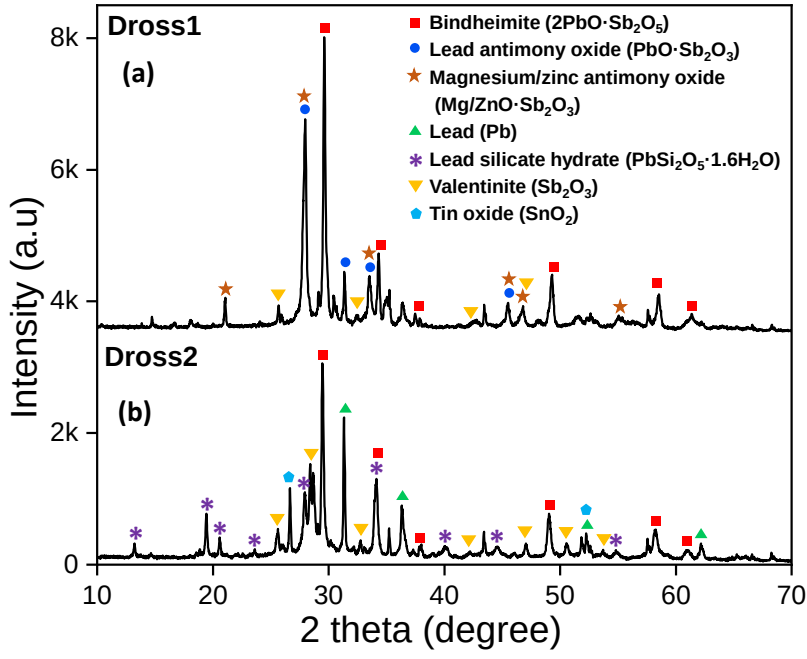


Figure 5.2: XRD pattern of (a) dross1 and (b) dross2.

### 5.3.2 Evaluation of solvometallurgical lixiviants

Different chloride-based solvometallurgical lixiviants were compared in order to determine their suitability for the selective leaching of antimony from the two drosses. The tested lixiviants were mostly alcohols containing dissolved hydrochloric acid: 2 mol $L^{-1}$ hydrochloric acid dissolved in ethanol, 1-octanol and ethylene glycol, and Aliquat 336 ([A336][Cl]) equilibrated by 12 mol $L^{-1}$ hydrochloric acid. The ideal lixiviant should allow for a high recovery of antimony and a limited co-dissolution of lead. All tested lixiviants showed high leaching efficiency of antimony (60−76%) from the drosses but the leaching efficiency of lead varied between the lixiviants (Figure 5.3 a-b). The lowest co-dissolution of lead was achieved using 2 mol $L^{-1}$ hydrochloric acid in ethanol and 1-octanol, while both lixiviant leached less than 0.1% of lead, making it highly selective against lead. The low dissolution of lead in ethanol and 1-octanol is because these molecular solvents are not very polar and are, therefore, not solvating the produced lead(II) chloro complexes, which most likely resulted in a precipitation of lead(II) chloride ($PbCl_2$). The higher leaching efficiency of lead in ethylene glycol than in ethanol or 1-octanol is due to the presence of two hydroxyl functional groups per molecule which can coordinate bidentately to lead(II) ions, thereby, keeping them dissolved in the leachate.[121] The high leaching efficiency of lead in Aliquat 336 equilibrated by 12 mol $L^{-1}$ is because quaternary ammonium cations can more easily accommodate anionic species such as $[PbCl_4]^{2-}$ than molecular solvents such as ethanol and 1-octanol. The best lixiviant candidates were 2 mol $L^{-1}$ hydrochloric acid in ethanol and 1-octanol, due their low co-dissolution of lead compared to the other lixiviants. Only ethanol was chosen for further investigation since it is much cheaper than 1-octanol. Moreover, ethanol is classified as an environmentally preferable green solvent because it is available by fermenting renewable sources such as sugars, starches, and lignocellulosics.[222] Dross 1 will be chosen as starting point for further experiments, and at the end, both dross 1 and dross 2 will be tested in the optimized leaching system.

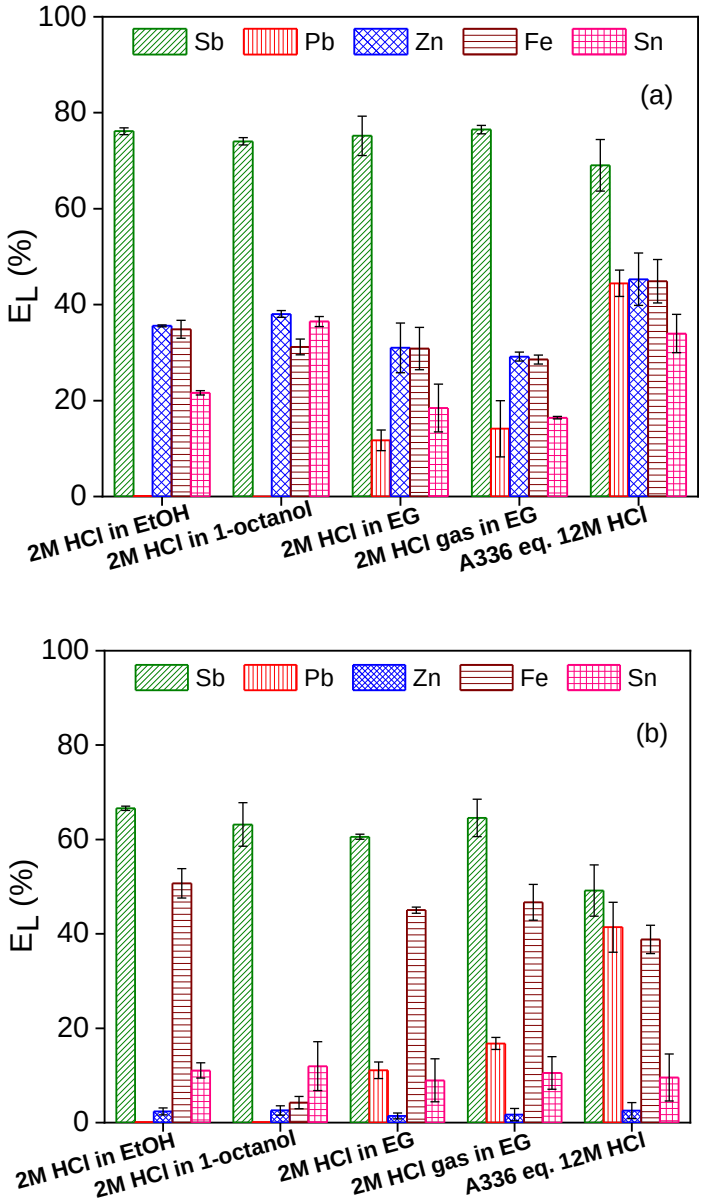


Figure 5.3: Leaching efficiency ($E_L$ %) of antimony, lead, zinc, iron and tin by various lixiviants from (a) dross1 and, (b) dross2. Leaching parameters: L/S ratio 10 mL $g^{-1}$, leaching time 2 h, temperature 50 °C, stirring speed 800 rpm. (A336 = Aliquat 336 and EG = ethylene glycol)

### 5.3.3 Comparison of the solvo- and hydro-metallurgical leaching routes

The leaching of dross by HCl dissolved in ethanol was compared to that of HCl in water (Figure 5.4). At low HCl concentrations (≤ 2 mol $L^{-1}$), antimony leaching was higher in ethanol than in water. For instance, the antimony leaching efficiency at 0.5 mol $L^{-1}$ HCl in ethanol and water were 21% and 0.3%, respectively. The better leaching of antimony at dilute HCl in ethanol than in water is most likely due to higher chloride ion activity in ethanol than water (Figure 5.4). Jana *et al.* also found that metal (Cu, Ni, Co, Mn and Fe) recoveries were considerably improved if appropriate amounts of methanol or ethanol were incorporated in dilute HCl solution in water.[88] The addition of certain organic reagents such as ethanol in an aqueous chloride solution sharply increases the chloride ion activity, thereby, promotes the chloro-complex formation with metals. In fact, the chloride ion activity increases more by incorporating higher alcohols, which would further reduce the requirement of HCl to leach similar amount of metals.[88] However, high cost and viscosity of higher alcohols such as 1-octanol need to be taken into account before using them in a commercial process.

The maximum antimony leaching efficiency in ethanol was 76%, using ≥2 mol $L^{-1}$ HCl and the antimony leaching efficiency at the same HCl concentration in water was 15%. Therefore, the advantage of using ethanol over water is evident from the fact that a lower chloride concentration was sufficient to achieve high antimony leaching efficiency, which could reduce the corrosion problems associated with the chloride-based hydrometallurgical leaching of antimony. Another important difference between using ethanol and water was in the leaching efficiency of lead. At the maximum antimony leaching of 76% using 2 mol $L^{-1}$ HCl in ethanol, the lead leaching was 0.1% (30 mg $L^{-1}$), whereas the lead leaching was 8% (2144 mg $L^{-1}$) using 4 mol $L^{-1}$ HCl in water where maximum antimony leaching of 85% was achieved. The higher leaching of lead using water is due to the higher solvating power of water than that of ethanol, which enables high solubility of lead(II)-chloro complexes in water. The lead leaching efficiency in water increased sharply after >6 mol $L^{-1}$ HCl, where lead leaching efficiency of 90% was obtained at 12 mol $L^{-1}$ HCl in water. The significant difference in lead leaching efficiency between low and high chloride concentrations in water is because lead(II) ion forms insoluble $PbCl_2$ at low chloride concentrations, while it forms the soluble $[PbCl_4]^{2-}$ complex in concentrated chloride solutions in water.[45] Therefore, the main advantage of using ethanol over water in chloride-based leaching of lead-rich dross is two-fold: (1) lower chloride concentration is

required to leach similar amounts of antimony and (2) the organic solvent is highly selective for antimony with barely any co-dissolution of lead.

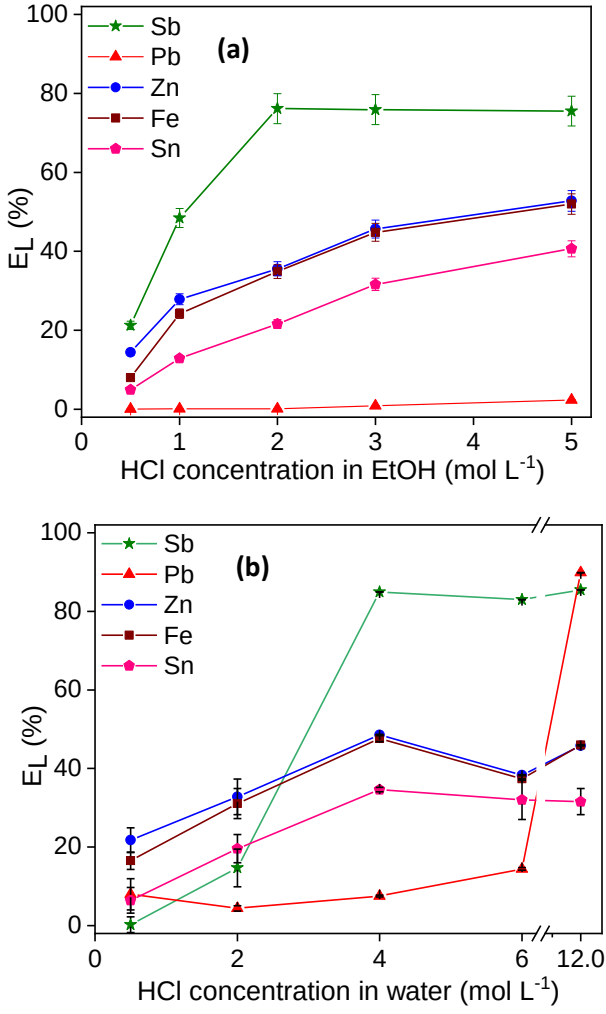


Figure 5.4: Leaching efficiency ($E_L$%) of antimony, lead, zinc, iron and tin from dross1 by using varying HCl concentration in (a) water and, (b) ethanol. Leaching parameters: L/S ratio 10 mL $g^{-1}$, leaching time 2 h, temperature 50 °C, stirring speed 800 rpm.

The effect of water content in 2 mol $L^{-1}$ HCl in ethanol was studied (Figure 5.5). The antimony leaching remains more or less the same at low water content (<40 vol%) but it decreased sharply with further increasing the water content. The decrease in the antimony leaching efficiency is most likely due to the hydrolysis and precipitation of antimony as antimony(III) oxychloride (SbOCl) from antimony(III) chloride solution.[58] The lead leaching efficiency increased slowly from 0.1% to 4% when water content was increased from 16 vol% to 100 vol%, which is due to the higher solubility of lead in water than in ethanol.

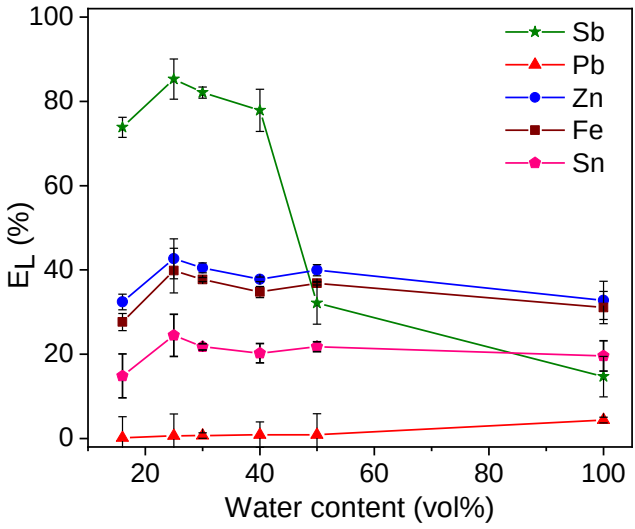


Figure 5.5: Effect of water content in leaching efficiency ($E_L$ %) of antimony, lead, zinc, iron and tin from dross1 by using 2 mol $L^{-1}$ HCl in ethanol. Leaching parameters: L/S ratio 10 mL $g^{-1}$, leaching time 2 h, temperature 50 °C, stirring speed 800 rpm.

### 5.3.4 Optimization of solvoleaching parameters

The effect of the temperature, liquid-to-solid (L/S) ratio and the leaching time on the leaching of dross1 with 2 mol $L^{-1}$ HCl in ethanol was studied by varying the temperature from 25 to 70 °C, L/S ratio from 5 to 40 mL $g^{-1}$ and the leaching time from 5 min to 96 h. Temperature has minimal effect on the leaching efficiency of lead and antimony (Figure 5.6). The antimony leaching efficiency increased with increasing temperature but at a slow rate. The leaching efficiency of antimony increased from 53 to 75% when the L/S ratio

was increased from 5 to 10 mL $g^{-1}$ (Figure 5.7 a). Further increase in the L/S ratio did not change the leaching efficiency of antimony, while the leaching efficiency of lead remained low (0.1 to 0.8%) with increase in the L/S ratio. The leaching kinetics of antimony from dross1 was fast since 57% of the antimony was leached within 5 min (Figure 5.7 b). With increasing leaching time, the leaching efficiency of antimony continually increased at a fast rate up to 6 h, when 80% of antimony was leached. When the leaching time was further increased, the leaching efficiency of antimony increased at much slower rate, with 88% leaching yield after 96 h. The leaching time did not have any effect on the leaching efficiency of lead. The difficulty of increasing the antimony leaching efficiency above 80% could be due to the stability of some antimony mineral phases, which do not dissolve by the lixiviant. The optimum leaching conditions were chosen to be temperature: 25 °C, L/S ratio 10 mL $g^{-1}$, and leaching time 6 h, at which about 80% of antimony and about 0.3% of lead were leached. Higher temperature and longer leaching time resulted in higher leaching efficiency of antimony, but the increase was too incremental to justify the increased cost of using such conditions.

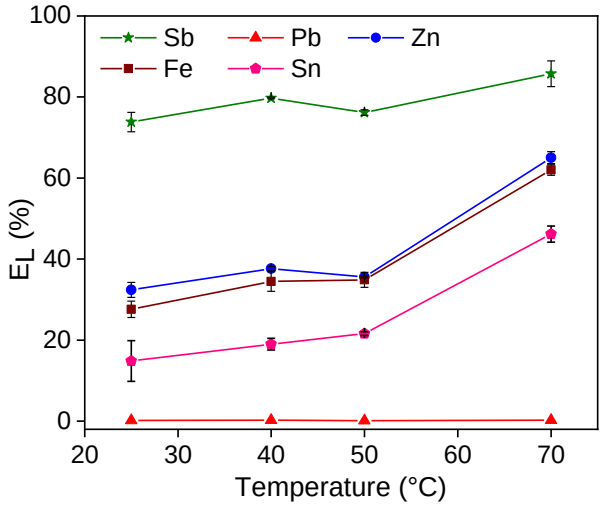


Figure 5.6: Effect of (a) temperature on the leaching efficiency ($E_L$ %) of antimony, lead, zinc, iron and tin from dross1 by using 2 mol $L^{-1}$ HCl in ethanol. Stirring speed 800 rpm.

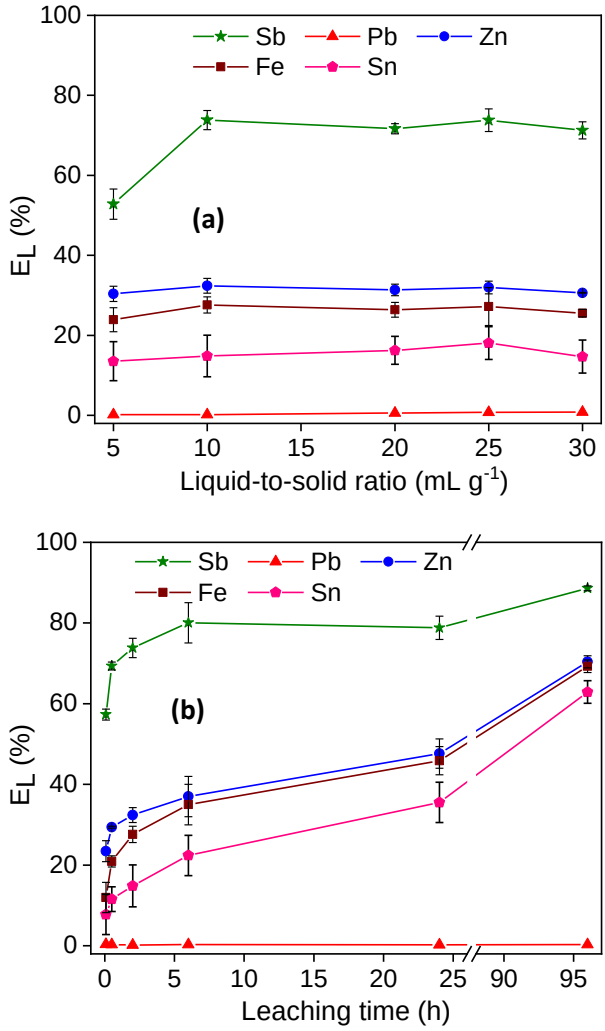


Figure 5.7: Effect of (a) liquid-to-solid ratio and (b) leaching time, on the leaching efficiency ($E_L$ %) of antimony, lead, zinc, iron and tin from dross1 by using 2 mol $L^{-1}$ HCl in ethanol. Stirring speed 800 rpm.

### 5.3.5 Upscaling and characterization of leaching residues

The leaching of both dross1 and dross2 at optimal conditions was tested on a larger scale in a 1 L temperature-controlled leaching reactor (Figure 4.12) with overhead stirring and automatic filtration starting from 100 g of a solid residue and 1 L of 2 mol $L^{-1}$ HCl in ethanol, which corresponded to upscaling by a factor of 500 compared to the screening experiments. The upscaling

resulted in improvement of the antimony leaching efficiency of dross1 from 80 to 90%, while maintaining a low co-dissolution of lead (Table 5.2). Similarly, the leaching efficiency of antimony from dross2 was high, despite the optimization of leaching parameters was not done on this sample. Hence, the leaching of drosses by hydrochloric acid in ethanol was reproducible and showed potential for upscaling to a larger scale.

Table 5.2: Leaching efficiency ($E_L$ %) and concentration (mg $L^{-1}$) of antimony, lead, zinc, iron and tin after scaled up leaching of dross1 and dross2 in a temperature-controlled batch reactor using 2 mol $L^{-1}$ HCl in ethanol.

| | Sb | | Pb | | Zn | | Fe | | Sn | |
|---|---|---|---|---|---|---|---|---|---|---|
| | % | mg $L^{-1}$ | % | mg $L^{-1}$ | % | mg $L^{-1}$ | % | mg $L^{-1}$ | % | mg $L^{-1}$ |
| Dross1 | 90 | 28000 | 0.4 | 100 | 40 | 2050 | 38 | 800 | 20 | 400 |
| Dross2 | 80 | 23000 | 0.5 | 130 | 5 | 90 | 57 | 560 | 11 | 561 |

Leaching parameters: L/S ratio 10 mL $g^{-1}$, leaching time 6 h, temperature 25 °C, stirring speed 300 rpm

The main mineralogical compositions of the leaching residues of dross1 and dross2 (Figure 5.8) were compared with that of fresh residues (Figure 5.2). The minerals such as lead(II) antimony (III) oxide ($PbO{\cdot}Sb_2O_3$), magnesium/zinc antimony(III) oxide ($Mg/ZnO{\cdot}Sb_2O_3$) and lead(II) silicate hydrate ($PbSi_2O_5{\cdot}1.6H_2O$) were completely dissolved by the lixiviant solution since these were not present in the leach residue. Bindheimite ($2PbO{\cdot}Sb_2O_5$) and valentinite ($Sb_2O_3$) were still present in the leach residues, indicating that the minerals were either only partially leached or not leached at all in the lixiviant. Bindheimite ($2PbO{\cdot}Sb_2O_5$) is a mixture of lead(II) oxide and antimony(V) oxide. The fact that antimony(V)-containing bindheimite was not leached whereas its counterpart antimony(III)-containing lead antimony oxide was leached shows that pentavalent lead antimony(V) oxide is more stable than the trivalent lead antimony(III) oxide in the chloride-based lixiviant. Cotunnite ($PbCl_2$) was present in both leach residues of the dross1 and dross2 which shows that the dissolved lead was precipitated as lead(II) chloride due to the poor solubility of lead(II)-chloro complexes in ethanol (Figure 5.8).

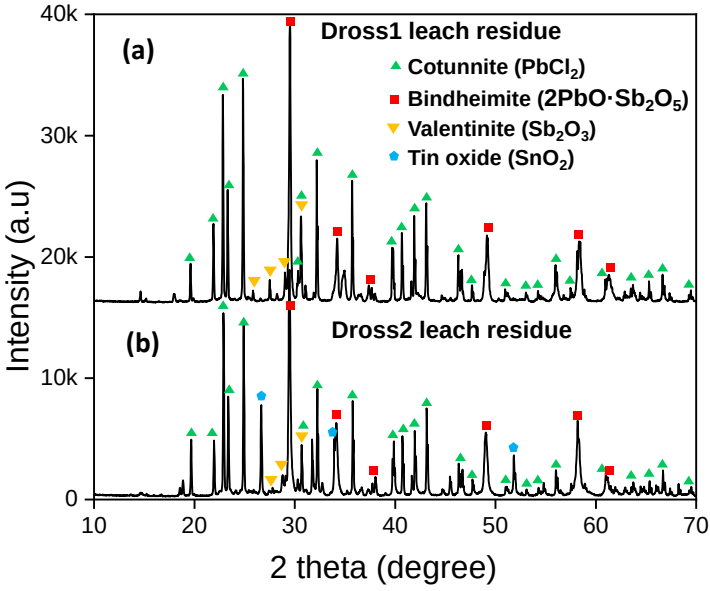


Figure 5.8: XRD pattern of the leach residues of (a) dross1 and (b) dross2.

### 5.3.6 Metal recovery from pregnant leach solution

The pregnant leach solution (PLS) after leaching dross1 in the 1L reactor using 2 mol $L^{-1}$ HCl in ethanol contained 28000 mg $L^{-1}$ Sb, 2050 mg $L^{-1}$ Zn, 800 mg $L^{-1}$ Fe, 400 mg $L^{-1}$ Sn and 90 mg $L^{-1}$ Pb (Table 5.2). Different precipitating agents were compared for recovery of antimony and other metals from the PLS by precipitation (Figure 5.9). The investigated precipitating agents are potassium carbonate, sodium sulfide and water. First, with using different concentrations of potassium carbonate, lead precipitated in the first place followed by antimony precipitation at 0.6 mol $L^{-1}$, which is about 3 times the stoichiometric amount of antimony (Figure 5.9a). Tin, iron and zinc precipitated at higher potassium carbonate concentration. The precipitate was yellow and it was identified as a mixture of antimony(III) oxide ($Sb_2O_3$ – valentinite) and potassium chloride salt (KCl – sylvite) (Figure 5.10a, 5.11a, 5.12a). Potassium chloride is soluble in water but not in ethanol, hence it precipitated in the organic solvent. Potassium carbonate reacted with antimony chloride solution in ethanol to form insoluble antimony(III) oxide and potassium chloride salt, as shown in the equation (5.3). Second, with sodium sulfide, antimony was fully precipitated at 0.3 mol $L^{-1}$, which is about 1.5 times the stoichiometric amount of antimony (Figure 5.9b). Nearly all lead was co-precipitated, but its concentration was low.

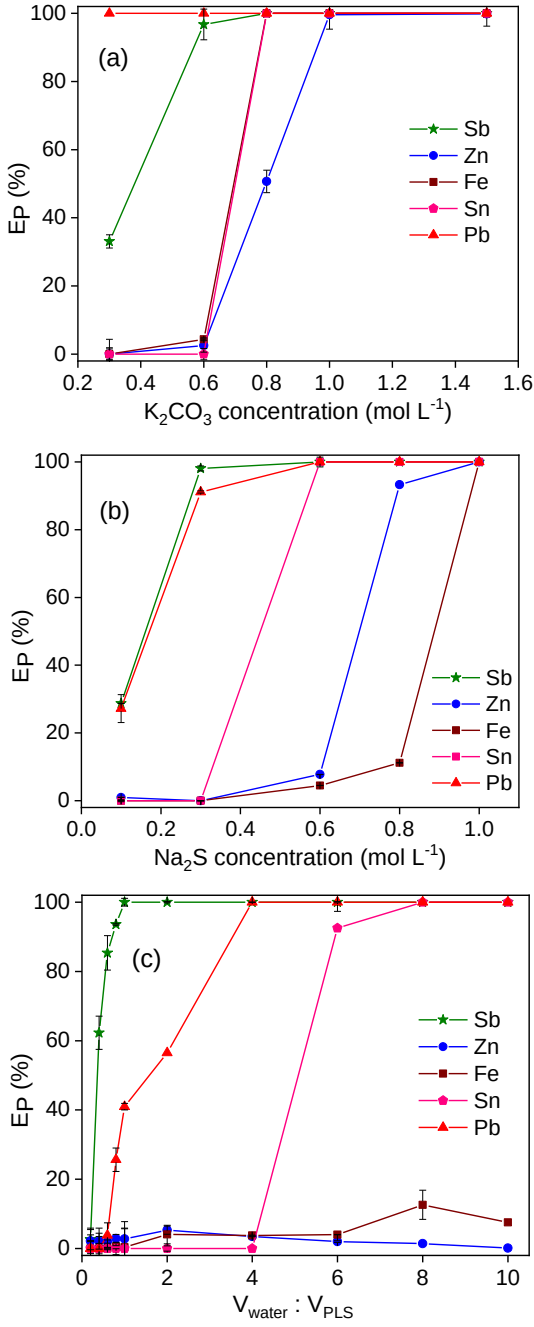


Figure 5.9 : The precipitating efficiency $E_P$ (%) of antimony, lead, zinc, iron and tin from HCl-ethanol leachate using (a) potassium carbonate, (b) sodium sulfide and (c) pure water as a precipitating agent. Precipitating parameters: room temperature, precipitating time 1 h, 800 rpm.

With further increasing the sodium sulfide concentration, tin precipitated followed by zinc and finally iron, allowing selective precipitation of each metal using different concentrations of sodium sulfide. The newly formed precipitate was a mixture of antimony(III) sulfide ($Sb_2S_3$ − stibnite) and sodium chloride (NaCl − halite) (Figure 5.10b, 5.11b, 5.12b). Sodium sulfide reacted with antimony chloride solution in ethanol to form insoluble antimony(III) sulfide and sodium chloride, as shown in the equation (5.4). Finally, the antimony recovery by precipitation was investigated by adding excess amount of water to the chloride PLS. Complete precipitation of antimony was achieved when equivalent volume of water was added to the PLS (Figure 5.9c). Lead co-precipitated with antimony, and tin precipitated after adding 6 times the volume of PLS. Iron and zinc did not precipitate. The hydrolysis precipitation of antimony(III) chloride solution formed a white solid, which was identified as a pure antimony oxide chloride ($Sb_4O_5Cl_2$) (Figure 5.10c, 5.11c, 5.12c). Water, added in considerable quantity to the acid solution of $SbCl_3$, gives a white precipitate of antimony(III) oxychloride (SbOCl) and addition of more water further hydrolyses antimony(III) oxychloride to antimony(III) oxide chloride ($Sb_4O_5Cl_2$) as shown in equation (5.5) and (5.6).[200,60]

$$4SbCl_3\ (l) + 6K_2CO_3\ (s) \rightarrow\ Sb_4O_6(s) + 12KCl\ (s) +\ 6CO_2(g) \quad (5.3)$$

$$2SbCl_3\ (l) + 3Na_2S\ (s) \rightarrow\ Sb_2S_3(s) + 6NaCl\ (s) \quad (5.4)$$

$$SbCl_3\ (l) + H_2O\ (l) \rightarrow\ SbOCl(s) + 2HCl\ (l) \quad (5.5)$$

$$4SbOCl\ (s) + H_2O\ (s) \rightarrow\ Sb_4O_5Cl_2(s) + 2HCl\ (l) \quad (5.6)$$

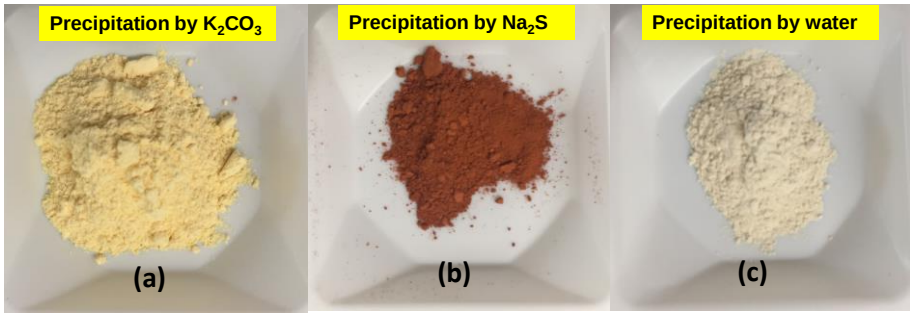


Figure 5.10: Photographs of precipitates formed after addition of: a) potassium carbonate, b) sodium sulfide and c) water to the pregnant leach solution after leaching dross1 with 2 mol $L^{-1}$ hydrochloric acid in ethanol.

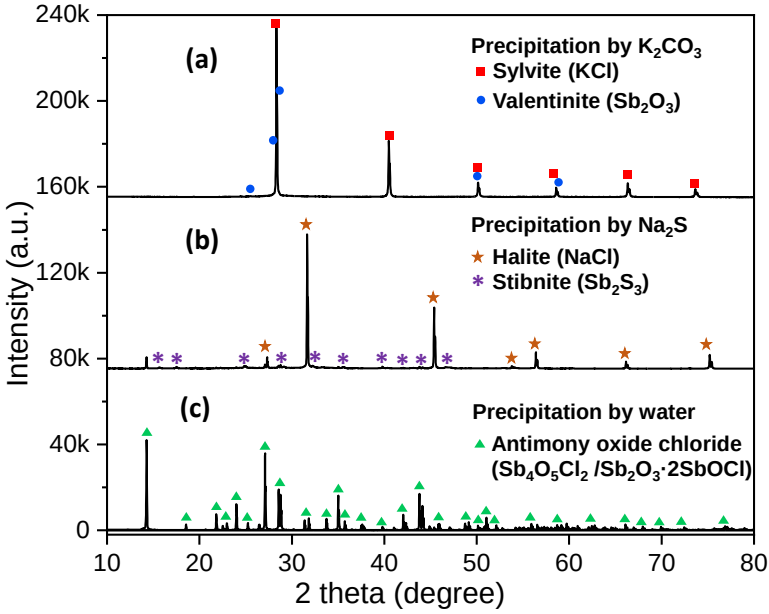


Figure 5.11: XRD patterns of the precipitates formed after using (a) potassium carbonate and (b) sodium sulfide and (c) water to recover metals from the pregnant leach solutions.

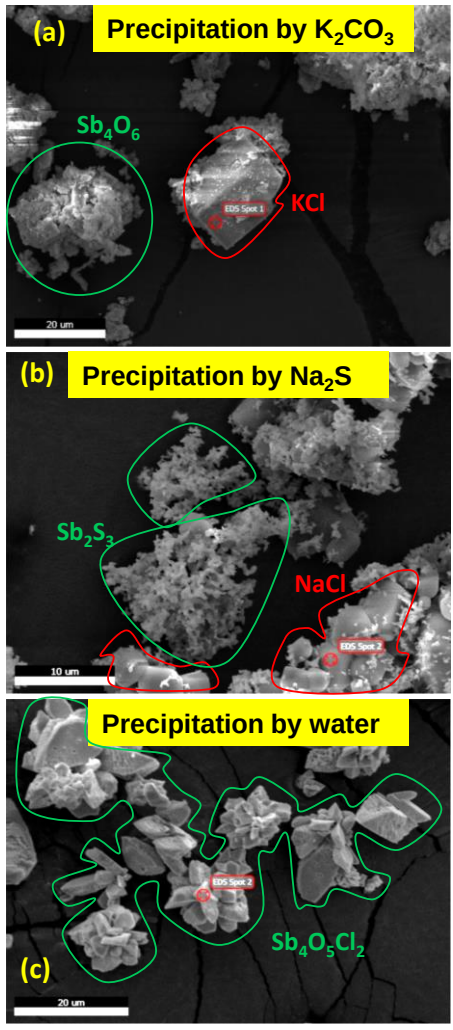


Figure 5.12: SEM micrographs of the precipitates formed by precipitation with (a) potassium carbonate and (b) sodium sulfide and (c) water to recover metals from the pregnant leach solutions. (The corresponding EDS spectra of the SEM micrographs does not fit well and, thus not included in the chapter)

Precipitation of antimony using water is a more viable method compared to that with sodium sulfide and potassium carbonate since water is a green and cheap reagent, and produced a pure product in the form of antimony(III) oxide chloride ($Sb_4O_5Cl_2$). Moreover, antimony(III) oxide chloride can find applications as flame retardant and anode material in lithium-ion batteries or aqueous chloride batteries.[216–221] The ethanol remaining in the PLS after

antimony precipitation was recovered by distillation. The FTIR spectra of fresh and distilled ethanol were comparable, indicating that the distilled ethanol is pure and can be reused again for leaching (Figure 5.13).

Finally, a conceptual flowsheet of the leaching of dross by 2 mol $L^{-1}$ hydrochloric acid in ethanol was proposed (Figure 5.14). The dross, which contains 30 wt% of lead and 30 wt% of antimony, was leached by 2 mol $L^{-1}$ hydrochloric acid in ethanol at optimized conditions. The PLS after the leaching contains 90% of the antimony in the original dross with no lead. The removal of majority of the antimony by leaching results in a leach residue enriched in lead with 100% of the lead in the original dross and only 10% of the antimony. The leach residue can be re-fed in the lead recycling. The dissolved antimony in the PLS is precipitated by adding water to produce a highly pure antimony oxide chloride ($Sb_4O_5Cl_2$), which can be directly used as a flame retardant. Subsequently, the ethanol from the PLS is distilled and a fresh lixiviant (2 mol $L^{-1}$ hydrochloric acid in ethanol) is prepared and reused for leaching dross.

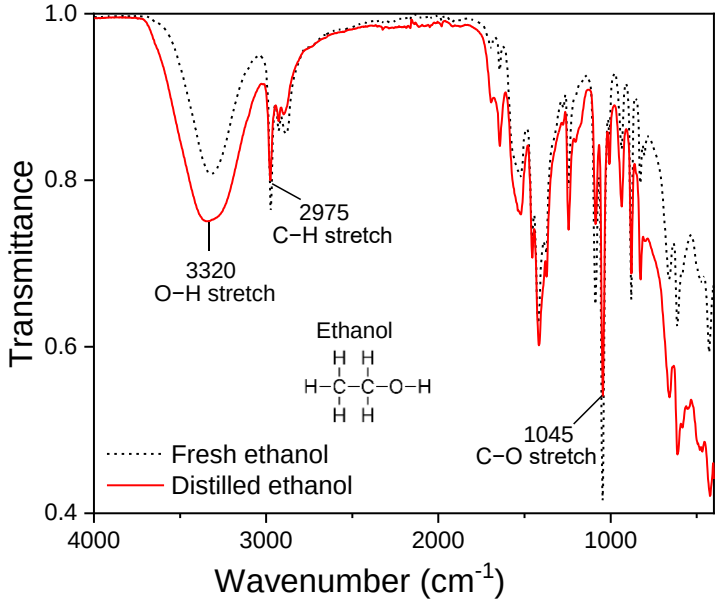


Figure 5.13: FTIR spectra of fresh ethanol and distilled ethanol.

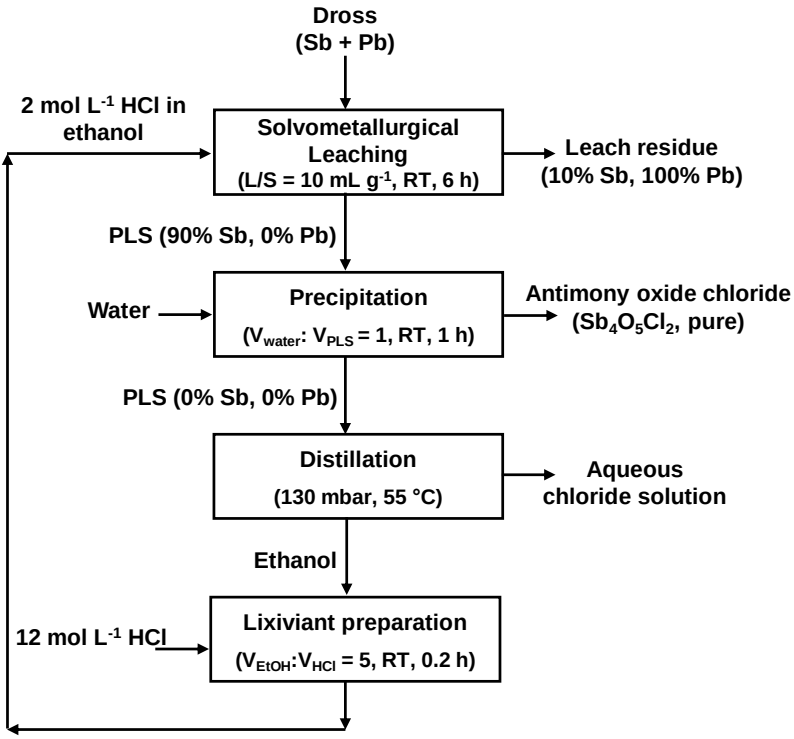


Figure 5.14: Conceptual flow chart for conversion of lead-rich dross into antimony oxide chloride by selective leaching of antimony using hydrochloric acid in ethanol and precipitation with water. (The % in the flow chart refers to the percentage of the initial amount in the fresh residue)

## 5.4 Conclusion

Solvometallurgical leaching was applied on lead-rich drosses from a lead recycling plant to selectively recover antimony. After screening various chloride-based organic lixiviants, hydrochloric acid in ethanol and 1-octanol were found to give high leaching efficiencies of antimony with minimal co-dissolution of lead. The low dissolution of lead in these lixiviant is attributed to the low solvating power of the low-polarity molecular solvents for the produced lead(II)-chloro complexes, which resulted in a precipitation of lead(II) chloride ($PbCl_2$). Other tested lixiviants such as hydrochloric acid in ethylene glycol and in Aliquat 336 chloride can dissolve larger amounts of lead(II)-chloro complexes by the bidentate hydroxyl functional groups and the cationic counter-ions, respectively. Using ethanol instead of water as a solvent for hydrochloric acid not only improved the selectivity towards

antimony over lead but it also required less chloride concentration to leach similar amounts of antimony, which would significantly diminish the usual corrosion issues faced by the industries for using high chloride concentrations. By using 2 mol $L^{-1}$ hydrochloric acid in ethanol, lead(II) antimony(III) oxide ($PbO{\cdot}Sb_2O_3$), magnesium/zinc antimony(III) oxide ($Mg/ZnO{\cdot}Sb_2O_3$) and lead(II) silicate hydrate ($PbSi_2O_5{\cdot}1.6H_2O$) were completely leached whereas lead(II) antimony(V) oxide ($2PbO{\cdot}Sb_2O_5$) and valentinite ($Sb_2O_3$) were still present in the leach residue, indicating that they are either only partially leached or not leached at all. The antimony in the PLS was recovered by hydrolysis precipitation using water, producing a pure antimony oxide chloride ($Sb_4O_5Cl_2$). The ethanol in the remaining PLS was distilled and it can be reused for leaching of more drosses.

# Chapter 6: Selective leaching of lead from lead smelter residues using EDTA

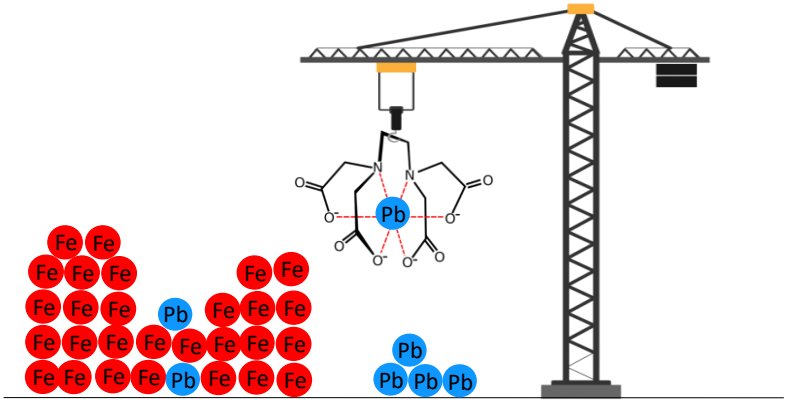


This chapter is based on the published paper:

**Palden, T**.; Machiels, L.; Onghena, B.; Regadío, M.; Binnemans, K. Selective Leaching of Lead from Lead Smelter Residues Using EDTA. *RSC Adv.* 2020, *10* (69), 42147–42156. https://doi.org/10.1039/D0RA08517K.

The text may contain slight adjustments compared to the original publication.

*Author contributions:*

K.B., B.O. and T.P. conceived the original research idea. T.P. designed and executed the experiments, treated the data, drew the conclusions, and wrote the article. L.M. performed the Q-XRD measurements and treated its data. All authors contributed to the discussion of the results and helped in the correction of the manuscript.

## Abstract

Ethylenediaminetetraacetic acid (EDTA) has been widely used as an effective reagent for the removal of lead from soil because of its high lead extraction efficiency caused by the high thermodynamic stability of Pb(II)-EDTA complex. In this study, EDTA was used as a lixiviant for the recovery of lead from residues (matte and slag) of a secondary lead smelter plant. The residues were composed mainly of iron (34−66 wt%) and lead (7−11 wt%). Leaching parameters (EDTA concentration, pH, temperature, liquid-to-solid ratio and leaching time) were optimized. The optimum leaching efficiency was achieved when leached for 1 h at room temperature using 0.05 mol $L^{-1}$ EDTA at a liquid-to-solid ratio of 5 mL $g^{-1}$. At such conditions, 72 to 80% of lead and less than 1% of iron were leached from both matte and slag. The high selectivity towards lead with minimal co-dissolution of iron is a major advantage since it reduces the chemical consumption and simplifies the downstream processes. Although the stability constants of the complexes Fe(III)-EDTA, Fe(II)-EDTA and Pb-EDTA are all large (log $K_S$ 25.1, 14.33 and 18.04, respectively), the leaching of iron was most likely limited by its presence in insoluble phases such as iron oxides, sulfides and silicates in the residues. 100% leaching of lead was achieved by a multi-step leaching process where the leaching residues were contacted three times by a fresh EDTA solution. To recover EDTA, first iron was precipitated as iron hydroxide by raising the pH of pregnant leach solution (PLS) above 12.6 by sodium hydroxide, followed by precipitation of lead as lead sulfide by adding ammonium sulfide. The recovered EDTA was successfully reused two times for leaching without significant changes in leaching yields.

## 6.1 Introduction

A total of 11.9 million tons of lead metal was produced globally in 2019, and 61% of that amount was produced by recycling of lead-containing scrap by secondary lead smelters.[223] The secondary lead smelters produce metallic lead as their main product but also a large amount of by−products. During the smelting process, molten lead sinks to the bottom of the furnace and is tapped separately for further refining. The less dense mineral phases (i.e., the smelting residue) float on the top of the molten lead and these are tapped into a separate pot to settle. There, the denser matte consisting mostly of molten sulfide sinks to the bottom and the slag consisting of molten silicate floats on the top.[53,223,224] After cooling, the matte is physically separated from the slag. About 200,000 tonnes of lead−rich residues (matte and slag) are being produced yearly in Europe alone during this smelting process.[225] These residues are composed mostly of iron (30−70%) and lead (6−10%), but some amounts of tin, antimony, nickel and zinc are present as well. Therefore, they can be reused as secondary resources for many valuable metals. In addition, matte and slag landfills are known to release lead, a toxic but economically important metal, to the environment, and recovery of the valuable metals such as lead will generate a new residue that is safer to landfill.[83]

Some research has focused on the valorization of these residues as a construction material.[50,51] However, the recovery of the valuable and toxic metals and metalloids prior to their application as construction material was not considered. Hence these approaches result in a great loss of valuable metals in addition to the potential risk of leaching the toxic metals to the environment. Few studies have investigated the recovery of valuable metals from these lead-containing residues. Kim *et al.* studied the selective leaching of lead and other minor metals from lead smelter residues using nitric acid.[223,226] They investigated in detail the effect of roasting, pressure leaching, and addition of the ferric ion as an oxidant to enhance lead leaching. With their optimized system, about 90% of lead was leached with minimal co−dissolution of iron. However, the leaching system employs nitric acid which is highly corrosive and powerful oxidant and, requires roasting which is energy intensive. Moreover, it did not leach any lead from slag making it only applicable for matte. Forte *et al.* employed a solvometallurgical leaching process using concentrated acetic acid to recover the valuable metals from the lead smelter residues.[62] The process could leach 90% of lead with 6% co−leaching of iron from matte and lower lead leaching

of 70% from the slag. Although this process is novel and promising, its main challenge is to convince the stakeholders to use a pure acetic acid at industrial scale since it has a strong stringent odor and it has not been applied on a commercial scale by a metallurgical industry yet. Moreover, liquid-to-solid ratio of 20 L $kg^{-1}$ required for the acetic acid leaching is too high, making the process unattractive for commercialization.

Ethylenediaminetetraacetic acid (EDTA) is a chelating agent that can form stable Pb(II)−EDTA complexes.[62] In fact, EDTA has been widely used as an effective reagent for decontamination of lead from soil because of its high lead extraction efficiency enabled by high thermodynamic stability of lead-EDTA complexes.[78,79,232–235,80,81,84,227–231] Moreover, EDTA can be recovered and recycled, which is of great economic and environmental importance since EDTA is relatively expensive and only slowly biodegradable.[82,144,236] In a recent study, Smaniotto *et al.* investigated the recovery of lead from recycled lead−acid battery slag using EDTA as a lixiviant.[83]

In this paper, we present the development of a process to selectively recover lead from the residues (matte and slag) of a secondary lead smelter using EDTA as lixiviant. Firstly, the operative parameters (concentration, pH, liquid−to−solid ratio, temperature) were optimized. Secondly, the recovery of EDTA and its subsequent reusability with fresh residues, was studied in detail. Finally, the scaling up of the leaching system was tested in a 1L reactor.

## 6.2 Experimental

### 6.2.1 Chemicals

The slag and matte were kindly provided by a European secondary lead producer. Disodium ethylenediaminetetraacetic acid (0.1 mol $L^{-1}$, $Na_2EDTA$) and sodium hydroxide (NaOH, pearl) was purchased from Fisher Scientific (Loughborough, United Kingdom). Disodium ethylenediaminetetraacetic acid (0.2 mol $L^{-1}$, $Na_2EDTA$) was purchased from Honeywell Fluka (Seelze, Germany). Hydrochloric acid (37 wt%, HCl in water) and boric acid (99.5%, $H_3BO_4$ in water) was supplied by VWR Chemicals (Leuven, Belgium). Nitric acid (65 wt% $HNO_3$ in water) and iron, lead, zinc and rhodium standard solutions (1000 mg $L^{-1}$) were purchased from Chem−Lab NV (Zedelgem, Belgium). Hydrofluoric acid (48 wt%, HF in water) and ammonium sulfide (20 wt%, $(NH_4)_2S$ in water) were purchased from Sigma−Aldrich (Diegem,

Belgium). All chemicals were used as received without any further purification.

### 6.2.2 Instrumentation

The matte and slag were ground and sieved using a mortar grinder (Pulverisette 2, Fritsch, Germany) and a vibratory sieve shaker (Analysette 3, Fritsch,Germany). The materials were digested using a microwave digester (Mars 6, CEM, USA). The metal content in solution was measured by inductively coupled plasma optical emission spectroscopy (ICP−OES, Optima 8300, Perkin Elmer, USA) from PerkinElmer. The mineral phases in the solid materials were identified by powder X−ray diffraction (XRD) analysis using a Bruker D2 Phaser diffractometer. The leaching was carried out on a RCT classic heating plate (IKA). The phase disengagement between the solid and liquid after leaching was carried out by centrifugation using Heraeus Labofuge 200. The scalability of the leaching at optimized conditions was studied using a customized 1 L jacketed laboratory reactor, linked to an automatic filtration unit (LabKit 36167) constructed by HiTec Zang GmbH (Herzogenrath, Germany).

### 6.2.3 Methodology

All the experiments were carried out in duplicates and relative standard deviations were within ± 5%. The matte and slag (as received) were dried in an oven at 100 °C for 24 h to remove any trace of moisture. The materials were ground using a mortar grinder and sieved below 250 µm in particle size using a vibratory sieve shaker. The procedure for quantitative X-ray diffraction analysis (QXRD) was adapted from the work of Snellings *et al*. and Machiels *et al*.[237,238] Samples were spiked with 20 wt.% of $Al_2O_3$ internal standard and ground in ethanol for 5 min using a McCrone Micronizing Mill. X-ray powder diffraction (XRD) was used for the phase identification of the crystalline fraction. Experimental parameters for XRD analysis were: 2θ: 10°–80°, $CuK_\alpha$, acceleration voltage: 45 kV, acceleration current: 30 mA, a step size of 0.020° and a counting time of 1 s per step, spin mode. Phase identification was done using the Bruker Diffrac+ software while Rietveld quantitative phase analysis (QPA) was performed using the Topas Academic software. A fundamental parameter approach was used, meaning that instrumental contributions to the peak shapes were directly calculated. The following parameters were refined: background, sample displacement, scale

factors of all phases, lattice parameters, crystallite size and lattice strain. The background was refined using a cosine Chebyshev polynomial function of 15 parameters. The metal content of the materials was determined after fully dissolving 100 mg of the milled sample in an acid mixture of 4 mL of 37 wt% HCl, 5 mL of 65 wt% $HNO_3$ and 1mL of 48 wt% HF using microwave−assisted acid digestion. The samples were digested using a one stage program where the samples heated from room temperature to 180 °C in 5.5 min and held for 9.5 min at 1000 W. After the digestion, the excess HF was rendered safe by complexation with 10 mL of 4 wt% of $H_3BO_3$ and enhanced by microwave digestion where the samples were heated up to 170 °C in 15 min and held for 10 min. After the neutralization, the digestion vessels were cooled and the digested solutions were transferred to volumetric flasks and filled up to 100 mL with ultrapure water for analysis. The sample dissolution via microwave digestion was done in triplicates to check the reproducibility of the composition. The metal concentrations in each of the digested acid solution was measured by ICP-OES with ±5% of error associated with the measurements.

The initial leaching experiments were carried out by adding 200 mg of matte or slag and 2 mL of EDTA solution in a 4 mL glass vial and magnetically stirred on a heating plate. The following leaching conditions were applied: a liquid−to−solid ratio (L/S) of 10 mL $g^{-1}$, a temperature of 60 °C, a contact time of 2 h and a stirring speed of 600 rpm. The upscaling of the leaching system was tested for 1 L of EDTA in a 1 L batch reactor. Attention had to be paid when choosing the type of vial for leaching experiments. The iron- and lead-rich residues have a high mass density and were difficult to stir by a magnetic stirring bar. As a result, the solids residues were not homogenously distributed in the EDTA solution, especially in the longitudinal leaching vials giving a low leaching efficiency of lead. An appropriate vial must be chosen for each volume of the lixiviant. Otherwise, maximum leaching of lead could not be realised using inappropriate vial. Therefore, 4 mL vials were used for lixiviant volume of less than 2 mL and 10 ml vial for lixiviant volume between 2−5 mL.

The *pregnant leach solution* (PLS) was separated from the solid residue by centrifugation (5300 rpm, 10 min). The finer particles suspended in the PLS were further separated by a syringe filter made of a polyester membrane (Chromafil PET, 0.45 µm pore size). The metal concentration in the PLS was measured using ICP−OES and the *leaching efficiency* $E_L$ *(%),* was calculated according to equation (6.1):

$$E_L(\%) = \frac{c_M \times v_{LIX}}{m_I \times c_I} \times 100 \quad (6.1)$$

where $c_M$ is the metal concentration in the PLS after leaching (mg $L^{-1}$), $v_{LIX}$ is the volume of leaching agent used for leaching (L), $m_I$ is the mass of the solid material used for leaching (kg), and $c_I$ is the concentration of the metal in the slag or matte before leaching (mg $kg^{-1}$).

The EDTA in the PLS was recovered by precipitation of the dissolved iron by adding 12 mol $L^{-1}$ NaOH; followed by precipitation of lead by adding 2.93 mol $L^{-1}$ $(NH_4)_2S$. The *precipitation efficiency* $E_P$ (%) was calculated by mass balance according to the following equation (6.2):

$$E_P(\%) = 100 - \left(\frac{c_P}{c_M} \times 100\right) \quad (6.2)$$

where $c_P$ is the concentration of metals in PLS after precipitation (mg $L^{-1}$) and $c_M$ is the concentration of metals in PLS before precipitation (mg $L^{-1}$).

## 6.3 Results and discussion

### 6.3.1 Characterization of matte and slag

The matte and slag were composed mainly of iron (34−66 wt%) and lead (7−11 wt%) (Table 6.1). The iron and lead were present in several mineral phases (Table 6.2). In the matte, iron was mainly present in the form of sulfide (FeS) with small amounts of oxides (FeO, $Fe_3O_4$). In the slag, iron was mainly present as silicates ($Fe_2SiO_4$, $CaFeSiO_4$) with a significant amount of sulfide (FeS) and small amounts of oxides ($Fe_3O_4$, FeO). It must be noted that 91% of the iron in matte and slag were in divalent state. Lead was present in elemental state (Pb), oxide (PbO) and carbonate hydroxide ($Pb_3(CO_3)_2(OH)_2$) form in both matte and slag, and additionally, in sulfide (PbS) form in the slag. Amorphous phases and the minor phases that were in low concentration were not detected by XRD. These unidentified phases contributed to less than 5% of the mass of the residues. To avoid complications in presenting a very large array of data, only data for iron and lead are compared and further

discussed. The other metals were in low concentrations and their impact on iron and lead leaching would be minimal.

Table 6.1: Element composition of matte and slag

| Metal | Matte (wt%) | Slag (wt%) |
|---|---|---|
| Fe | 66.30 ± 0.73 | 34.45 ± 1.16 |
| Pb | 10.94 ± 0.15 | 6.8 ± 0.34 |
| Zn | 0.347 ± 0.001 | 0.608 ± 0.004 |
| Cu | 0.82 ± 0.05 | 0.27 ± 0.01 |
| Si | 0.26 ± 0.01 | 13.49 ± 0.01 |
| Sn | 0.21 ± 0.01 | 0.34 ± 0.02 |
| Ni | 0.111 ± 0.003 | 0.028 ± 0.002 |
| Ca | 0.063 ± 0.002 | 4.28 ± 0.21 |
| Cr | 0.049 ± 0.003 | 0.334 ± 0.012 |

Table 6.2: Mineral phases present in the matte and slag

| Mineral phases | Matte wt% | Slag wt% |
|---|---|---|
| FeS (troilite) | 71 | 29 |
| $Fe_2SiO_4$ (fayalite) | - | 34 |
| $CaFeSiO_4$ (monticellite) | - | 19 |
| FeO (wüstite) | 12 | 2 |
| $Fe_3O_4$ (magnetite) | 8 | 7 |
| $Pb_3(CO_3)_2(OH)_2$ (hydrocerussite) | 1 | 0.5 |
| PbO (massicotite) | 1 | - |
| PbO (litharge) | 1 | <0.5 |
| Pb (lead) | 0.5 | 0.5 |
| galena (PbS) | - | 1 |
| quartz ($SiO_2$) | - | 1 |
| not calculated/amorphous | 5 | 5 |

### 6.3.2 Leaching matte and slag with EDTA

Leaching matte and slag using 0.1 mol $L^{-1}$ EDTA resulted in leaching of about 64-73 % of lead and 1-12% of iron, making it selective for lead over iron (Figure 6.1). This favourable selectivity towards lead with minimal co-dissolution of iron significantly reduces the chemical consumption and simplifies the downstream processes. The lower leaching efficiency of iron compared to that of lead was unanticipated as EDTA usually forms a highly stable complex with iron. The equilibration reactions (equation (6.3), (6.4) and (6.5) and stability constants (log $K_S$, 25 °C and $\mu$ = 0.1) of EDTA with Fe(III), Fe(II) and Pb(II) are shown below:[78]

$$Fe^{3+}(aq) + H_2EDTA(aq) \rightleftharpoons FeHEDTA(aq) + H^+(aq) \quad \log K_S = 25.1 \quad (6.3)$$

$$Fe^{2+}(aq) + H_2EDTA(aq) \rightleftharpoons FeH_2EDTA\ (aq) \quad \log K_S = 14.33 \quad (6.4)$$

$$Pb^{2+}(aq) + H_2EDTA(aq) \rightleftharpoons PbH_2EDTA\ (aq) \quad \log K_S = 18.04 \quad (6.5)$$

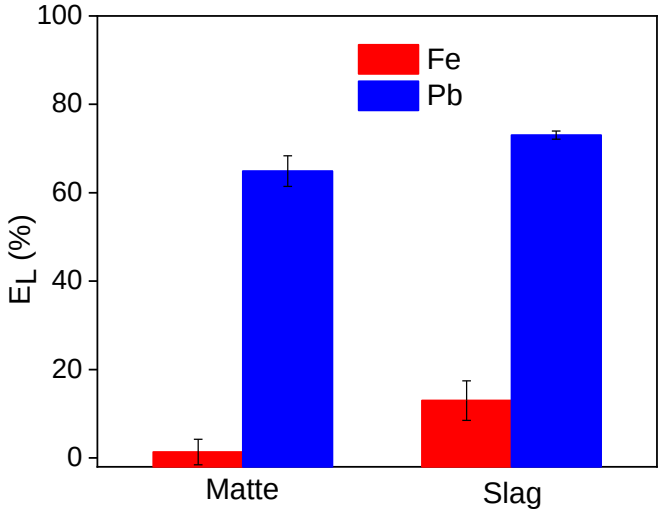


Figure 6.1: Leaching efficiency $E_L$ (%) of lead and iron from matte and slag by EDTA. Leaching parameters: EDTA concentration 0.1 mol $L^{-1}$, L/S ratio 10 mL $g^{-1}$, 25 °C, pH (initial) = 8, stirring speed 600 rpm, leaching time 1 h.

Based on the stability constants, one could draw the wrong conclusion that most of the iron would be leached because of the high stability constant of Fe-EDTA complexes and the abundance of iron in the residues. However, the leachability of any metal depends primarily on the solubility of its mineral form. In matte and slag, the iron was present in crystalline sulfide, oxide, and/or silicate form, which are relatively stable and thus difficult to be leached by chelating lixiviants like EDTA or weak acids. The high stability constants of the Fe-EDTA complexes does positively influence the leachability of the iron minerals but the fact that iron was barely leached by the EDTA solution means that the insolubility of the iron minerals is probably the limiting factor. Nevertheless, the high stability constant of Fe-EDTA complexes does ensure that the already dissolved iron remains in solution, and does not precipitate easily. The presence of lead in more soluble minerals in the residues, together with the high stability constant of Pb-EDTA complexes resulted in a higher leaching efficiency of lead than of iron. Independent studies by Clevenger *et al.* and Elles *et al.* already showed that EDTA can solubilize many of the common inorganic lead phases such as $PbCO_3$, $PbSO_4$, $PbCl_2$, $Pb(NO_3)_2$, PbO, $Pb_3O_4$, $PbO_2$ and $Pb(OAc)_2$ except for PbS and $PbCrO_4$.[239,240] Thus, the main limiting factor in leaching of iron and lead from the residues was the solubility of the metal phases. The solubility

product constants of the iron phases (log $K_S$ at 25° C, $\mu$ = 0.1: magnetite = 2, wustite = 0.8 and troilitle = 5.25)[241,242] are also significantly lower than that of the lead phases (log $K_S$ at 25° C, $\mu$ = 0.1: litharge = 12.89, hydrocerussite = 17.51),[243] supporting the discussion that the good solubility of the mineral phases is crucial in achieving a high leaching efficiency of the metals. The Cu-EDTA and Zn-EDTA complexes are also stable with stability constant (log $K_S$, 25 °C and $\mu$ = 0.1) of 18.7 and 16.44, respectively.[78] However, their influence in the selective leaching of lead over iron would be minimal, since their concentration (Cu = 0.3-0.8 wt%, Zn = 0.3-0.6 wt%) were low in the residues.

### 6.3.3 Optimization of leaching of lead

The leaching of lead and iron from matte and slag was studied as a function of the leaching time (Figure 6.2). The leaching of lead was relatively fast: about ~50% of the lead was leached from both matte and slag within the first few minutes. For the matte, it reached a maximum of 74% after 6 hours and then remained stable. For the slag, the leaching efficiency of lead increased sharply until 73% after 2 hours and then it remained constant at longer leaching time. The leaching efficiency of iron remained low for both residues: less than 1.5% after 1 hour of leaching. Forte *et al.* also reported fast leaching kinetics where the lead leaching efficiency reached a plateau within 2 h.[62] Since the objective was to use the same condition for both matte and slag and to achieve high selectivity over iron, the optimum leaching time was chosen as 1 hour for both matte and slag. After 1 hour, about 60% of lead and 1.5% of iron were leached, making it highly selective for lead with minimal co-dissolution of iron.

Next, the effect of the concentration of EDTA on leaching of slag and matte was investigated by increasing the EDTA concentration stepwise from 0.01 to 0.2 mol $L^{-1}$ (Figure 6.3). The leaching of lead increased sharply with increasing EDTA concentration from 0.01 to 0.05 mol $L^{-1}$ EDTA for both matte and slag. Further increase in the concentration led to a small decrease in leaching efficiency of lead in the matte and a gradual increase for the slag. The leaching efficiency of iron increased gradually with increasing EDTA concentration, but remained less than 14%. Due to good selectivity and the reduced cost of less concentrated EDTA solutions, the optimum concentration was chosen to be 0.05 mol $L^{-1}$ at which about 60% of lead and <2% of iron were leached. However, leaching by 0.1 mol $L^{-1}$ EDTA concentration was also investigated to avoid limiting the leaching efficiency of lead by the lack of sufficient EDTA molecules.

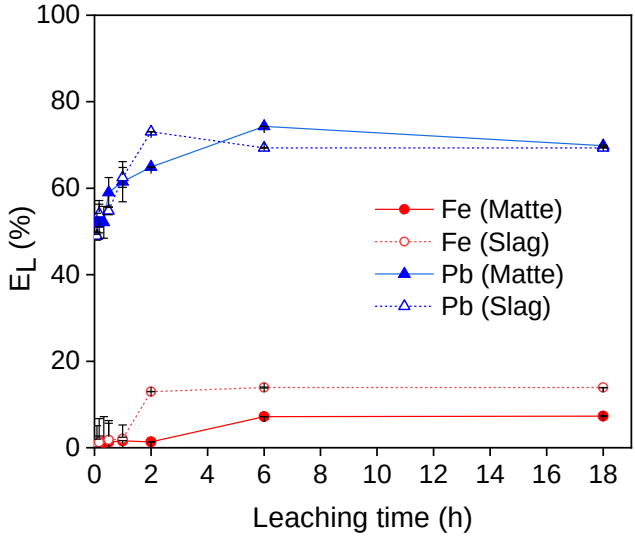


Figure 6.2: Effect of the leaching time on the leaching efficiency $E_L$ (%) of lead and iron from matte and slag by EDTA. Leaching parameters: EDTA concentration 0.1 mol $L^{-1}$, L/S ratio 10 mL $g^{-1}$, 25°C, pH (initial) 8, stirring speed 600 rpm.

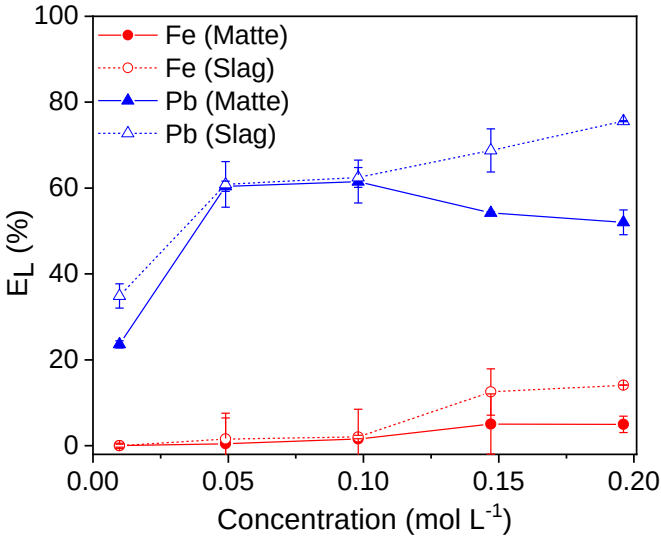


Figure 6.3: Effect of the EDTA concentration on the leaching efficiency $E_L$ (%) of lead and iron from matte and slag. Leaching parameters: L/S ratio 10 mL $g^{-1}$, 25°C, pH (initial) = 8, stirring speed 600 rpm, leaching time 1 h.

The leaching of lead and iron from matte and slag was studied as a function of pH at 0.05 and 0.1 mol $L^{-1}$ EDTA concentration (Figure 6.4 a and b, respectively). The pH of the EDTA solution did not have a significant effect on the leaching efficiency of lead for both residues. Previous studies have also shown that pH did not influence the extraction of potentially toxic metal(loid)s by EDTA.[78] As confirmed here, the pH of the EDTA solution was indeed not important for the leaching efficiency of lead. However, the leaching efficiency of iron decreased with increasing pH, and at pH = 12 there was no iron in the PLS. This was due to the precipitation of Fe(II) and Fe(III) as $Fe(OH)_2$ and $Fe(OH)_3$, respectively, at higher pH with a red-brown precipitate formed quickly in the PLS after filtration of the leaching residue. Fe(III) in aqueous solutions usually precipitates at much lower pH, but it is reported to be stable up to pH =12 in EDTA solutions due to the high stability constant of Fe(III)-EDTA complexes.[79] The pH of the solution was expected to remain unchanged (initial pH = 8) or to slightly decrease after equilibration due to the release of free protons by the EDTA molecule. However, the equilibration pH of the PLS increased after leaching. When pure water was used to leach matte and slag, the equilibration pH of water after leaching also increased to 10.6 and 9.5, respectively. After analyzing the PLS resulting from leaching with pure water, trace amounts of Pb, Zn, Ca, Sn and K were found to be present but one specific chemical reaction could not be linked to this pH change. Dissolution of calcium oxide in water would generate hydroxide ions but the concentration of calcium did not show positive correlation with the change in pH of the PLS. The increase in pH could be due to the release of hydroxide ions by more than one reaction taking place during leaching. The selectivity of lead over iron was better at pH 12 than pH 8. However, the iron leaching efficiency was already low and further reducing the iron leaching efficiency by increasing pH was not a sufficient justification to choose a more complicated leaching process whereby a pH adjustment of the lixiviant is required prior to the leaching. Therefore, the pH of fresh EDTA solution (~pH 8) was chosen as the optimum pH to have simple leaching process where pH adjustment is not required.

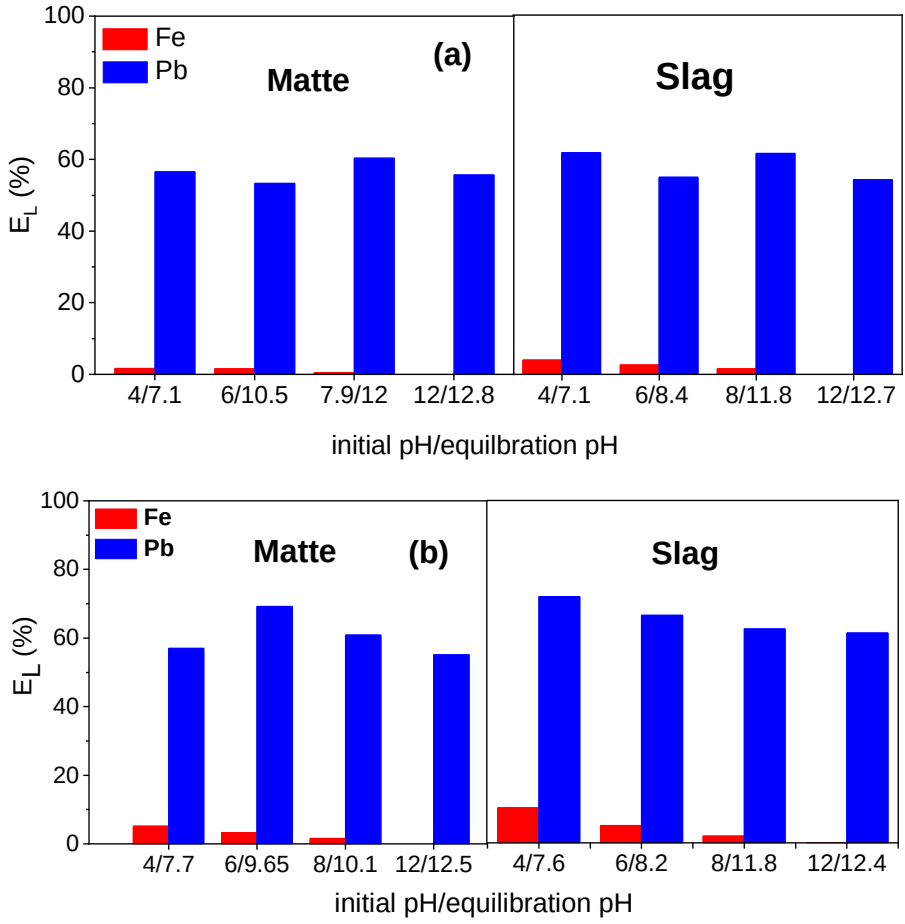


Figure 6.4: Effect of the pH on the leaching efficiency $E_L$ (%) of lead and iron from matte and slag using a) 0.05 mol $L^{-1}$ and b) 0.1 mol $L^{-1}$ EDTA. Leaching parameters: L/S ratio 10 mL $g^{-1}$, 25°C, stirring speed 600 rpm, leaching time 1 h.

The influence of liquid−to−solid ratio (L/S) on leaching of lead and iron from matte and slag using 0.05 and 0.1 mol $L^{-1}$ EDTA solution was investigated (Figure 6.5). The leaching of lead increased sharply when the L/S ratio was increased up to 5. Further increase in the L/S did not significantly change the leaching efficiency of lead. The leaching of iron gradually increased but remained low with increasing L/S ratio. For matte, the leaching efficiency of lead was about 20−25% higher using 0.1 mol $L^{-1}$ EDTA solution compared to that of the 0.05 mol $L^{-1}$ solution. However, for slag, the lead leaching

efficiency only increased by 10% when the EDTA concentration was increased from 0.05 to 0.1 mol $L^{-1}$. The optimum conditions were selected to be L/S ratio of 5 and EDTA concentration of 0.1 mol $L^{-1}$. At such conditions, lead and iron leaching efficiency were 77% and 0.04%, respectively, for matte and, 72% and 1.2%, respectively, for slag.

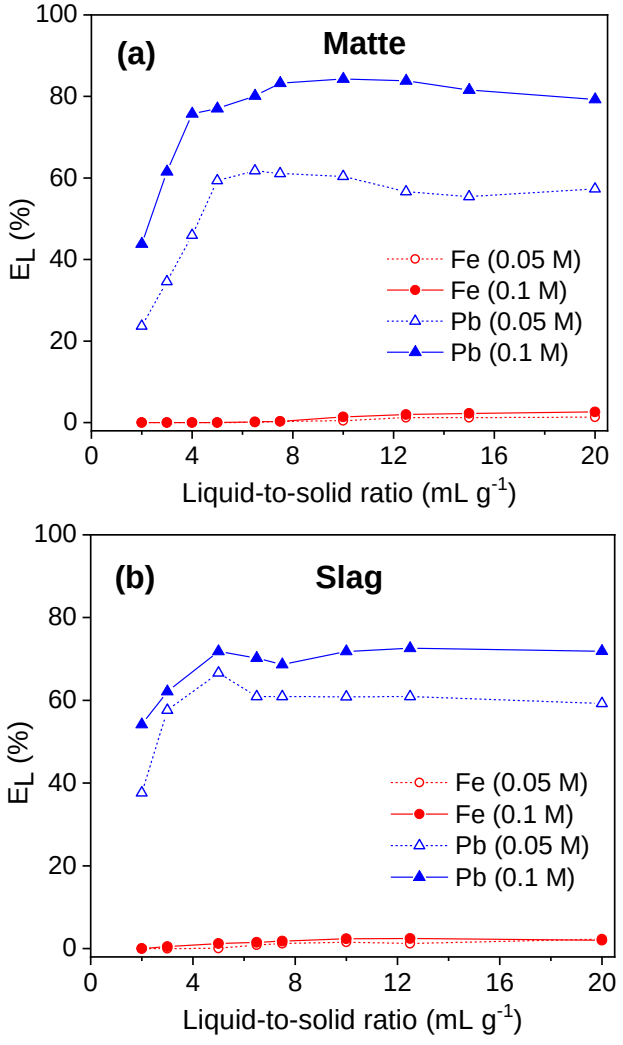


Figure 6.5: Effect of the liquid-to-solid ratio on the leaching efficiency $E_L$ (%) of lead and iron from a) matte and b) slag. Leaching parameters: 25 °C, stirring speed 600 rpm, leaching time 1 h, pH (initial) = 8, EDTA concentration 0.05 and 0.1 mol $L^{-1}$.

The influence of temperature on leaching of lead and iron from the residues was studied at L/S ratio 4 and 5 mL $g^{-1}$ (Figure 6.6). The temperature had only a small effect on the leaching efficiency of lead and iron, so room temperature (25 °C) was chosen as the optimum temperature for further experiments. Lead could not be fully leached even at higher temperatures, indicating the low reactivity of some lead phases which are still insoluble even at more severe reaction conditions. In a few studies, the lead leaching efficiency even decreased with increasing temperature, which was attributed to the precipitation of lead as a lead sulfate.[62,226] In this study, the absence of lead sulfate precipitation at high temperatures may be due to the high stability constant of Pb(II)-EDTA complexes. At optimized conditions (T = 25 °C, t = 1 h, L/S = 5 mL $g^{-1}$), EDTA leached about 72 to 80% of lead and less than 1% of iron from both matte and slag. Forte *et al.* leached 72-90% of lead and less than 3-6% of iron was co-dissolved from matte and slag at optimized conditions (T = 25 °C, t = 2h, L/S = 20 mL $g^{-1}$)[62] The slightly higher leaching of lead and iron by acetic acid compared to that of EDTA could be because the lead and iron solubilizing power of acetic acid due to its acidity, is slightly higher than that of EDTA due to its chelation. Kim *et al.* leached 69% of lead and 14% of iron from matte using 0.5 mol $L^{-1}$ nitric acid, which increased lead and iron leaching efficiency to 89% and 23%, respectively by adding ferric ion as an additional oxidant increased (T = 25 °C, t = 2 h, L/S = 10).[53]

In another study, Kim *et al*. successfully leached lead sulfide and iron sulfide minerals using 1 mol $L^{-1}$ citric acid and 0.5 mol $L^{-1}$ hydrogen peroxide as a lixiviant.[226] The hydrogen peroxide oxidized the lead sulfide and iron sulfide minerals, and brought lead(II) and iron(III) ions into the citric acid solution. To limit the dissolution of iron, the pH of the solution was maintained between 5 and 8.5, at which iron was precipitated as iron(III) oxide, but lead remained dissolved in solution by forming a stable lead(II)-citrate complex. This process leached 93% of lead and 0.6% of iron. In the process developed in this study, the leaching efficiency of lead could not be increased above 80% and this could be due to the lack of a strong acidity and oxidative power to dissolve the lead sulfide. An oxidizing agent such as hydrogen peroxide was not used in the process developed in this study because, it would also oxidize iron sulfide minerals and bring iron(III) ions into the solution, which would require pH adjustment to separate iron by precipitation. Moreover, some studies have also shown that EDTA decomposes over time in the presence of hydrogen peroxide.[244,245]

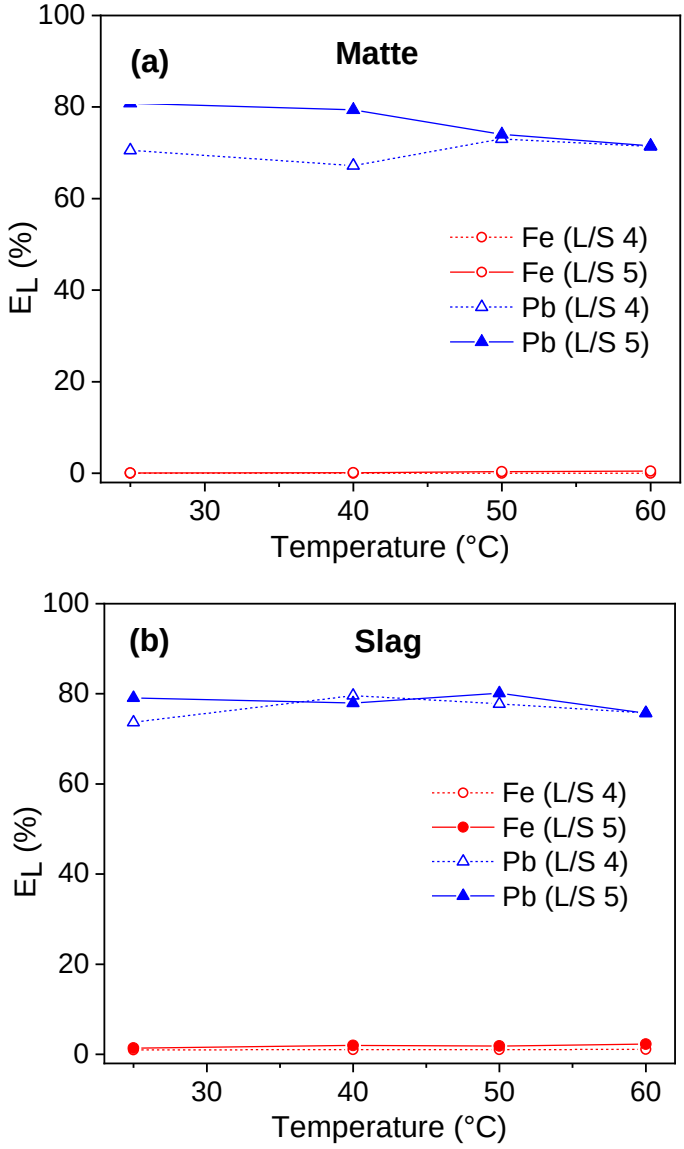


Figure 6.6: Effect of the temperature on the leaching efficiency $E_L$ (%) of lead and iron from a) matte and b) slag. Leaching parameters: stirring speed 600 rpm, leaching time 1 h, L/S ratio 4 and 5 mL $g^{-1}$, pH (initial) = 8, EDTA concentration 0.05 mol $L^{-1}$.

### 6.3.4 Multi–step leaching and EDTA recovery

Since one leaching step cannot achieve 100% leaching of lead, multistep leaching was carried out where the leached residue was contacted again with a fresh EDTA solution. After contacting the residue three times with a fresh EDTA solution, 100% lead was finally leached (Figure 6.7). This result is consistent with the findings of others. During the remediation of contaminated soils, it is commonly found that significantly more lead was leached when the same amount of EDTA was applied in several leaching steps.[78,246–249] Metals such as iron compete with potentially toxic metal(loid)s to form complexes with EDTA.[78] The high lead leaching efficiency of multi-step leaching is most likely because iron interferes more strongly with lead complexation when the residues were leached in single-step mode. However, a more in-depth study will be needed to understand why leaching with an application of EDTA solution in multiple steps is more efficient and how multistep leaching facilitate the dissolution of insoluble lead solids, like metallic lead and galena.

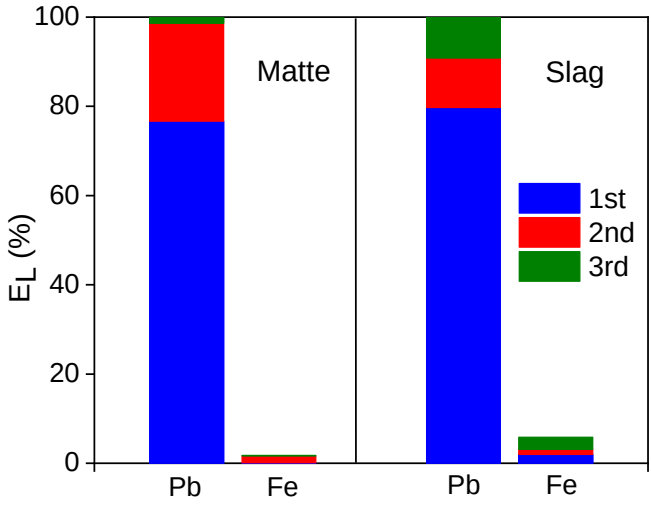


Figure 6.7: Multi-step leaching of lead matte and slag with EDTA. Leaching parameters: temperature 25 °C, stirring speed 600 rpm, leaching time 1 h, L/S ratio 5 mL $g^{-1}$, pH (initial) = 8, EDTA concentration 0.05 mol $L^{-1}$.

EDTA is a rather expensive chemical and it is only slowly biodegradable. Therefore, it is crucial that EDTA can be recovered and reused to reduce cost and to avoid environmental issues. To allow the recyclability of the leaching agent, the unreacted EDTA solution in PLS of matte and slag was recovered by two precipitation steps; iron was precipitated first by increasing the pH of the PLS by adding NaOH followed by precipitation of lead by adding $(NH_4)_2S$ solution. Having a 0.12 mol $L^{-1}$ NaOH concentration in the PLSs was sufficient to increase their pH to 12.6 and consequently to precipitate all dissolved iron as iron hydrous oxide.[83,84] The completeness of the precipitation of iron was also visually evident from the change in color of the PLS from red-brown to transparent. The red-brown color of the precipitate indicated that the precipitate was ferric hydroxide, $Fe(OH)_3$, since ferrous hydroxide, $Fe(OH)_2$, is either white or green. Moreover, the reddish color of PLS turns darker within few hours after leaching, indicating that the Fe(II) was being oxidized to Fe(III) by the air. Therefore, all the iron complexed with EDTA in the PLS were most likely in trivalent state, which has a higher stability constant with EDTA than the divalent state and lead. The PLS without the iron was again contacted with $(NH_4)_2S$ to precipitate lead as lead sulfide. Lead was completely precipitated at 0.12 mol $L^{-1}$ and 0.15 mol $L^{-1}$ $(NH_4)_2S$ for matte and slag, respectively (Figure 6.8). Excess of unreacted $(NH_4)_2S$ in the PLS was evident from the bright yellowish color of otherwise transparent PLS and the sulfurous odor. Therefore, excess of $(NH_4)_2S$ must not be used during precipitation of lead. The XRD pattern of the leach residue was compared to the one of the fresh residue, and the remaining lead phases could not be identified because the diffraction peaks corresponding to lead phases were small and often overlapping with those of the iron phases. The leached residue can be used by the iron and steel industry as a secondary iron resources, because of its high iron content. Direct precipitation of lead as lead sulfide from the residues in one step using alkaline sulfide might work due to the strong affinity between lead ($Pb^{2+}$) and sulfide ($S^{2-}$) based on the Pearson's acid base (HSAB) principle. However, direct precipitation is not always preferred since the precipitates are mixed with the leach residue and separating them can pose an even bigger challenge than a two-step process of leaching followed by precipitation.

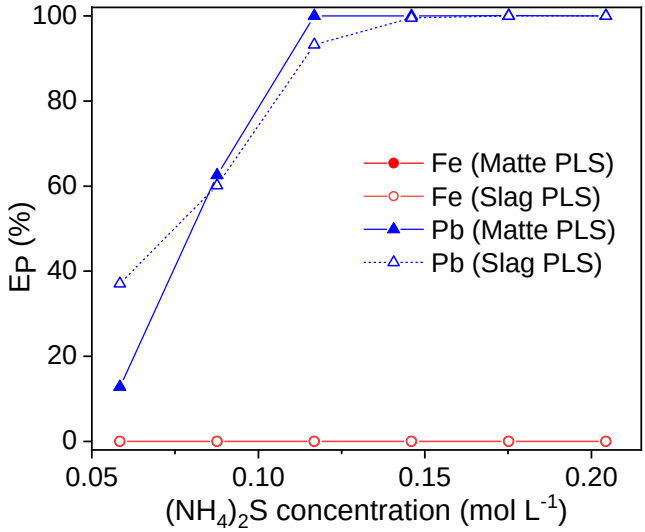


Figure 6.8: Precipitation of lead from the pregnant leach solution as lead sulfide by addition of $(NH_4)_2S$. Precipitation parameters: temperature 25 °C, stirring speed 600 rpm, time 1 h.

### 6.3.5 Scale up and reusability of EDTA

The EDTA leaching of lead matte and slag at optimal conditions was tested on a larger scale in a 1 L temperature-controlled leaching reactor (See Figure 4.12 in chapter 4) with overhead stirring and automatic filtration starting from 200 g of a solid residue and 1 L of 0.1 mol $L^{-1}$ EDTA solution, which corresponds to 500 times upscaling compared to the screening experiments. The results show that the leaching efficiency of lead using the leaching reactor was about 15−20% lower than the small−scale experiments (Figure 6.9, fresh). This may be due to ineffective stirring of the residues in a longitudinal reactor, resulting in a heterogeneous distribution of the high mass density residues. The leaching efficiency of lead in the leaching reactor can be increased to that of small−scale experiments by changing the stirring speed or reducing the amount of solids and liquid. However, the optimization of leaching in the 1 L reactor was not carried out as it was outside the scope of this study. Nevertheless, the leaching yield of lead was high with minimal co−dissolution of iron, showing potential for upscaling to a larger scale.

The reusability of the recovered EDTA solution was tested by reusing it to leaching of fresh matte and slag samples. The process of leaching and precipitation was repeated for two cycles and the leaching results were

compared to that of fresh EDTA (Figure 6.9). The leaching result between fresh and 1st recycled EDTA were quite similar. However, the leaching efficiency of lead by 2nd recycled EDTA was about 20% higher than that of the fresh and 1st recycle. The pH of the regenerated EDTA were slightly different but, as mentioned above, the pH has little influence on the leaching of lead. The lower leaching efficiency of lead using fresh and 1st cycle was most likely due to the fact that the leaching was carried out in larger reactors without optimization of the stirring. The 2nd cycle leaching was carried out using the same vial as the small−scale screening experiments and thus the leaching efficiency of lead was closer to the optimized small-scale experiments. Nevertheless, the leaching efficiencies were still high, indicating that the recovered EDTA solution could be reused successfully. A conceptual flowsheet of the leaching of lead matte and slag and subsequent recovery of the EDTA by two precipitation steps is shown in Figure 6.10.

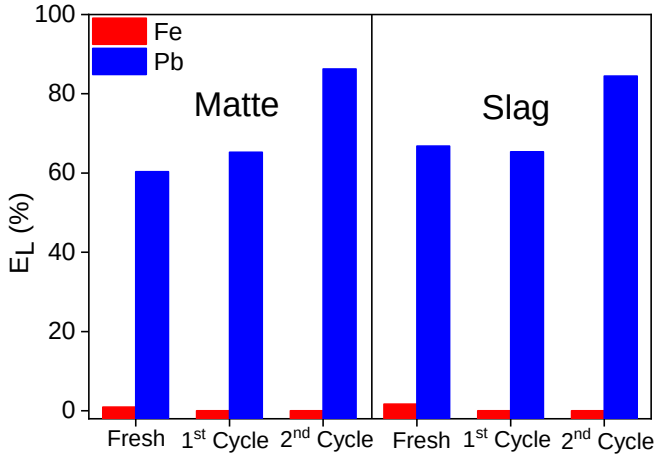


Figure 6.9: Comparative leaching efficiencies of lead and iron from matte and slag by fresh EDTA and recycled EDTA. Leaching parameters: temperature 25 °C, stirring speed 600 rpm, leaching time 1 h, L/S ratio 5 mL $g^{-1}$, pH (initial) = 8, EDTA concentration 0.05 mol $L^{-1}$.

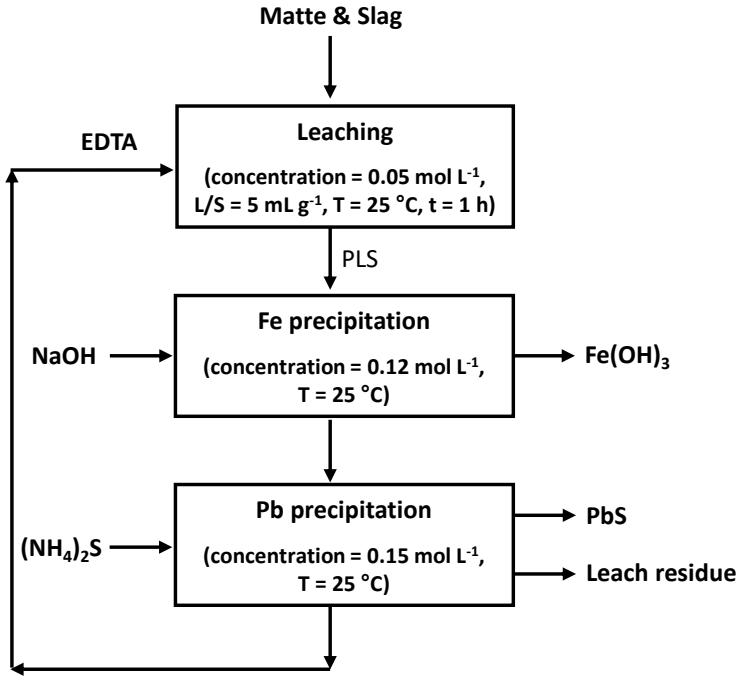


Figure 6.10: Conceptual flow sheet for the selective leaching of lead from matte and slag of the secondary lead smelters by EDTA.

## 6.4 Conclusion

EDTA was used for the leaching of lead from residues (matte and slag) of a secondary lead smelter plant. The residues were composed mainly of iron (34−66%) and lead (7−11%). The use of EDTA in leaching metals from matte and slag resulted in a highly selective leaching of lead over iron: only about 1% of iron was co-dissolved alongside about 80% of the lead. Having a PLS with lead as a major component reduces the cost of downstream processes for obtaining high purity lead and, at the same time, less lead was left in the original residue, which reduces its pollution potential when disposed. The poor leaching of iron by EDTA can be attributed to the low solubility of crystalline iron oxides, iron sulfide and iron silicates which were the major iron phases in the residues. The leaching efficiency of lead increased to 100% when the leaching residues were contacted three times by a fresh EDTA solution. The EDTA in the PLS was recovered by precipitation of iron and lead by sodium hydroxide and ammonium sulfide respectively. The recycled EDTA

was successfully reused for leaching of fresh residues, making the process cheaper and environmentally friendlier.

# Chapter 7: Conclusions and outlook

In this PhD thesis, the potential of organic lixiviants for the selective recovery of toxic and valuable metals from low-grade industrial process residues was investigated. Chapter 3 and 4 were focussed on the selective leaching of lead and zinc over iron from the jarosite of the zinc hydrometallurgy plants. Chapter 5 entailed the selective leaching of antimony over lead from the dross of the lead smelter. Chapter 7 was focussed on the selective leaching of lead over iron from the matte and slag of the lead smelter. The developed leaching processes showed potential for upscaling when the leaching volumes were increased from few milliliters to hundreds of milliliters. The organic lixiviants were also recovered and reused multiples times without significant changes in the leaching efficiencies, which would reduce the overall cost and the environmental impact, and make the processes more industrially viable.

**Factors influencing the selectivity of the leaching processes**

The stability of dissolved metal complexes in a given lixiviant greatly affects the selectivity, since more stable complexes remain in the solution, whereas the less stable ones are precipitated. Some organic lixiviants (e.g. 1.2 mol $L^{-1}$ HCl in ethanol, 1-octanol equilibrated with 12 mol $L^{-1}$ HCl, and TBP equilibrated with 12 mol $L^{-1}$ HCl) leached significant concentration of zinc and iron from jarosite but not lead **(Chapter 3)**. The low leaching efficiency of lead by these lixiviant is most likely due to the low stability of the dissolved lead-chloro complexes in those organic solvents, which led to the precipitation of lead as lead(II) chloride. However, the IL lixiviants [A336][Cl] or [C101][Cl] equilibrated with 12 mol $L^{-1}$ HCl achieved high leaching efficiency of lead (51–66%) and zinc (56–66%) and iron (81–87%). The high leaching efficiency of lead by these lixiviants is due to the presence of cationic counter-ions, which can more easily accommodate large anionic species such as $[PbCl_4]^{2-}$ than molecular solvents such as ethanol or 1-octanol. Methanesulfonic acid (MSA) reacted readily with lead, zinc and iron minerals in the jarosite due to its high acid strength **(Chapter 4)**. The dissolved lead remained in the MSA, but significant amounts of dissolved iron and zinc precipitated as methanesulfonate salts due to their low stability in pure MSA. The presence of ≥10 vol% of water in the MSA solution avoided these precipitate

formations, as the high hydration energy of the metal ions kept them well-solvated in the mixed aqueous-MSA solution. For leaching dross, some of the tested organic lixiviants (e.g. 2 mol $L^{-1}$ HCl in ethanol and 2 mol $L^{-1}$ HCl in 1-octanol), barely leached any lead due to the low stability of lead(II) chloro complexes in these molecular solvent, and thus resulted in the precipitation of the dissolved lead as lead(II) chloride **(Chapter 5)**. The lixiviant 2 mol $L^{-1}$ HCl in ethylene glycol leached some amount of lead (11%), because the two hydroxyl functional groups of ethylene glycol can coordinate bidentately to lead(II) ions, thereby, keeping them solubilized in the lixiviant. The IL [A336][Cl] equilibrated with 12 mol $L^{-1}$ HCl achieved the highest leaching efficiency for lead (45%), as expected due to the stabilization of the dissolved anionic lead(II) complexes ($[PbCl_4]^{2-}$) by the counter cations of the ionic liquid. Unlike lead, the leaching efficiency of antimony by the abovementioned lixiviants were 60−76%, which shows the high stability of antimony(III) chloro complexes in the organic lixiviants.

The selectivity of a leaching process is also influenced by the stability of the metal containing minerals in the residues since stable minerals are hard to leach and vice versa. The lixiviant 2 mol $L^{-1}$ HCl in ethanol leached about 80-90% of antimony from dross **(Chapter 5)**. The XRD analysis of the fresh dross and the leaching residue showed that this lixiviant fully leached the trivalent antimony containing minerals (i.e., $PbO{\cdot}Sb_2O_3$, $Mg/ZnO{\cdot}Sb_2O_3$ and $PbSi_2O_5{\cdot}1.6H_2O$) but the stable pentavalent antimony mineral bindheimite ($2PbO{\cdot}Sb_2O_5$) and trivalent valentinite ($Sb_2O_3$) were only partially leached or not leached at all. By using 0.1 mol $L^{-1}$ EDTA in water as a lixiviant, lead was selectively leached over iron from matte and slag **(Chapter 6)**. The selective leaching of lead over iron was mainly influenced by the stability of different minerals phases in the residues. In a single step leaching, the lixiviant leached about 72 to 80% of lead and less than 1% of iron from both matte and slag. The iron of matte was mainly present as sulfide, and of slag, as silicates and sulfides. Lead of matte and slag was present as elemental state, oxide and carbonate hydroxide, and additionally in the slag, as sulfide. The presence of lead in more reactive mineral phases (oxide and carbonate hydroxide), together with the high stability constant of the Pb(II)-EDTA complex in aqueous solutions resulted in high leaching efficiency of lead. Conversely, the high stability of iron minerals (oxides, sulfide and silicates) in the residues resulted in a low leaching efficiency of iron.

The reactivity of the lixiviant towards the minerals in the residue affects the selectivity of leaching processes. Strong lixiviants can leach very stable minerals whereas weak lixiviants can be inactive towards highly stable

minerals. Strong mineral acids such as 12 mol $L^{-1}$ HCl in water leached 100% of the lead, 76% of the zinc and 92% of the iron from jarosite. Weak organic acids (formic acid, acetic acid, Versatic Acid 10, Cyanex 272) barely leached any metals from jarosite, because they are a poorer lixiviant compared to the mineral acids and thus did not dissolve the metal-containing minerals in jarosite **(chapter 3).** However, the HCl containing organic lixiviants (e.g. 1.2 mol $L^{-1}$ HCl in ethanol, 1-octanol equilibrated with 12 mol $L^{-1}$ HCl, TBP/[A336][Cl]/[C101][Cl] equilibrated with 12 mol $L^{-1}$ HCl) leached higher amounts of metals than the organic acids. Similarly, methanesulfonic acid (MSA) reacted readily with lead, zinc and iron minerals in the jarosite due to its high acid strength **(Chapter 4)**.

**Superior selectivity of solvometallurgy over hydrometallurgy**

Strong hydrometallurgical lixiviants such as HCl in water are usually not selective as they leached both the target metals and undesired metals, and the dissolved metals remained in the solution due to the high solvating power of water. For instance, using 12 mol $L^{-1}$ HCl in water for jarosite leached 100% of the lead, 76% of the zinc and 92% of the iron and thus generated an impure PLS containing mostly iron **(Chapter 4)**. Strong organic lixiviants are obtained by dissolving HCl in organic solvents (e.g. [A336][Cl], [C101][Cl] or ethanol), but the resulting lixiviants are not as good a solvent as water, and subsequently some dissolved metal complexes precipitated, which resulted in a PLS rich in the target metals. The IL lixiviants [A336][Cl] or [C101][Cl] equilibrated with 12 mol $L^{-1}$ HCl achieved high leaching efficiency of lead (51–66%) and zinc (56–66%) and iron (81–87%) **(Chapter 3)**. However, the selectivity towards lead and zinc over iron significantly improved when leaching with [A336][Cl] or [C101][Cl] equilibrated with 0.5 mol $L^{-1}$ HCl, achieving leaching efficiencies of 60–70% lead, 27–30% zinc and 7–10% iron. The competition between the metals for complexation with low concentration of chloride ions most likely favored the formation of lead- and zinc-chloro complexes over iron-chloro complexes. Using 0.5 mol $L^{-1}$ HCl in water was not selective and barely leached any lead ( 12% iron, 32% zinc and 3% lead). Like jarosite, using 12 mol $L^{-1}$ HCl in water for leaching dross was not selective as it leached 90% of the lead and 85% of the antimony **(Chapter 5)**. Using 2 mol $L^{-1}$ HCl in water leached only 4% of lead and 15% of antimony. The organic lixiviant 2 mol $L^{-1}$ HCl in ethanol achieved highly selective leaching of antimony (80–90%) over lead (0.4%). Lead was dissolved by the lixiviant but it precipitated as lead(II) chloride, due to the low stability

stability of lead(II)-chloro complexes in ethanol. The high leaching efficiency of antimony was due to the high stability of antimony(III) chloro complexes in the organic solvent.

Another example of superior selectivity achieved by solvometallurgical lixiviant is the MSA leaching of jarosite **(Chapter 4)**. MSA is a very strong lixiviant that leached both the target (lead and zinc) and undesired metals (iron) from jarosite, but the undesired metal precipitated due to the low stability of iron(III)-methanesulfonate complexes in the organic acid, and subsequently a PLS with only the target metals was obtained. The target metals remained solubilized due to the high stability of lead- and zinc methanesulfonate complexes in the acid. The pure MSA achieved high selectivity towards lead and zinc in the PLS, with leaching efficiencies of 100% lead, 50% zinc and 9% iron. The leaching of matte and slag by 0.1 mol $L^{-1}$ EDTA was also highly selective, with 100% of the lead and only 2-6% of iron leached after contacting the residues three times by a fresh EDTA solution **(Chapter 6)**.

**Economic feasibility of the leaching processes**

The following is an analysis of the economic feasibility of the leaching processes studied in this PhD thesis based on the data of the tables 7.1 and 7.2. Table 7.1 presents the maximum monetary value obtained from the metals removed/recovered from one ton of the industrial process residues, and table 7.2 assesses the economic feasibility of the leaching processes by comparing: the total cost of all the chemicals used, the total value of the recovered metals, and the avoidance of costs and taxes related to the disposal of hazardous metal residues. Note that the energy consumption was not included in the assessment for simplification and due to the lack of and difficult access to reliable data. This would tip the balance towards costs. However, the commercialization of a material that could be safely used in other applications, the landfill cost, and the depletion of hazardous metal waste landfills, causing damage at an average remediation cost of 124,000 €/site[250], was also not included in the analysis, which would tip the balance towards revenues.

The assessment shows that the leaching processes developed for jarosite, matte and slag result in financial loss, mainly due to the low price of the target metals (Pb and Zn) and their low concentrations in the residues. However, the leaching process for dross results in financial gain, mainly due to the high concentration of the target metals and the high price of

specifically antimony metal. In any case, around 90% of the organic lixiviants can be recovered and reused, whereas the remaining 10% is lost in the solid leaching residues and on the equipment surfaces, which was the quantity accounted for in the cost assessment (Table 7.2). The possibility of decomposition of the organic lixiviants after several cycles was not considered in the cost.

Table 7.1: Monetary value of the target metals per ton of the industrial process residues. The metal prices are obtained from www.lme.com.

| Residues | Target metals | Concentration (ton/ton) | Metal price per ton ($) | Maximum metal value per ton ($) | Total metal value per ton ($) |
|---|---|---|---|---|---|
| Jarosite | Pb | 0.04 | 1943 | 78 | 146 |
| | Zn | 0.024 | 2814 | 68 | |
| Matte | Pb | 0.109 | 1943 | 212 | 212 |
| Slag | Pb | 0.068 | 1943 | 132 | 132 |
| Dross | Pb | 0.3 | 1943 | 583 | 3823 |
| | Sb | 0.3 | 10800 | 3240 | |

The assessment shows that the removal/recovery of base metals such as lead and zinc from low-grade industrial process residues (e.g. jarosite, matte, slag) is not economically feasible, when the recovered metals are considered as the only commercial products of the process. In addition, the cost of energy for drying, crushing and milling of the residues prior to leaching, and for heating, stirring and vacuum distillation during the recovery process should be added. In this sense, the energy cost of the process for leaching jarosite using MSA in Chapter 4 can be very high. The leaching was carried out at a high temperature of 130 °C, and the metals were recovered by vacuum distillation at 115 °C and 0.04 mbar. The use of such energy-intensive methods further lessens the economic viability of the process. For developing an economically feasible process for valorization of such residues, the primary objective must be to find a suitable application (e.g. catalyst, cement) for the residues where the majority of the residues can be used with

minimal treatment. In cases where a specific metal(s) is required to be removed before the application, a hydrometallurgical process using relatively cheap chemicals can be employed but using expensive organic lixiviants such as ionic liquids, EDTA and MSA reduces the economic feasibility of the process.

The recovery of lead and antimony from the dross by the ethanol–HCl process is still economically promising, provided that the dross is generated continuously in large volumes by the lead smelters. In this process, antimony is selectively recovered as antimony oxide chloride and the lead remains in the leaching residue. The European industrial company which provided the residue is currently testing the recovered antimony oxide chloride as a flame retardant. The lead-rich leaching residue can be refed into the lead smelter along with other primary and secondary lead sources.

In this PhD thesis, the primary focus was on developing a solvometallurgical process for the removal/recovery of toxic and valuable metals from the given low-grade residues. Rendering the processes economical is a huge challenge, and also beyond the scope of the SOCRATES project which focuses on lower technology readiness levels. Although the developed processes for metal recovery from jarosite, matte and slag are not economically viable, the selective removal of lead from the residues still renders the processes relevant from an environmental point of view. Moreover, the developed processes demonstrate the potential of using organic lixiviant for selective recovery of metals from low-grade metal sources. It can serve for future research on the use of organic lixiviant for selective metal recovery from high-grade residues or low-grade residues containing more expensive metals.

Table 7.2: Comparison of the total cost of chemicals used during the leaching processes to the monetary value of the recovered metals. The price of the chemicals are obtained from www.alibaba.com.

| Leaching process | Chemicals used | Price per ton ($) | Amount required for leaching 1 ton of residue (ton) | Recoverable (%) | Cost ($) | Total chemical cost ($) | Total metal value ($) | Profit-loss per ton ($) |
|---|---|---|---|---|---|---|---|---|
| A336−jarosite | Aliquat 336 | 21000 | 22.3 | 90 | 23669 | 24012 | 66 | -23945 |
| | HCl 35% | 169 | 0.1 | 0 | 18.62 | | | |
| | $NH_3$ sol. 25% | 300 | 1.1 | 0 | 324 | | | |
| MSA−jarosite | MSA | 2500 | 29.6 | 90 | 7400 | 7400 | 112 | -7289* |
| EDTA−matte | $Na_2EDTA$ | 1100 | 507.3 | 90 | 55806 | 84090 | 212 | -83878 |
| | NaOH (pearl) | 760 | 4.1 | 0 | 3549 | | | |
| | $(NH_4)_2S$ | 1100 | 22.5 | 0 | 24735 | | | |
| EDTA−slag | $Na_2EDTA$ | 1100 | 507.3 | 90 | 55806 | 75583 | 132 | -75452 |
| | NaOH (pearl) | 760 | 4.1 | 0 | 3100 | | | |
| | $(NH_3)_2S$ | 1100 | 15.2 | 0 | 16677 | | | |
| EtOH-HCl−dross | Ethanol 96% | 600 | 6.6 | 90 | 395 | 469 | 3823 | 3354* |
| | HCl 35% | 166 | 0.3 | 0 | 55 | | | |
| | Water | 2 | 10 | 0 | 19 | | | |

*Expected to have the highest cost for energy consumption

**Outlook**

This PhD thesis successfully demonstrated the advantages of using organic lixiviants over mineral acids in water for the metal recovery from some industrial process residues but there are still other opportunities to develop new metal recovery processes using organic lixiviants. Fundamental studies about the chemical reactions and metal speciation in different solution are strongly recommended since it will help, firstly, in further improving the processes and, secondly, in applying the processes to other type of materials. The developed processes in this PhD thesis are applicable only to the specific residues studied here. The processes might not work when applied to similar residues from different production plants, since each production plants are different and therefore, the residue generated may differ in terms of chemical composition and mineralogical phases. Therefore, more work is needed to optimize and adjust the leaching processes when applied to similar residues coming from different metallurgical plants. The solvometallurgical processes can be applied to not just industrial process residues but also other materials such as low-grade ores, keeping in mind that the process must be specifically optimized on each material. It would be meaningful to investigate the degree of liberation of the target metals/minerals in the residues, and its effect on the leaching yields. The "degree of liberation" represents the percentage of free or liberated mineral particles in the residue/ore in relation to the total content.[251] The residues to be leached can be milled to different sizes and the degree of the liberation can be determined from the images and elemental maps of SEM or by QEMSCAN instruments (FEI, US).[251,252]

In addition, more research is needed at larger scales (pilot scale) to demonstrate the feasibility and robustness of the developed processes. In this PhD thesis, the scalability was studied on few hundred milliliters to one liter scale, but it needs to be tested on a pilot scale of hundreds of liters over a longer period of time to truly know the associated problems of upscaling. Since the organic lixiviants are more viscous than water, more work on the engineering aspects is required in order to achieve similar leaching efficiencies as in the lab scale tests. This PhD thesis showed the potential reusability of the organic lixiviants for few times but more studies are needed on the reusability of the organic solvents on the long term and in a continuous process. Lastly, organic solvents tend to decompose over time and especially in the presence of acids. Therefore, the rate and the

mechanism of chemical decomposition need to be studied and understood better, by reusing the lixiviants multiple times and monitoring the stability of the organic components.

# References


(1) Korhonen, J.; Honkasalo, A.; Seppälä, J. Circular Economy: The Concept and Its Limitations. *Ecol. Econ.* **2018**, *143*, 37–46. https://doi.org/10.1016/j.ecolecon.2017.06.041.

(2) OECD. *Global Material Resources Outlook to 2060: Economic Drivers and Environmental Consequences*; OECD Publishing: Paris, France, 2019. https://doi.org/10.1787/9789264307452-en.

(3) World Bank. *What a Waste 2.0: A Global Snapshot of Solid Waste Management to 2050*; 2018. https://doi.org/10.1596/978-1-4648-1329-0.

(4) European Commision. Towards a Circular Economy: A Zero Waste Programme for Europe. **2014**, COM/2014/0398.

(5) European Commision. Closing the Loop - An EU Action Plan for the Circular Economy. **2015**, COM/2015/614.

(6) European Commission. Circular Economy Action Plan: For a Cleaner and More Competitive Europe. **2020**, COM/2020/98.

(7) Binnemans, K.; Jones, P. T. Solvometallurgy: An Emerging Branch of Extractive Metallurgy. *J. Sustain. Metall.* **2017**, *3* (3), 570–600. https://doi.org/10.1007/s40831-017-0128-2.

(8) European Training Network for the sustainable, zero-waste valorisation of critical-metal-containing industrial process residues (SOCRATES) https://etn-socrates.eu/.

(9) Dutrizac, J. E.; Jambor, J. L. Jarosites and Their Application in Hydrometallurgy. *Rev. Mineral. Geochemistry* **2000**, *40* (1), 405–452. https://doi.org/10.2138/rmg.2000.40.8.

(10) Hoang, J.; Reuter, M. A.; Matusewicz, R.; Hughes, S.; Piret, N. Top Submerged Lance Direct Zinc Smelting. *Miner. Eng.* **2009**, *22* (9–10), 742–751. https://doi.org/10.1016/j.mineng.2008.12.014.

(11) Wang, Y.; Yang, H.; Zhang, W.; Song, R.; Jiang, B. Study on Recovery of Lead, Zinc, Iron from Jarosite Residues and Simultaneous Sulfur Fixation by Direct Reduction. *Physicochem. Probl. Miner. Process.* **2018**, *54* (2), 517–526. https://doi.org/10.5277/ppmp1859.

(12) Liu, C.; Ju, S. H.; Zhang, L. B.; Srinivasakannan, C.; Peng, J. H.; Le, T. Q. X.; Guo, Z. Y. Recovery of Valuable Metals from Jarosite by Sulphuric

Acid Roasting Using Microwave and Water Leaching. *Can. Metall. Q.* **2017**, *56* (1), 1–9. https://doi.org/10.1080/00084433.2016.1242972.

(13) Wang, Y. yun; Yang, H. fen; Jiang, B.; Song, R. long; Zhang, W. hao. Comprehensive Recovery of Lead, Zinc, and Iron from Hazardous Jarosite Residues Using Direct Reduction Followed by Magnetic Separation. *Int. J. Miner. Metall. Mater.* **2018**, *25* (2), 123–130. https://doi.org/10.1007/s12613-018-1555-1.

(14) Monhemius, A. J. The Iron Elephant: A Brief History of Hydrometallurgists' Struggles with Element No. 26. *CIM J.* **2017**, *8*, 1–13. https://doi.org/10.15834/cimj.2017.21.

(15) Ismael, M.; Carvalho, J. Iron Recovery from Sulphate Leach Liquors in Zinc Hydrometallurgy. *Miner. Eng.* **2003**, *16*, 31–39. https://doi.org/10.1016/S0892-6875(02)00310-2.

(16) Steintveit, G. Treatment of Zinc Leach Plant Residue by the Jarosite Process. In *Proceedings of the Institute of Mining and Metallurgy Symposium*; London, UK, 1971; pp 521–528.

(17) Haigh, C.; Wood, J. Jarosite Process Boosts Zn Recovery in Electrolytic Plants. *World Min.* **1972**, 34–38.

(18) Arregui, B.; Gordon, A. R.; Steintvelt, G. The Jarosite Process − Past, Present, and Future. In *Lead–Zinc–Tin'80*; Cigan, J. M., Mackey, T. S., O'Keefe, T., Eds.; Warrendale, USA, 1979; p 97.

(19) Scott, J.; Donyina, D.; Mouland, J. Iron-the Good with the Bad—Kidd Creek Zinc Plant Experience. In *Iron Control in Hydrometallurgy*; Dutrizac, J., Monhemius, A., Eds.; Ellis Horwood: Chichester, UK, 1986; pp 666–675.

(20) Tamargo, F.; San, M.; Valcarcel, M. Asturiana de Zinc: More than 30 Years of Experience with Jarosite Process. In *Iron Control and Disposal*; Dutrizac, J., Harris, G., Eds.; The Canadian Institute of Mining, Metallurgy and Petroleum: Montreal, Canada, 1996; pp 93–100.

(21) Buban, K. R.; Collins, M. J.; Masters, I. M. Iron Control in Zinc Pressure Leach Processes. *JOM* **1999**, *51*, 23–25. https://doi.org/10.1007/s11837-999-0166-8.

(22) Boxal, J. M.; James, S. E. Experience with the Goethite Process at National Zinc. In *Iron Control in Hydrometallurgy*; Dutrizac, J., Monhemius, A., Eds.; Ellis Horwood: Chichester, 1986; pp 676–686.

(23) Torfs, K.; Vliegen, J. The Union Miniere Goethite Process: Plant Practice and Future Prospects. In *Iron Control and Disposal*; Dutrizac, J., Harris, G., Eds.; The Canadian Institute of Mining, Metallurgy and

Petroleum,: Montreal, 1996; pp 135–146.

(24) Ropenack, A. . Hematite—the Solution to a Disposal Problem—an Example from the Zinc Industry. In *Iron Control in Hydrometallurgy*; Dutrizac, J., Monhemius, A., Eds.; Ellis Horwood: Chichester, UK, 1986; pp 730–741.

(25) Pappu, A.; Saxena, M.; Asolekar, S. R. Jarosite Characteristics and Its Utilisation Potentials. *Sci. Total Environ.* **2006**, *359* (1–3), 232–243. https://doi.org/10.1016/j.scitotenv.2005.04.024.

(26) Romero, M.; Rincón, J. M. Microstructural Characterization of a Goethite Waste from Zinc Hydrometallurgical Process. *Mater. Lett.* **1997**, *31*, 67–73. https://doi.org/10.1016/S0167-577X(96)00235-2.

(27) Ju, S.; Zhang, Y.; Zhang, Y.; Xue, P.; Wang, Y. Clean Hydrometallurgical Route to Recover Zinc, Silver, Lead, Copper, Cadmium and Iron from Hazardous Jarosite Residues Produced during Zinc Hydrometallurgy. *J. Hazard. Mater.* **2011**, *192* (2), 554–558. https://doi.org/10.1016/j.jhazmat.2011.05.049.

(28) Kerolli-Mustafa, M.; Ćurković, L.; Fajković, H.; Rončević, S. Ecological Risk Assessment of Jarosite Waste Disposal. *Croat. Chem. Acta* **2015**, *88* (2), 189–196. https://doi.org/10.5562/cca2554.

(29) Mäkinen, J.; Salo, M.; Hassinen, H.; Kinnunen, P. Comparison of Reductive and Oxidative Bioleaching of Jarosite for Valuable Metals Recovery. *Solid State Phenom.* **2017**, *262*, 24–27. https://doi.org/10.4028/www.scientific.net/SSP.262.24.

(30) Kerolli–Mustafa, M.; Fajković, H.; Rončević, S.; Ćurković, L. Assessment of Metal Risks from Different Depths of Jarosite Tailing Waste of Trepça Zinc Industry, Kosovo Based on BCR Procedure. *J. Geochemical Explor.* **2015**, *148*, 161–168. https://doi.org/10.1016/j.gexplo.2014.09.001.

(31) Glinin, A.; Creedy, S.; Matusewicz, R.; Hughes, S.; Reuter, M. Outotec® Ausmelt Technology for Treating Zinc Residues. In *European Metallurgical Conference (EMC)*; Clausthal-Zellerfeld, Germany, 2013; pp 485–494.

(32) Garcia, A.; Valdez, C. Jarosite Disposal Practices at the Penoles Zinc Plant. In *Iron Control and Disposal*; Dutrizac, J. E., Harris, G. B., Eds.; Canadian Institute of Mining, Metallurgy and Petroleum: Montreal, Canada, 1996; pp 643–650.

(33) Chen, T. T.; Dutrizac, J. E. Mineralogical Study of Jarofix Products for the Stabilization of Zinc Industry Jarosite Residues. In *Second International Symposium on Extraction and Processing for the*

*Treatment and Minimization of Wastes*; Ramachandran, V., Nesbitt, C., Eds.; TMS: Warrendale, USA, 1996; pp 659–672.

(34) Asokan, P.; Saxena, M.; Asolekar, S. R. Recycling Hazardous Jarosite Waste Using Coal Combustion Residues. *Mater. Charact.* **2010**, *61* (12), 1342–1355. https://doi.org/10.1016/j.matchar.2010.09.005.

(35) Asokan, P.; Saxena, M.; Asolekar, S. R. Hazardous Jarosite Use in Developing Non-Hazardous Product for Engineering Application. *J. Hazard. Mater.* **2006**, *137* (3), 1589–1599. https://doi.org/10.1016/j.jhazmat.2006.04.054.

(36) Mehra, P.; Gupta, R. C.; Thomas, B. S. Properties of Concrete Containing Jarosite as a Partial Substitute for Fine Aggregate. *J. Clean. Prod.* **2016**, *120*, 241–248. https://doi.org/10.1016/j.jclepro.2016.01.015.

(37) Pelino, M. Recycling of Zinc-Hydrometallurgy Wastes in Glass and Glass Ceramic Materials. *Waste Manag.* **2000**, *20* (7), 561–568. https://doi.org/10.1016/S0956-053X(00)00002-7.

(38) Pisciella, P.; Crisucci, S.; Karamanov, A.; Pelino, M. Chemical Durability of Glasses Obtained by Vitrification of Industrial Wastes. *Waste Manag.* **2001**, *21* (1), 1–9. https://doi.org/10.1016/S0956-053X(00)00077-5.

(39) Ruşen, A.; Sunkar, A. S.; Topkaya, Y. A. Zinc and Lead Extraction from Çinkur Leach Residues by Using Hydrometallurgical Method. *Hydrometallurgy* **2008**, *93* (1–2), 45–50. https://doi.org/10.1016/j.hydromet.2008.02.018.

(40) Turan, M. D.; Altundoğan, H. S.; Tümen, F. Recovery of Zinc and Lead from Zinc Plant Residue. *Hydrometallurgy* **2004**, *75* (1–4), 169–176. https://doi.org/10.1016/j.hydromet.2004.07.008.

(41) Chen, Y.-M.; Tang, M.-T.; Yang, S.-H.; He, J.; Tang, C.-B.; Yang, J.-G.; Lu, J.-Y. Novel Technique of Decomposition of Ammonium Jarosite Bearing Indium in NaOH Medium. *Zhongguo Youse Jinshu Xuebao/Chinese J. Nonferrous Met.* **2009**, *19* (7), 1322–1331.

(42) Han, H.; Sun, W.; Hu, Y.; Jia, B.; Tang, H. Anglesite and Silver Recovery from Jarosite Residues through Roasting and Sulfidization-Flotation in Zinc Hydrometallurgy. *J. Hazard. Mater.* **2014**, *278*, 49–54. https://doi.org/10.1016/j.jhazmat.2014.05.091.

(43) Ntumba Malenga, E.; Mulaba-Bafubiandi, A. F.; Nheta, W. Alkaline Leaching of Nickel Bearing Ammonium Jarosite Precipitate Using KOH, NaOH and $NH_4OH$ in the Presence of EDTA and $Na_2S$. *Hydrometallurgy* **2015**, *155*, 69–78.

https://doi.org/10.1016/j.hydromet.2015.04.004.

(44) Xue, P.-Y.; Ju, S.-H.; Zhang, Y.-F.; Wang, X.-W. Recovery of Valuable Metals by Leaching of Roasted Jarosite Residue. *Guocheng Gongcheng Xuebao/The Chinese J. Process Eng.* **2011**, *11* (1), 56–60.

(45) Palden, T.; Regadío, M.; Onghena, B.; Binnemans, K. Selective Metal Recovery from Jarosite Residue by Leaching with Acid-Equilibrated Ionic Liquids and Precipitation-Stripping. *ACS Sustain. Chem. Eng.* **2019**, *7*, 4239–4246. https://doi.org/10.1021/acssuschemeng.8b05938.

(46) Besser, A. D.; Sorokina, V. S.; Sokolov, O. K.; Paretskii, V. M. Processing of Utilized Lead-Acid Storage Batteries-The Basis of Lead Recycling. *Russ. Metall.* **2009**, *2009*, 781–787. https://doi.org/10.1134/S0036029509080217.

(47) Dupont, D.; Arnout, S.; Jones, P. T.; Binnemans, K. Antimony Recovery from End-of-Life Products and Industrial Process Residues: A Critical Review. *J. Sustain. Metall.* **2016**, *2*, 79–103. https://doi.org/10.1007/s40831-016-0043-y.

(48) German Federal Environmental Agency (UBA). *Report on Best Available Techniques (BAT) in German Zinc and Lead Production*; Berlin, Germany, 1999.

(49) Blanpain, B.; Arnout, S.; Chintinne, M.; R. Swinbourne, D. Chapter 8: Lead Recycling. In *Handbook of Recycling*; Worrell, E., Reuter, M., Eds.; Elsevier: Amsterdam, the Netherlands, 2014; pp 95–111. https://doi.org/10.1016/B978-0-12-396459-5.00008-8.

(50) De Angelis, G.; Medici, F.; Montereali, M. .; Pietrelli, L. Reuse of Residues Arising from Lead Batteries Recycle: A Feasibility Study. *Waste Manag.* **2002**, *22*, 925–930. https://doi.org/10.1016/S0956-053X(02)00082-X.

(51) Penpolcharoen, M. Utilization of Secondary Lead Slag as Construction Material. *Cem. Concr. Res.* **2005**, *35*, 1050–1055. https://doi.org/10.1016/j.cemconres.2004.11.001.

(52) Kim, E.; Roosen, J.; Horckmans, L.; Spooren, J.; Broos, K.; Binnemans, K.; Vrancken, K. C.; Quaghebeur, M. Process Development for Hydrometallurgical Recovery of Valuable Metals from Sulfide-Rich Residue Generated in a Secondary Lead Smelter. *Hydrometallurgy* **2017**, *169*, 589–598. https://doi.org/10.1016/j.hydromet.2017.04.002.

(53) Kim, E.; Horckmans, L.; Spooren, J.; Vrancken, K. C.; Quaghebeur, M.; Broos, K. Selective Leaching of Pb, Cu, Ni and Zn from Secondary

Lead Smelting Residues. *Hydrometallurgy* **2017**, *169*, 372–381. https://doi.org/10.1016/j.hydromet.2017.02.027.

(54) Lin, D.; Qiu, K. Removal of Arsenic and Antimony from Anode Slime by Vacuum Dynamic Flash Reduction. *Environ. Sci. Technol.* **2011**, *45*, 3361–3366. https://doi.org/10.1021/es103424u.

(55) Qiu, K.; Lin, D.; Yang, X. Vacuum Evaporation Technology for Treating Antimony-Rich Anode Slime. *JOM* **2012**, *64*, 1321–1325. https://doi.org/10.1007/s11837-012-0458-2.

(56) Peterson, M.; Twidwell, L. G. Removal of Arsenic from Lead Smelter Speiss. *J. Hazard. Mater.* **1985**, *12*, 225–229. https://doi.org/10.1016/0304-3894(85)85009-3.

(57) Itoh, S.; Ono, J.; Hino, M.; Nagasaka, T. Kinetic Study on Recovery of Antimony in Anode Slime from Used Lead Batteries Utilizing Volatile Oxide Formation. *Mater. Trans.* **2005**, *46*, 658–664. https://doi.org/10.2320/matertrans.46.658.

(58) Anderson, C. G. Hydrometallurgically Treating Antimony-Bearing Industrial Wastes. *JOM* **2001**, *53*, 18–20. https://doi.org/10.1007/s11837-001-0156-y.

(59) Ye, L.; Ouyang, Z.; Chen, Y.; Chen, Y. Ferric Chloride Leaching of Antimony from Stibnite. *Hydrometallurgy* **2019**, *186*, 210–217. https://doi.org/10.1016/j.hydromet.2019.04.021.

(60) Singh, L. N. Synthesis of Potassium Antimony Tartrate from the Antimony Dross of Lead Smelters. *Hydrometallurgy* **1990**, *25*, 19–25. https://doi.org/10.1016/0304-386X(90)90061-6.

(61) Cao, H. Z.; Chen, J. Z.; Yuan, H. J.; Zheng, G. Q. Preparation of Pure $SbCl_3$ from Lead Anode Slime Bearing High Antimony and Low Silver. *Trans. Nonferrous Met. Soc. China (English Ed.* **2010**, *20*, 2397–2403. https://doi.org/10.1016/S1003-6326(10)60661-9.

(62) Forte, F.; Horckmans, L.; Broos, K.; Kim, E.; Kukurugya, F.; Binnemans, K. Closed-Loop Solvometallurgical Process for Recovery of Lead from Iron-Rich Secondary Lead Smelter Residues. *RSC Adv.* **2017**, *7* (79), 49999–50005. https://doi.org/10.1039/C7RA09150H.

(63) Binz, F.; Friedrich, B. Development of Secondary Antimony Oxides from Metallurgical Slags for the Application in Plastic Products. *J. Sustain. Metall.* **2017**, *3* (4), 683–689. https://doi.org/10.1007/s40831-017-0125-5.

(64) Liu, W.; Yang, T.; Zhang, D.; Chen, L.; Liu, Y. A New Pyrometallurgical Process for Producing Antimony White from By-Product of Lead Smelting. *JOM* **2014**, *66*, 1694–1700.

https://doi.org/10.1007/s11837-014-1026-8.

(65) Habashi, F. Handbook of Extractive Metallurgy. Wiley: Weinheim 1997.

(66) Habashi, F. Pyro- Versus Hydrometallurgy or Dry Versus Wet Methods. *JOJ Mater. Sci.* **2017**, *3*, 555618. https://doi.org/10.19080/JOJMS.2018.03.555618.

(67) Haldar, S. K. Mineral Processing. In *Mineral Exploration*; Elsevier, 2018; pp 259–290. https://doi.org/10.1016/B978-0-12-814022-2.00013-7.

(68) Fernández-González, D.; Ruiz-Bustinza, I.; Mochón, J.; González-Gasca, C.; Verdeja, L. F. Iron Ore Sintering: Process. *Miner. Process. Extr. Metall. Rev.* **2017**, *38* (4), 215–227. https://doi.org/10.1080/08827508.2017.1288115.

(69) Habashi, F. A Short History of Hydrometallurgy. *Hydrometallurgy* **2005**, *79*, 15–22. https://doi.org/10.1016/j.hydromet.2004.01.008.

(70) Shamsuddin, M. Chapter 11: Hydrometallurgy. In *Physical Chemistry of Metallurgical Processes*; Wiley-TMS, 2016; pp 423–522. https://doi.org/10.1002/9781119078326.

(71) Habashi, F. *Textbook of Hydrometallurgy*, Second Edi.; Metallurie Extractive Quebec: Quebec, Canada, 1999.

(72) Wang, S. Aqueous Lixiviants: Principle, Types, and Applications. *JOM* **2007**, *59*, 37–42. https://doi.org/10.1007/s11837-007-0129-x.

(73) Peelman, S.; Sun, Z. H. I.; Sietsma, J.; Yang, Y. Chapter 21 - Leaching of Rare Earth Elements: Review of Past and Present Technologies. In *Rare Earths Industry*; Lima, I. B. De, Filho, W. L., Eds.; Elsevier: Amsterdam, the Netherlands, 2016; pp 319–334. https://doi.org/10.1016/B978-0-12-802328-0.00021-8.

(74) Bhargava, S. K.; Ram, R.; Pownceby, M.; Grocott, S.; Ring, B.; Tardio, J.; Jones, L. A Review of Acid Leaching of Uraninite. *Hydrometallurgy* **2015**, *151*, 10–24. https://doi.org/10.1016/j.hydromet.2014.10.015.

(75) Shen, L.; Li, X.; Lindberg, D.; Taskinen, P. Tungsten Extractive Metallurgy: A Review of Processes and Their Challenges for Sustainability. *Miner. Eng.* **2019**, *142*, 105934. https://doi.org/10.1016/j.mineng.2019.105934.

(76) Radmehr, V.; Koleini, S. M. J.; Khalesi, M. R.; Tavakoli Mohammadi, M. R. Ammonia Leaching: A New Approach of Copper Industry in Hydrometallurgical Processes. *J. Inst. Eng. Ser. D* **2013**, *94*, 95–104. https://doi.org/10.1007/s40033-013-0029-x.

(77) Hind, A. R.; Bhargava, S. K.; Grocott, S. C. The Surface Chemistry of Bayer Process Solids: A Review. *Colloids Surf, A Physicochem. Eng. Asp.* **1999**, *146*, 359–374. https://doi.org/10.1016/S0927-7757(98)00798-5.

(78) Finžgar, N.; Leštan, D. Multi-Step Leaching of Pb and Zn Contaminated Soils with EDTA. *Chemosphere* **2007**, *66*, 824–832. https://doi.org/10.1016/j.chemosphere.2006.06.029.

(79) Kim, C.; Lee, Y.; Ong, S. K. Factors Affecting EDTA Extraction of Lead from Lead-Contaminated Soils. *Chemosphere* **2003**, *51*, 845–853. https://doi.org/10.1016/S0045-6535(03)00155-3.

(80) Heil, D. M.; Samani, Z.; Hanson, A. T.; Rudd, B. Remediation of Lead Contaminated Soil by EDTA. I. Batch and Column Studies. *Water. Air. Soil Pollut.* **1999**, *113*, 77–95. https://doi.org/10.1023/A:1005032504487.

(81) Leštan, D.; Luo, C.; Li, X. The Use of Chelating Agents in the Remediation of Metal-Contaminated Soils: A Review. *Environ. Pollut.* **2008**, *153*, 3–13. https://doi.org/10.1016/j.envpol.2007.11.015.

(82) Gitipour, S.; Ahmadi, S.; Madadian, E.; Ardestani, M. Soil Washing of Chromium- and Cadmium-Contaminated Sludge Using Acids and Ethylenediaminetetra Acetic Acid Chelating Agent. *Environ. Technol.* **2016**, *37*, 145–151. https://doi.org/10.1080/09593330.2011.597784.

(83) Smaniotto, A.; Antunes, A.; Filho, I. do N.; Venquiaruto, L. D.; de Oliveira, D.; Mossi, A.; Di Luccio, M.; Treichel, H.; Dallago, R. Qualitative Lead Extraction from Recycled Lead–Acid Batteries Slag. *J. Hazard. Mater.* **2009**, *172*, 1677–1680. https://doi.org/10.1016/j.jhazmat.2009.07.026.

(84) Sasai, R.; Kubo, H.; Kamiya, M.; Itoh, H. Development of an Eco-Friendly Material Recycling Process for Spent Lead Glass Using a Mechanochemical Process and $Na_2EDTA$ Reagent. *Environ. Sci. Technol.* **2008**, *42*, 4159–4164. https://doi.org/10.1021/es0719576.

(85) Li, L.; Ge, J.; Wu, F.; Chen, R.; Chen, S.; Wu, B. Recovery of Cobalt and Lithium from Spent Lithium Ion Batteries Using Organic Citric Acid as Leachant. *J. Hazard. Mater.* **2010**, *176*, 288–293. https://doi.org/10.1016/j.jhazmat.2009.11.026.

(86) Meng, F.; Liu, Q.; Kim, R.; Wang, J.; Liu, G.; Ghahreman, A. Selective Recovery of Valuable Metals from Industrial Waste Lithium-Ion Batteries Using Citric Acid under Reductive Conditions: Leaching Optimization and Kinetic Analysis. *Hydrometallurgy* **2020**, *191*, 105160. https://doi.org/10.1016/j.hydromet.2019.105160.

(87) Rodriguez, N. R.; Onghena, B.; Binnemans, K. Recovery of Lead and Silver from Zinc Leaching Residue Using Methanesulfonic Acid. *ACS Sustain. Chem. Eng.* **2019**, *7* (24), 19807–19815. https://doi.org/10.1021/acssuschemeng.9b05116.

(88) Jana, R. K.; Singh, D. D. N.; Roy, S. K. Hydrochloric Acid Leaching of Sea Nodules with Methanol and Ethanol Addition. *Mater. Trans. JIM* **1993**, *34* (7), 593–598. https://doi.org/10.2320/matertrans1989.34.593.

(89) Kimball, R. B.; Ewing, R. A. Uranium Recovery from Ores with Hydrochloric Acid and Acetone. US Patent 2800387, 1957.

(90) Jana, R. K.; Singh, D. D. N.; Roy, S. K. Alcohol-Modified Hydrochloric Acid Leaching of Sea Nodules. *Hydrometallurgy* **1995**, *38*, 289–298. https://doi.org/10.1016/0304-386X(94)00069-F.

(91) Patterson, C. G.; Runnells, D. D. Geochemistry, Low-Temperature. In *Encyclopedia of Physical Science and Technology*; Meyers, R. A., Ed.; Elsevier: Amsterdam, the Netherlands, 2003; pp 531–547. https://doi.org/10.1016/B0-12-227410-5/00281-7.

(92) *Quantities, Units and Symbols in Physical Chemistry*; Cohen, E. R., Cvitas, T., Frey, J. G., Holström, B., Kuchitsu, K., Marquardt, R., Mills, I., Pavese, F., Quack, M., Stohner, J., Strauss, H. L., Takami, M., Thor, A. J., Eds.; IUPAC: Singapore, 2007. https://doi.org/10.1039/9781847557889.

(93) Ahmad, Z. Basic Concepts in Corrosion. In *Principles of Corrosion Engineering and Corrosion Control*; Butterworth-Heinemann: Oxford, UK, 2006; pp 9–56. https://doi.org/10.1016/B978-075065924-6/50003-9.

(94) Brookins, D. G. *Eh-PH Diagrams for Geochemistry*; Springer: Berlin, Heidelberg, Germany, 1988. https://doi.org/10.1007/978-3-642-73093-1.

(95) Habashi, F. *Principles of Extractive Metallurgy*, Second Edi.; Gordon & Breach: New York, USA, 1980.

(96) *Solvent Extraction Principles and Practice, Revised and Expanded*, 2nd ed.; Rydberg, J., Ed.; CRC Press: New York, USA, 2004. https://doi.org/10.1201/9780203021460.

(97) Ritcey, G. M. Solvent Extraction—Projection to the Future. *Sep. Sci. Tech* **1983**, *18*, 1617–1646. https://doi.org/10.1080/01496398308056118.

(98) Xie, F.; Zhang, T. A.; Dreisinger, D.; Doyle, F. A Critical Review on Solvent Extraction of Rare Earths from Aqueous Solutions. *Miner.*

*Eng.* **2014**, *56*, 10–28. https://doi.org/10.1016/j.mineng.2013.10.021.

(99) Gijsemans, L.; Roosen, J.; Riaño, S.; Jones, P. T.; Binnemans, K. Ammoniacal Solvoleaching of Copper from High-Grade Chrysocolla. *J. Sustain. Met.* **2020**, *6*, 589–598. https://doi.org/10.1007/s40831-020-00294-3.

(100) Wellens, S.; Thijs, B.; Möller, C.; Binnemans, K. Separation of Cobalt and Nickel by Solvent Extraction with Two Mutually Immiscible Ionic Liquids. *Phys. Chem. Chem. Phys.* **2013**, *15*, 9663. https://doi.org/10.1039/c3cp50819f.

(101) Rout, A.; Wellens, S.; Binnemans, K. Separation of Rare Earths and Nickel by Solvent Extraction with Two Mutually Immiscible Ionic Liquids. *RSC Adv.* **2014**, *4*, 5753. https://doi.org/10.1039/c3ra46261g.

(102) Peeters, N.; Binnemans, K.; Riaño, S. Solvometallurgical Recovery of Cobalt from Lithium-Ion Battery Cathode Materials Using Deep-Eutectic Solvents. *Green Chem.* **2020**, *22*, 4210–4221. https://doi.org/10.1039/D0GC00940G.

(103) Deferm, C.; Onghena, B.; Nguyen, V. T.; Banerjee, D.; Fransaer, J.; Binnemans, K. Non-Aqueous Solvent Extraction of Indium from an Ethylene Glycol Feed Solution by the Ionic Liquid Cyphos IL 101: Speciation Study and Continuous Counter-Current Process in Mixer–Settlers. *RSC Adv.* **2020**, *10*, 24595–24612. https://doi.org/10.1039/D0RA04684A.

(104) Li, Z.; Li, X.; Raiguel, S.; Binnemans, K. Separation of Transition Metals from Rare Earths by Non-Aqueous Solvent Extraction from Ethylene Glycol Solutions Using Aliquat 336. *Sep. Purif. Technol* **2018**, *201*, 318–326. https://doi.org/10.1016/j.seppur.2018.03.022.

(105) Jackson, W. M.; Drury, J. S. Miscibility of Organic Solvent Pairs. *Ind. Eng. Chem* **1959**, *51*, 1491–1493. https://doi.org/10.1021/ie50600a039.

(106) Reichardt, C. *Solvents and Solvent Effects in Organic Chemistry*, 3rd ed.; Wiley: Weinheim, Germany, 2003.

(107) Hecker, E. Verteilungsverfahren Im Laboratorium; Verlag Chemie: Weinheim, Germany, 1955.

(108) Hecker, E. Auswahl von Losungsmittelsystemen Zur Multiplikativen Verteilung. *Chimia (Aarau).* **1954**, *8*, 229–236.

(109) Riaño Torres, S. Recovery of Neodymium and Dysprosium from NdFeB Magnets Using Ionic Liquid Technology, KU Leuven, 2017.

(110) Sethurajan, M. Metallurgical Sludges, Bio/Leaching and Heavy Metals Recovery (Zn, Cu), Université Paris-Est, 2015.

(111) Benning, L. G.; Waychunas, G. A. Nucleation, Growth, and Aggregation of Mineral Phases: Mechanisms and Kinetic Controls. In *Kinetics of Water-Rock Interaction*; Springer: New York, USA, 2008; pp 259–333. https://doi.org/10.1007/978-0-387-73563-4_7.

(112) Önal, M. A. R.; Riaño, S.; Binnemans, K. Alkali Baking and Solvometallurgical Leaching of NdFeB Magnets. *Hydrometallurgy* **2020**, *191*, 105213. https://doi.org/10.1016/j.hydromet.2019.105213.

(113) Subrahmanyam, J.; Sastri, M. N. Use of Non-Aqueous Solvents in Anion Exchange Separation of Cobalt and Nickel. *Z. Anal. Chem.* **1962**, *189*, 175–179. https://doi.org/10.1007/BF00468734.

(114) Endres, F.; MacFarlane, D.; Abbott, A. *Electrodeposition from Ionic Liquids*; Wiley: Weinheim, Germany, 2008. https://doi.org/10.1002/9783527622917.

(115) Smith, E. L.; Fullarton, C.; Harris, R. C.; Saleem, S.; Abbott, A. P.; Ryder, K. S. Metal Finishing with Ionic Liquids: Scale-up and Pilot Plants from IONMET Consortium. *Trans. Inst. Met. Finish.* **2010**, *88*, 285–293. https://doi.org/10.1179/174591910X12856686485734.

(116) Abbott, A. P.; McKenzie, K. J. Application of Ionic Liquids to the Electrodeposition of Metals. *Phys. Chem. Chem. Phys.* **2006**, *8*, 4265. https://doi.org/10.1039/b607329h.

(117) Abbott, A. P.; Collins, J.; Dalrymple, I.; Harris, R. C.; Mistry, R.; Qiu, F.; Scheirer, J.; Wise, W. R. Processing of Electric Arc Furnace Dust Using Deep Eutectic Solvents. *Aust. J. Chem.* **2009**, *62*, 341. https://doi.org/10.1071/CH08476.

(118) Abbott, A. P.; Capper, G.; McKenzie, K. J.; Ryder, K. S. Electrodeposition of Zinc–Tin Alloys from Deep Eutectic Solvents Based on Choline Chloride. *J. Electroanal. Chem.* **2007**, *599*, 288–294. https://doi.org/10.1016/j.jelechem.2006.04.024.

(119) Abbott, A. P.; Ballantyne, A.; Harris, R. C.; Juma, J. A.; Ryder, K. S.; Forrest, G. A Comparative Study of Nickel Electrodeposition Using Deep Eutectic Solvents and Aqueous Solutions. *Electrochim. Acta* **2015**, *176*, 718–726. https://doi.org/10.1016/j.electacta.2015.07.051.

(120) Abbott, A. P.; El Ttaib, K.; Frisch, G.; McKenzie, K. J.; Ryder, K. S. Electrodeposition of Copper Composites from Deep Eutectic Solvents Based on Choline Chloride. *Phys. Chem. Chem. Phys.* **2009**,

*11*, 4269. https://doi.org/10.1039/b817881j.

(121) Li, X.; Monnens, W.; Li, Z.; Fransaer, J.; Binnemans, K. Solvometallurgical Process for Extraction of Copper from Chalcopyrite and Other Sulfidic Ore Minerals. *Green Chem.* **2020**, *22*, 417–426. https://doi.org/10.1039/c9gc02983d.

(122) Spathariotis, S.; Peeters, N.; Ryder, K. S.; Abbott, A. P.; Binnemans, K.; Riaño, S. Separation of Iron(III), Zinc(II) and Lead(II) from a Choline Chloride–Ethylene Glycol Deep Eutectic Solvent by Solvent Extraction. *RSC Adv.* **2020**, *10* (55), 33161–33170. https://doi.org/10.1039/D0RA06091G.

(123) Özdemir, S.; Girgin, I. Decomposition of Scheelite in Acid-Alcohol Solutions. *Miner. Eng.* **1991**, *4* (2), 179–184. https://doi.org/10.1016/0892-6875(91)90034-S.

(124) Kopkova, E. K.; Shchelokova, E. A.; Gromov, P. B. Processing of Titanomagnetite Concentrate with a Hydrochloric Extract of N-Octanol. *Hydrometallurgy* **2015**, *156*, 21–27. https://doi.org/10.1016/j.hydromet.2015.05.007.

(125) Girgin, I.; Erkal, F. Dissolution Characteristics of Scheelite in HCl-$C_2H_5OH$-$H_2O$ and HCl-$C_2H_5OH$ Solutions. *Hydrometallurgy* **1993**, *34*, 221–230.

(126) Wongnawa, S.; Boonsin, P.; Sombatchaikul, T. Determination of Impurities in Ilmenite Ore and Residues after Leaching with HCl-Ethylene Glycol by Energy Dispersive X-Ray Fluorescence (EDXRF) Spectrometry. *Hydrometallurgy* **1997**, *45*, 161–167. https://doi.org/10.1016/S0304-386X(96)00071-0.

(127) Girgin, I. Leaching of Ilmenite in HCl-$H_2O$, HCl-$CH_3OH$-$H_2O$ and HCl-$CH_3OH$ Solutions. *Hydrometallurgy* **1990**, *24*, 127–134.

(128) Gernon, M. D.; Wu, M.; Buszta, T.; Janney, P. Environmental Benefits of Methanesulfonic Acid: Comparative Properties and Advantages. *Green Chem.* **1999**, *1*, 127–140. https://doi.org/10.1039/a900157c.

(129) Patai, S.; Rappoport, Z. *The Chemistry of Sulphonic Acids, Esters and Their Derivatives*; Wiley: New Jersey, US, 1991. https://doi.org/10.1002/0470034394.

(130) Raza, N.; Zafar, Z. I.; Najam-ul-Haq, M. Utilization of Formic Acid Solutions in Leaching Reaction Kinetics of Natural Magnesite Ores. *Hydrometallurgy* **2014**, *149*, 183–188. https://doi.org/10.1016/j.hydromet.2014.08.008.

(131) Yaras, A.; Arslanoglu, H. Leaching Behaviour of Low-Grade Copper Ore in the Presence of Organic Acid. *Can. Metall. Q.* **2018**, *57*, 319–

327. https://doi.org/10.1080/00084433.2018.1473136.

(132) Edtmaier, C.; Schiesser, R.; Meissl, C.; Schubert, W. D.; Bock, A.; Schoen, A.; Zeiler, B. Selective Removal of the Cobalt Binder in WC/Co Based Hardmetal Scraps by Acetic Acid Leaching. *Hydrometallurgy* **2005**, *76*, 63–71. https://doi.org/10.1016/j.hydromet.2004.09.002.

(133) Gijsemans, L.; Forte, F.; Onghena, B.; Binnemans, K. Recovery of Rare Earths from the Green Lamp Phosphor $LaPO_4:Ce^{3+},Tb^{3+}$ (LAP) by Dissolution in Concentrated Methanesulphonic Acid. *RSC Adv.* **2018**, *8*, 26349–26355. https://doi.org/10.1039/c8ra04532a.

(134) Thorsen, G.; Grislingås, A.; Steintveit, G. Recovery of Zinc from Zinc Ash and Flue Dusts by Hydrometallurgical Processing. *JOM* **1981**, *33*, 24–29. https://doi.org/https://doi.org/10.1007/BF03354397.

(135) Duan, W.; Zhu, L.; Jing, S.; Zhu, Y.; Chen, J. Study on Properties of TBP-$HNO_3$ Complex Used for Direct Dissolution of Lanthanide and Actinide Oxides in Supercritical Fluid $CO_2$. *Chinese J. Chem.* **2007**, *25*, 319–322.

(136) Kumar, B.; Kumar, S.; Sampath, M.; Sivakumar, D.; Mudali, U. K.; Natarajan, R. Direct Dissolution of $UO_2$ and in Situ Extraction by TBP–$HNO_3$ and TiAP–$HNO_3$ Organic Solutions at Atmospheric Pressure. *J. Radioanal. Nucl. Chem.* **2011**, *288* (2), 443–445. https://doi.org/10.1007/s10967-010-0941-6.

(137) Wellens, S.; Vander Hoogerstraete, T.; Möller, C.; Thijs, B.; Luyten, J.; Binnemans, K. Dissolution of Metal Oxides in an Acid-Saturated Ionic Liquid Solution and Investigation of the Back-Extraction Behaviour to the Aqueous Phase. *Hydrometallurgy* **2014**, *144–145*, 27–33. https://doi.org/10.1016/j.hydromet.2014.01.015.

(138) Dupont, D.; Binnemans, K. Rare-Earth Recycling Using a Functionalized Ionic Liquid for the Selective Dissolution and Revalorization of $Y_2O_3:Eu^{3+}$ from Lamp Phosphor Waste. *Green Chem.* **2015**, *17*, 856–868. https://doi.org/10.1039/C4GC02107J.

(139) Smith, E. L.; Abbott, A. P.; Ryder, K. S. Deep Eutectic Solvents (DESs) and Their Applications. *Chem. Rev.* **2014**, *114*, 11060–11082. https://doi.org/10.1021/cr300162p.

(140) Rodriguez Rodriguez, N.; Machiels, L.; Onghena, B.; Spooren, J.; Binnemans, K. Selective Recovery of Zinc from Goethite Residue in the Zinc Industry Using Deep-Eutectic Solvents. *RSC Adv.* **2020**, *10*, 7328–7335. https://doi.org/10.1039/D0RA00277A.

(141) Pateli, I. M.; Abbott, A. P.; Binnemans, K.; Rodriguez Rodriguez, N.

Recovery of Yttrium and Europium from Spent Fluorescent Lamps Using Pure Levulinic Acid and the Deep Eutectic Solvent Levulinic Acid–Choline Chloride. *RSC Adv.* **2020**, *10*, 28879–28890. https://doi.org/10.1039/D0RA05508E.

(142) Riaño, S.; Petranikova, M.; Onghena, B.; Vander Hoogerstraete, T.; Banerjee, D.; Foreman, M. R. S.; Ekberg, C.; Binnemans, K. Separation of Rare Earths and Other Valuable Metals from Deep-Eutectic Solvents: A New Alternative for the Recycling of Used NdFeB Magnets. *RSC Adv.* **2017**, *7*, 32100–32113. https://doi.org/10.1039/C7RA06540J.

(143) Longo Jr., L.; Craveiro, M. Deep Eutectic Solvents as Unconventional Media for Multicomponent Reactions. *J. Braz. Chem. Soc.* **2018**, *29*, 1999–2025. https://doi.org/10.21577/0103-5053.20180147.

(144) Wang, Q.; Chen, J.; Zheng, A.; Shi, L. Dechelation of Cd-EDTA Complex and Recovery of EDTA from Simulated Soil-Washing Solution with Sodium Sulfide. *Chemosphere* **2019**, *220*, 1200–1207. https://doi.org/10.1016/j.chemosphere.2018.12.212.

(145) Gergoric, M.; Ravaux, C.; Steenari, B.-M.; Espegren, F.; Retegan, T. Leaching and Recovery of Rare-Earth Elements from Neodymium Magnet Waste Using Organic Acids. *Metals (Basel).* **2018**, *8* (9), 721. https://doi.org/10.3390/met8090721.

(146) Ma, D.; Su, M.; Qian, J.; Wang, Q.; Meng, F.; Ge, X.; Ye, Y.; Song, C. Heavy Metal Removal from Sewage Sludge under Citric Acid and Electroosmotic Leaching Processes. *Sep. Purif. Technol.* **2020**, *242*, 116822. https://doi.org/10.1016/j.seppur.2020.116822.

(147) Gargul, K.; Boryczko, B.; Bukowska, A.; Jarosz, P.; Małecki, S. Leaching of Lead and Copper from Flash Smelting Slag by Citric Acid. *Arch. Civ. Mech. Eng.* **2019**, *19*, 648–656. https://doi.org/10.1016/j.acme.2019.02.001.

(148) Ke, X.; Zhang, F. J.; Zhou, Y.; Zhang, H. J.; Guo, G. L.; Tian, Y. Removal of Cd, Pb, Zn, Cu in Smelter Soil by Citric Acid Leaching. *Chemosphere* **2020**, *255*, 126690. https://doi.org/10.1016/j.chemosphere.2020.126690.

(149) Liu, C.; Yan, Q.; Zhang, X.; Lei, L.; Xiao, C. Efficient Recovery of End-of-Life NdFeB Permanent Magnets by Selective Leaching with Deep Eutectic Solvents. *Environ. Sci. Technol.* **2020**, *54*, 10370–10379. https://doi.org/10.1021/acs.est.0c03278.

(150) Nguyen, V. T.; Riaño, S.; Aktan, E.; Deferm, C.; Fransaer, J.; Binnemans, K. Solvometallurgical Recovery of Platinum Group Metals from Spent Automotive Catalysts. *ACS Sustain. Chem. Eng*

**2020**. https://doi.org/10.1021/acssuschemeng.0c07355.

(151) Davris, P.; Balomenos, E.; Panias, D.; Paspaliaris, I. Selective Leaching of Rare Earth Elements from Bauxite Residue (Red Mud), Using a Functionalized Hydrophobic Ionic Liquid. *Hydrometallurgy* **2016**, *164*, 125–135. https://doi.org/10.1016/j.hydromet.2016.06.012.

(152) Rivera, R. M.; Ulenaers, B.; Ounoughene, G.; Binnemans, K.; Van Gerven, T. Extraction of Rare Earths from Bauxite Residue (Red Mud) by Dry Digestion Followed by Water Leaching. *Miner. Eng.* **2018**, *119*, 82–92. https://doi.org/10.1016/j.mineng.2018.01.023.

(153) Markiewicz, M.; Maszkowska, J.; Nardello-Rataj, V.; Stolte, S. Readily Biodegradable and Low-Toxic Biocompatible Ionic Liquids for Cellulose Processing. *RSC Adv.* **2016**, *6*, 87325–87331. https://doi.org/10.1039/C6RA14435G.

(154) Thuy Pham, T. P.; Cho, C.-W.; Yun, Y.-S. Environmental Fate and Toxicity of Ionic Liquids: A Review. *Water Res.* **2010**, *44*, 352–372. https://doi.org/10.1016/j.watres.2009.09.030.

(155) Costa, V.; Urban, F. Lead and Its Alloys: Metallurgy, Deterioration and Conservation. *Stud. Conserv.* **2005**, *50*, 48–62. https://doi.org/10.1179/sic.2005.50.Supplement-1.48.

(156) ILA https://www.ila-lead.org/lead-facts/lead-uses--statistics.

(157) Tchounwou, P. B.; Yedjou, C. G.; Patlolla, A. K.; Sutton, D. J. Heavy Metal Toxicity and the Environment. In *EXS*; 2012; pp 133–164. https://doi.org/10.1007/978-3-7643-8340-4_6.

(158) Blanpain, B.; Reuter, M. A.; Malfliet, A. Lead Metallurgy Is Fundamental to the Circular Economy. *SOCRATES Policy Br.* **2019**, https://kuleuven.sim2.be/wp-content/uploads/2019/0.

(159) Reuter, M. A.; Matusewicz, R.; Van Schaik, A. Lead, Zinc and Their Minor Elements: Enablers of a Circular Economy. *World Metall. - ERZMETALL* **2015**, *68*, 132–146.

(160) van Schalkwyk, R. F.; Reuter, M. A.; Gutzmer, J.; Stelter, M. Challenges of Digitalizing the Circular Economy: Assessment of the State-of-the-Art of Metallurgical Carrier Metal Platform for Lead and Its Associated Technology Elements. *J. Clean. Prod.* **2018**, *186*, 585–601. https://doi.org/10.1016/j.jclepro.2018.03.111.

(161) Dutrizac, J. E. The Behavior of Impurities during Jarosite Precipitation. In *Hydrometallurgical Process Fundamentals*; Bautista, R. G., Ed.; Springer: Boston, USA, 1984; pp 125–169. https://doi.org/10.1007/978-1-4899-2274-8_6.

(162) Dutrizac, J. Jarosite-Type Compounds and Their Application in the Metallurgical Industry. *J. Met.* **1982**, *35*, A70.

(163) Goldstein, J. I.; Newbury, D. E.; Michael, J. R.; Ritchie, N. W. M.; Scott, J. H. J.; Joy, D. C. *Scanning Electron Microscopy and X-Ray Microanalysis*; 2017. https://doi.org/10.1007/978-1-4939-6676-9.

(164) Silva, S. G.; Oliveira, P. V.; Rocha, F. R. P. A Green Analytical Procedure for Determination of Copper and Iron in Plant Materials after Cloud Point Extraction. *J. Braz. Chem. Soc.* **2010**, *21* (2), 234–239. https://doi.org/10.1590/S0103-50532010000200007.

(165) Riaño, S.; Binnemans, K. Extraction and Separation of Neodymium and Dysprosium from Used NdFeB Magnets: An Application of Ionic Liquids in Solvent Extraction towards the Recycling of Magnets. *Green Chem.* **2015**, *17* (5), 2931–2942. https://doi.org/10.1039/c5gc00230c.

(166) Regadío, M.; Riaño, S.; Binnemans, K.; Vander Hoogerstraete, T. Direct Analysis of Metal Ions in Solutions with High Salt Concentrations by Total Reflection X-Ray Fluorescence. *Anal. Chem.* **2017**, *89* (8), 4595–4603. https://doi.org/10.1021/acs.analchem.7b00097.

(167) Svens, K. Outotec Atmospheric Zinc Concentrate Direct Leaching Process – Past, Present and Future. *World Metall. 63*, 136–144.

(168) Farahmand, F.; Moradkhani, D.; Safarzadeh, M. S.; Rashchi, F. Brine Leaching of Lead-Bearing Zinc Plant Residues: Process Optimization Using Orthogonal Array Design Methodology. *Hydrometallurgy* **2009**, *95* (3–4). https://doi.org/10.1016/j.hydromet.2008.07.012.

(169) Guo, Z. H.; Pan, F. K.; Xiao, X. Y.; Zhang, L.; Jiang, K. Q. Optimization of Brine Leaching of Metals from Hydrometallurgical Residue. *Trans. Nonferrous Met. Soc. China (English Ed.* **2010**, *20* (10), 2000–2005. https://doi.org/10.1016/S1003-6326(09)60408-8.

(170) Holdich, R. G.; Lawson, G. J. The Solubility of Aqueous Lead Chloride Solutions. *Hydrometallurgy* **1987**, *19* (2), 199–208. https://doi.org/10.1016/0304-386X(87)90005-3.

(171) Swamy, K. M.; Narayana, K. L. Intensification of Leaching Process by Dual-Frequency Ultrasound. *Ultrason. Sonochem.* **2001**, *8*, 341–346. https://doi.org/10.1016/S1350-4177(01)00067-0.

(172) Dijkstra, J. J.; van der Sloot, H. A.; Comans, R. N. J. The Leaching of Major and Trace Elements from MSWI Bottom Ash as a Function of PH and Time. *Appl. Geochemistry* **2006**, *21*, 335–351. https://doi.org/10.1016/j.apgeochem.2005.11.003.

(173) Fuerstenau, D. W.; Osseo-Asare, K. Adsorption of Copper, Nickel, and Cobalt by Oxide Adsorbents from Aqueous Ammoniacal Solutions. *J. Colloid Interface Sci.* **1987**, *118*, 524–542. https://doi.org/10.1016/0021-9797(87)90487-5.

(174) Monhemius, J. Precipitation Diagrams for Metal Hydroxides, Sulfides, Arsenates and Phosphates. *Trans. Inst. Min. Metall.* **1977**, *86* (Section C), C202–C206.

(175) Vogel, A. I.; Svehla, G. *Vogel's Textbook of Macro and Semimicro Qualitative Inorganic Analysis*; Longman: London, UK, 1979.

(176) BASF SE. Lutropur® - the Friendly Acid. The Purest Form of MSA, Methanesulfonic Acid Made by BASF. **2011**.

(177) Fonfe, B.; Cheung, C. K.; Hartwig, A.; Duerr, N. Process For Operating a Plant For Preparing An Alkanesulfonic Acid. 20190077748A1, 2019.

(178) Springborn Laboratories. *An Acute Oral Toxicity Study in Rats with 70% Methane Sulfonic Acid*; 1997.

(179) Baker, S. C.; Kelly, D. P.; Murrell, J. C. Microbial Degradation of Methanesulphonic Acid: A Missing Link in the Biogeochemical Sulphur Cycle. *Nature* **1991**, *350*, 627–628. https://doi.org/10.1038/350627a0.

(180) Florence, F.; Nisha, S. R.; Rajendran, S.; Srinivasan, K. N.; John, S. Studies on Electrodeposition of Copper from Methanesulphonic Acid Bath . **2011**, *3* (3), 1318–1325.

(181) Commarieu, A.; Hoelderich, W.; Laffitte, J. A.; Dupont, M.-P. Fries Rearrangement in Methane Sulfonic Acid, an Environmental Friendly Acid. *J. Mol. Catal. A Chem.* **2002**, *182–183*, 137–141. https://doi.org/10.1016/S1381-1169(01)00506-4.

(182) Kulkarni, P. Methane Sulphonic Acid Is Green Catalyst in Organic Synthesis. *Orient. J. Chem.* **2015**, *31*, 447–451. https://doi.org/10.13005/ojc/310154.

(183) Luong, B. X.; Petre, A. L.; Hoelderich, W.; Commarieu, A.; Laffitte, J. A. Use of Methanesulfonic Acid as Catalyst for the Production of Linear Alkylbenzenes. *J. Catal.* **2004**, *226*, 301–307. https://doi.org/10.1016/j.jcat.2004.05.025.

(184) Tian, Y.; Meng, X.; Duan, J.; Shi, L. A Novel Application of Methanesulfonic Acid as Catalyst for the Alkylation of Ole Fi Ns with Aromatics. *Ind. Eng. Chem. Res.* **2012**, *51*, 13627–13631. https://doi.org/10.1021/ie302015v.

(185) Góra, M.; Kozik, B.; Jamroży, K.; Łuczyński, M. K.; Brzuzan, P.; Woźny,

M. Solvent-Free Condensations of Ketones with Malononitrile Catalysed by Methanesulfonic Acid/Morpholine System. *Green Chem.* **2009**, *11*, 863. https://doi.org/10.1039/b820901d.

(186) Jehanno, C.; Flores, I.; Dove, A. P.; Müller, A. J.; Ruipérez, F.; Sardon, H. Organocatalysed Depolymerisation of PET in a Fully Sustainable Cycle Using Thermally Stable Protic Ionic Salt. *Green Chem.* **2018**, *20*, 1205–1212. https://doi.org/10.1039/c7gc03396f.

(187) Sara García-Argüelles; García, C.; Serrano, M. C.; Gutiérrez, M. C.; Ferrera, M. L.; Monte, F. del. Near-to-Eutectic Mixtures as Bifunctional Catalysts in the Low-Temperature-Ring-Opening-Polymerization of ε-Caprolactone. *Green Chem.* **2015**, *17*, 3632–3643. https://doi.org/10.1039/c5gc00348b.

(188) Wu, Z.; Dreisinger, D. B.; Urch, H.; Fassbender, S. Hydrometallurgy The Kinetics of Leaching Galena Concentrates with Ferric Methanesulfonate Solution. *Hydrometallurgy* **2014**, *142*, 121–130. https://doi.org/10.1016/j.hydromet.2013.10.017.

(189) Feng, Q.; Wen, S.; Zhao, W.; Bai, X.; Chen, Y. Dissolution Regularities of Smithsonite in Methane Sulfonic Acid 1. *Russ. J. Non-Ferrous Met.* **2015**, *56* (4), 365–371. https://doi.org/10.3103/S1067821215040033.

(190) FENG, Q.; WEN, S.; ZHAO, W.; LV, C.; BAI, X. Leaching of Copper from Malachite with Methane-Sulfonic Acid. *Solvent Extr. Res. Dev. Japan* **2015**, *22* (2), 159–168.

(191) Hidalgo, T.; Kuhar, L.; Beinlich, A.; Putnis, A. Kinetic Study of Chalcopyrite Dissolution with Iron ( III ) Chloride in Methanesulfonic Acid. *Miner. Eng.* **2018**, *125*, 66–74. https://doi.org/10.1016/j.mineng.2018.05.025.

(192) Zhang, Q.; Wen, S.; Feng, Q.; Nie, W.; Wu, D. Dissolution Kinetics of Hemimorphite in Methane Sulfonic Acid. *Physicochem. Probl. Miner. Process.* **2019**, *55* (1), 1–9. https://doi.org/10.5277/ppmp18105.

(193) Riley, A. L.; Pepper, S. E.; Canner, A. J.; Brown, S. F.; Ogden, M. D. Metal Recovery from Jarosite Waste – A Resin Screening Study. *Sep. Sci. Technol.* **2018**, *53*, 22–35. https://doi.org/10.1080/01496395.2017.1378679.

(194) Jones, P. T.; Binnemans, K. Towards Zero-Waste Valorisation of Landfilled Stocks and Fresh Flows of Critical-Metal-Containing Industrial Process Residues: A Critical Review. In *Third International Academic Symposium on Enhanced Landfill Mining (ELFM III)*; Lisboa, 2016; pp 150–173.

(195) Railsback, B. L. *Some Fundamentals of Mineralogy and Geochemistry*; Department of Geology, University of Georgia Athens, Georgia 30602-2501 U.SA.: Athens,Georgia, USA, 2006.

(196) Grosse, A. V; Snyder, J. C. Production of Organic Compounds from Methanesulfonic Acid. US2553576A, 1947.

(197) Eaton, P. E.; Carlson, G. R.; Lee, J. T. Phosphorus Pentoxide-Methanesulfonic Acid. Convenient Alternative to Polyphosphoric Acid. *J. Org. Chem.* **1973**, *38*, 4071–4073. https://doi.org/10.1021/jo00987a028.

(198) Kapoor, R.; Wadhawan, P.; Kapoor, P. Of Arsenic ( III ), Antimony ( III ), and Bismuth ( II1 ). *Can. J. Chem.* **1987**, *65* (6), 1195–1199. https://doi.org/10.1139/v87-200.

(199) Haynes, J. S.; Sams, J. R.; Thompson, R. C. Synthesis and Structural Studies of Iron(II) and Iron(III) Sulfonates. *Can. J. Chem.* **1981**, *59*, 669–678. https://doi.org/10.1139/v81-098.

(200) Anderson, C. G. The Metallurgy of Antimony. *Geochemistry* **2012**, *72*, 3–8. https://doi.org/10.1016/j.chemer.2012.04.001.

(201) Bruggen, B. Van der; Daniels, D.; Vanroelen, M.; Gerven, T. Van; Balta, S. Closing the Materials Cycle in Pyrometallurgical Production of Lead from Waste Fractions: Hydrometallurgical Purification of Iron Containing Waste in View of Recycling. *Environ. Eng. Manag. J.* **2018**, *17* (2), 381–390. https://doi.org/10.30638/eemj.2018.039.

(202) Ichlas, Z. T.; Rustandi, R. A.; Mubarok, M. Z. Selective Nitric Acid Leaching for Recycling of Lead-Bearing Solder Dross. *J. Clean. Prod.* **2020**, *264*, 121675–121681. https://doi.org/10.1016/j.jclepro.2020.121675.

(203) Palden, T.; Machiels, L.; Onghena, B.; Regadío, M.; Binnemans, K. Selective Leaching of Lead from Lead Smelter Residues Using EDTA. *RSC Adv.* **2020**, *10* (69), 42147–42156. https://doi.org/10.1039/D0RA08517K.

(204) Luo, H. L.; Liu, W.; Qin, W. Q.; Zheng, Y. X.; Yang, K. Cleaning of High Antimony Smelting Slag from an Oxygen-Enriched Bottom-Blown by Direct Reduction. *Rare Met.* **2019**, *38*, 800–804. https://doi.org/10.1007/s12598-015-0468-7.

(205) Keqiang, Q.; Rongliang, Z. Research on Preparation of Nanometer Antimony Trioxide from Slag Containing Antimony by Vacuum Evaporation Method. *Vacuum* **2006**, *80*, 1016–1020. https://doi.org/10.1016/j.vacuum.2006.01.010.

(206) Osmani, A.; Rizaj, M.; Terziqi, A.; Kamberaj, N. Slag Valorisation of

Reductive Smelting Process by Shaft Furnace in the Lead Metallurgy of “Trepça” Complex with Economical and Environmental Effects. *J. Int. Environ. Appl. Sci.* **2009**, *4*, 198–206.

(207) Zhang, B.; Li, Q.; Shen, W.; Min, X. Recovery of Bismuth and Antimony Metals from Pressure-Leaching Slag. *Rare Met.* **2012**, *31*, 102–106. https://doi.org/10.1007/s12598-012-0471-1.

(208) Binz, F.; Friedrich, B. Recovery of Antimony Trioxide Flame Retardants from Lead Refining Residues by Slag Conditioning and Fuming. *Chemie Ing. Tech.* **2015**, *87*, 1569–1579. https://doi.org/10.1002/cite.201500071.

(209) Awe, S. A.; Sandström, Å. Electrowinning of Antimony from Model Sulphide Alkaline Solutions. *Hydrometallurgy* **2013**. https://doi.org/10.1016/j.hydromet.2013.04.006.

(210) Awe, S. A.; Sandström, K. Selective Leaching of Arsenic and Antimony from a Tetrahedrite Rich Complex Sulphide Concentrate Using Alkaline Sulphide Solution. *Miner. Eng.* **2010**, *23*, 1227–1236. https://doi.org/10.1016/j.mineng.2010.08.018.

(211) Yang, T.; Rao, S.; Liu, W.; Zhang, D.; Chen, L. A Selective Process for Extracting Antimony from Refractory Gold Ore. *Hydrometallurgy* **2017**, *169*, 571–575. https://doi.org/10.1016/j.hydromet.2017.03.014.

(212) Yang, T. Z.; Jiang, M. X.; Lai, Q. L.; Chen, J. Z. Sodium Sulfide Leaching of Low-Grade Jamesonite Concentrate in Production of Sodium Pyroantimoniate. *J. Cent. South Univ. Technol. (English Ed.* **2005**, *12*, 1227–1236. https://doi.org/10.1007/s11771-005-0147-1.

(213) Tian, Q.; Wang, H.; Xin, Y.; Li, D.; Guo, X. Ozonation Leaching of a Complex Sulfidic Antimony Ore in Hydrochloric Acid Solution. *Hydrometallurgy* **2016**, *159*, 126–131. https://doi.org/10.1016/j.hydromet.2015.11.011.

(214) Rodríguez-Rodríguez, C.; Nava-Alonso, F.; Uribe-Salas, A.; Viñals, J. Pyrargyrite (Ag3SbS3): Silver and Antimony Dissolution by Ozone Oxidation in Acid Media. *Hydrometallurgy* **2016**, *164*, 15–23. https://doi.org/10.1016/j.hydromet.2016.04.014.

(215) Yang, J. G.; Wu, Y. T. A Hydrometallurgical Process for the Separation and Recovery of Antimony. *Hydrometallurgy* **2014**, *143*, 68–74. https://doi.org/10.1016/j.hydromet.2014.01.002.

(216) Chen, X. Y.; Huh, H. S.; Lee, S. W. Hydrothermal Synthesis of Antimony Oxychloride and Oxide Nanocrystals: $Sb_4O_5Cl_2$, $Sb_8O_{11}Cl_2$, and $Sb_2O_3$. *J. Solid State Chem.* **2008**, *181* (9), 2127–2132.

https://doi.org/10.1016/j.jssc.2008.04.043.

(217) Su, X.; Liu, Y.; Xiao, C.; Zhang, G.; Liu, T.; Qin, J.; Chen, C. A Facile, Clean and Quantitative Synthesis of Antimony Chloride Oxide Single Crystals. *Mater. Lett.* **2006**, *60*, 3879–3881. https://doi.org/10.1016/j.matlet.2006.03.148.

(218) Costa, L.; Goberti, P.; Paganetto, G.; Camino, G.; Sgarzi, P. Thermal Behaviour of Chlorine-Antimony Fire-Retardant Systems. *Polym. Degrad. Stab.* **1990**, *30*, 13–18. https://doi.org/10.1016/0141-3910(90)90114-M.

(219) Xie, J.; Pei, Y.; Liu, L.; Guo, S.; Xia, J.; Li, M.; Ouyang, Y.; Zhang, X.; Wang, X. Hydrothermal Synthesis of Antimony Oxychlorides Submicron Rods as Anode Materials for Lithium-Ion Batteries and Sodium-Ion Batteries. *Electrochim. Acta* **2017**, *254*, 246–254. https://doi.org/10.1016/j.electacta.2017.09.136.

(220) Hu, X.; Chen, F.; Wang, S.; Ru, Q.; Chu, B.; Wei, C.; Shi, Y.; Ye, Z.; Chu, Y.; Hou, X.; Sun, L. Electrochemical Performance of $Sb_4O_5Cl_2$ as a New Anode Material in Aqueous Chloride-Ion Battery. *ACS Appl. Mater. Interfaces* **2019**, *11* (9), 9144–9148. https://doi.org/10.1021/acsami.8b21652.

(221) Lakshmi, K. P.; Janas, K. J.; Shaijumon, M. M. Antimony Oxychloride Embedded Graphene Nanocomposite as Efficient Cathode Material for Chloride Ion Batteries. *J. Power Sources* **2019**, *433*, 126685. https://doi.org/10.1016/j.jpowsour.2019.05.091.

(222) Capello, C.; Fischer, U.; Hungerbühler, K. What Is a Green Solvent? A Comprehensive Framework for the Environmental Assessment of Solvents. *Green Chem.* **2007**, *9* (9), 927. https://doi.org/10.1039/b617536h.

(223) World Refined Lead Supply and Usage 2015−2020. *International Lead and Zinc Study Group (ILZSG)*.

(224) Pan, D.; Li, L.; Tian, X.; Wu, Y.; Cheng, N.; Yu, H. A Review on Lead Slag Generation, Characteristics, and Utilization. *Resour. Conserv. Recycl.* **2019**, *146*, 140–155. https://doi.org/10.1016/j.resconrec.2019.03.036.

(225) Lassin, A.; Piantone, P.; Burnol, A.; Bodénan, F.; Chateau, L.; Lerouge, C.; Crouzet, C.; Guyonnet, D.; Bailly, L. Reactivity of Waste Generated during Lead Recycling: An Integrated Study. *J. Hazard. Mater.* **2007**, *139*, 430–437. https://doi.org/10.1016/j.jhazmat.2006.02.055.

(226) Kim, E.; Horckmans, L.; Spooren, J.; Broos, K.; Vrancken, K. C.; Quaghebeur, M. Recycling of a Secondary Lead Smelting Matte by

Selective Citrate Leaching of Valuable Metals and Simultaneous Recovery of Hematite as a Secondary Resource. *Hydrometallurgy* **2017**, *169*, 290–296. https://doi.org/10.1016/j.hydromet.2017.02.007.

(227) Zhang, S.; Yang, Z.; Wu, B.; Wang, Y.; Wu, R.; Liao, Y. Removal of Cd and Pb in Calcareous Soils by Using $Na_2EDTA$ Recycling Washing. *CLEAN - Soil, Air, Water* **2014**, *42* (5), 641–647. https://doi.org/10.1002/clen.201200634.

(228) Lei, M.; Zeng, M.; Qin, P. feng; Liao, B. han; Tie, B. qing; Tanaka, M. Removal of Cd, Pb, Cu and Zn from Real Contaminated Soils with Fresh and Regenerated $Na_2EDTA$. *Int. J. Environ. Technol. Manag.* **2012**, *15*, 50–60. https://doi.org/10.1504/IJETM.2012.045145.

(229) Deng, T.; Zhang, B.; Li, F.; Jin, L. Sediment Washing by EDTA and Its Reclamation by Sodium Polyamidoamine-Multi Dithiocarbamate. *Chemosphere* **2017**, *168*, 450–456. https://doi.org/10.1016/j.chemosphere.2016.09.152.

(230) Wei, M.; Chen, J. Influence of Multi-Step Washing Using $Na_2EDTA$, Oxalic Acid and Phosphoric Acid on Metal Fractionation and Spectroscopy Characteristics from Contaminated Soil. *Environ. Sci. Pollut. Res.* **2016**, *23*, 23123–23133. https://doi.org/10.1007/s11356-016-7542-z.

(231) Wei, M.; Chen, J.; Wang, X. Removal of Arsenic and Cadmium with Sequential Soil Washing Techniques Using $Na_2EDTA$, Oxalic and Phosphoric Acid: Optimization Conditions, Removal Effectiveness and Ecological Risks. *Chemosphere* **2016**, *156*, 252–261. https://doi.org/10.1016/j.chemosphere.2016.04.106.

(232) Goel, S.; Pant, K. K.; Nigam, K. D. P. Extraction of Nickel from Spent Catalyst Using Fresh and Recovered EDTA. *J. Hazard. Mater.* **2009**, *171*, 253–261. https://doi.org/10.1016/j.jhazmat.2009.05.131.

(233) Fischer, K.; Bipp, H.-P.; Riemschneider, P.; Leidmann, P.; Bieniek, D.; Kettrup, A. Utilization of Biomass Residues for the Remediation of Metal-Polluted Soils. *Environ. Sci. Technol.* **1998**, *32*, 2154–2161. https://doi.org/10.1021/es9706209.

(234) Vuyyuru, K. R.; Pant, K. K.; Krishnan, V. V.; Nigam, K. D. P. Recovery of Nickel from Spent Industrial Catalysts Using Chelating Agents. *Ind. Eng. Chem. Res.* **2010**, *49*, 2014–2024. https://doi.org/10.1021/ie901406e.

(235) Peters, R. W. Chelant Extraction of Heavy Metals from Contaminated Soils. *J. Hazard. Mater.* **1999**, *66*, 151–210. https://doi.org/10.1016/S0304-3894(99)00010-2.

(236) Zeng, Q. R.; Sauvé, S.; Allen, H. E.; Hendershot, W. H. Recycling EDTA Solutions Used to Remediate Metal-Polluted Soils. *Environ. Pollut.* **2005**, *133*, 225–231. https://doi.org/10.1016/j.envpol.2004.06.006.

(237) Snellings, R.; Machiels, L.; Mertens, G.; Elsen, J. Rietveld Refinement Strategy for Quantitative Phase Analysis of Partially Amorphous Zeolitized Tuffaceous Rocks. *Geol. Belgica* **2010**, *13*, 183–196.

(238) Machiels, L.; Garcés, D.; Snellings, R.; Vilema, W.; Morante, F.; Paredes, C.; Elsen, J. Zeolite Occurrence and Genesis in the Late-Cretaceous Cayo Arc of Coastal Ecuador: Evidence for Zeolite Formation in Cooling Marine Pyroclastic Flow Deposits. *Appl. Clay Sci.* **2014**, *87*, 108–119. https://doi.org/10.1016/j.clay.2013.10.018.

(239) Elless, M. P.; Blaylock, M. J. Amendment Optimization to Enhance Lead Extractability from Contaminated Soils for Phytoremediation. *Int. J. Phytoremediation* **2000**, *2*, 75–89. https://doi.org/10.1080/15226510008500031.

(240) Clevenger, T. E.; Saiwan, C.; Koirtyohann, S. R. Lead Speciation of Particles on Air Filters Collected in the Vicinity of a Lead Smelter. *Environ. Sci. Technol.* **1991**, *25*, 1128–1133. https://doi.org/10.1021/es00018a017.

(241) Schwertmann, U.; Cornell, R. M. *Iron Oxides in the Laboratory*; VCH: New York, USA, 1991.

(242) Davison, W. The Solubility of Iron Sulphides in Synthetic and Natural Waters at Ambient Temperature. *Aquat. Sci.* **1991**, *53*, 309–329. https://doi.org/10.1007/BF00877139.

(243) Kim, C. Extraction of Lead Using EDTA: Factors Affecting Extraction, Effects of Amorphous Iron and Recycling of Used EDTA, Iowa State University, 1996.

(244) Rämö, J.; Sillanpää, M. Degradation of EDTA by Hydrogen Peroxide in Alkaline Conditions. *J. Clean. Prod.* **2001**, *9*, 191–195. https://doi.org/10.1016/S0959-6526(00)00049-4.

(245) Koppenol, W. H. The Reaction of Ferrous EDTA with Hydrogen Peroxide: Evidence against Hydroxyl Radical Formation. *J. Free Radic. Biol. Med.* **1985**, *1*, 281–285. https://doi.org/10.1016/0748-5514(85)90132-1.

(246) Elliott, H. A.; Brown, G. A. Comparative Evaluation of NTA and EDTA for Extractive Decontamination of Pb-Polluted Soils. *Water. Air. Soil Pollut.* **1989**, *45*, 361–369. https://doi.org/10.1007/BF00283464.

(247) Steele, M. C.; Pichtel, J. Ex-Situ Remediation of a Metal-Contaminated Superfund Soil Using Selective Extractants. *J. Environ.*

*Eng.* **1998**, *124* (7), 639–645. https://doi.org/10.1061/(asce)0733-9372(1998)124:7(639).

(248) Theodoratos, P.; Papassiopi, N.; Georgoudis, T.; Kontopoulos, A. Selective Removal of Lead from Calcareous Polluted Soils Using the Ca-EDTA Salt. *Water. Air. Soil Pollut.* **2000**, *122*, 351–368. https://doi.org/10.1023/a:1005295119231.

(249) Sun, B.; Zhao, F. J.; Lombi, E.; McGrath, S. P. Leaching of Heavy Metals from Contaminated Soils Using EDTA. *Environ. Pollut.* **2001**, *113*, 111–120. https://doi.org/10.1016/S0269-7491(00)00176-7.

(250) Pérez, A. P.; Eugenio, N. R. Status of Local Soil Contamination in Europe: Revision of the Indicator "Progress in the Management Contaminated Sites in Europe." *Publ. Off. Eur. Union* **2018**, 1–193. https://doi.org/10.2760/09380410.2760/503827.

(251) RAO, D. S.; RATH, S. S.; DASH, N.; MOHANTY, S.; BISWAL, S. K. Mineralogy, Liberation and Leaching Characteristics of Iron Oxide Phases in an Indian Diaspore Sample. *Trans. Nonferrous Met. Soc. China* **2018**, *28*, 1640–1651. https://doi.org/10.1016/S1003-6326(18)64807-1.

(252) Alarcón, A.; Segura, C.; Gamarra, C.; Rodriguez-Reyes, J. C. F. Green Chemistry in Mineral Processing: Chemical and Physical Methods to Enhance the Leaching of Silver and the Efficiency in Cyanide Consumption. *Pure Appl. Chem.* **2018**, *90*, 1109–1120. https://doi.org/10.1515/pac-2017-0904.

# Safety aspects

The experimental work performed during this PhD thesis was executed in compliance with:

- The code of practice for safety in the lab (https://admin.kuleuven.be/sab/vgm/kuleuven/risicoactiviteiten/cv/cglp#section-0)
- The safety guidelines of the department of chemistry of KU Leuven (http://chem.kuleuven.be/veiligheid/documenten/safety-brochure.pdf).

The following safety precautions were taken:

- Risk assessments were approved before each experiment and are available at: https://www.groupware.kuleuven.be/sites/hsecorefacilities/Pages/RA/default.aspx
- For unsupervised experiments, additional risk assessments were prepared and approved by the necessary people according to the procedure: https://admin.kuleuven.be/sab/vgm/kuleuven/en/riskactivities/ue/continuous-activities
- Safety goggle, labcoat and glove were worn while performing the experiments. A mask was used when dealing with powder samples.

The following safety courses were attended at the beginning of the doctoral research (January 2017 – March 2017):

- Introductory course about safety guidelines
- Safety in the Lab
- Radiation Protection

Majority of the chemicals used during this PhD project did not represent unusual safety risks. Care was taken to minimize direct exposure to toxic metal salts, corrosive chemicals (acids/bases) and hazardous organic compounds. Particular care was taken during the handling of solid residues and fine powders, since they are harmful to the respiratory system and potentially also carcinogenic. A mouth mask was worn (in addition to gloves, goggles and lab coat) during the handling of solid residues and fine powders. Attention was also paid to the correct disposal of chemical waste in the appropriate waste vessels, identified by color code and label. Methanesulfonic acid (MSA) reacts aggressively with organic solvents, and therefore, it was diluted with water prior to disposal in inorganic acid waste container. Similarly, nitric acid wastes were made sure to dispose in the oxidant waste container.

Hydrofluoric acid (HF) is one of the most dangerous inorganic acids known, since burns of as little as 1% body surface area can be fatal. Therefore, specific HSE information and work practices for the HF lab were complied, and hands-on training was received as well. HF was always handled in a fumehood equipped with scrubber and forearm-length neoprene gloves were worn. A trained coworker was made sure to be present alongside me in case of emergencies.

# List of publications

## Peer-reviewed publications

**Palden, T.**; Regadío, M.; Onghena, B.; Binnemans, K. Selective Metal Recovery from Jarosite Residue by Leaching with Acid-Equilibrated Ionic Liquids and Precipitation-Stripping. *ACS Sustainable Chemistry and Engineering.* **2019**, *7*, 4239–4246. https://doi.org/10.1021/acssuschemeng.8b05938.

**Palden, T.**; Onghena, B.; Regadío, M.; Binnemans, K. Methanesulfonic Acid: A Sustainable Acidic Solvent for Recovering Metals from the Jarosite Residue of the Zinc Industry. *Green Chemistry.* **2019**, *21*, 5394–5404. https://doi.org/10.1039/C9GC02238D.

**Palden, T**.; Machiels, L.; Onghena, B.; Regadío, M.; Binnemans, K. Selective Leaching of Lead from Lead Smelter Residues Using EDTA. *RSC Advances.* **2020**, *10*, 42147–42156. https://doi.org/10.1039/D0RA08517K.

**Palden, T**.; Machiels, L.; Regadío, M.; Binnemans, K. Antimony recovery from lead-rich dross of lead smelter and conversion into antimony oxide chloride ($Sb_4O_5Cl_2$). *ACS Sustain. Chem. Eng.* **2021**, 9, 5074–5084. https://doi.org/10.1021/acssuschemeng.0c09073.

## Conference proceedings

**Palden, T.**; Regadío, M.; Binnemans, K. Selective solvometallurgical leaching of lead and zinc from jarosite residue of the zinc industry, 4th International Symposium on Enhanced Landfill Mining (ELFM IV), Mechelen (Belgium), 5 – 6 February 2018.

# List of conferences and trainings

## Attended conferences

2nd European Rare Earth Resource (ERES), 28–31st May 2017, Santorini (Greece).

4th International Symposium on Enhanced Landfill Mining (ELFM IV), 5–6th February 2018, Mechelen (Belgium). Poster presentation. **Palden, T.**; Regadío, M.; Binnemans, K. "Selective solvometallurgical leaching of lead and zinc from jarosite residue of the zinc industry".

5th International Symposium on Green Chemistry (ISGC), 13–17 May 2019, La Rochelle (France). Oral presentation. **Palden, T.**; Onghena, B.; Regadío, M.; Binnemans, K. "Selective leaching of lead and zinc from jarosite using methanesulfonic acid".

International Process Metallurgy Symposium (IPMS), 5–6 November 2019, Espoo, Finland. Oral presentation. **Palden, T.**; Onghena, B.; Regadío, M.; Binnemans, K. "Biocompatible solvometallurgical leaching methods for low-grade industrial process residues".

## Secondments (MSCA ETN SOCRATES)

Metallo, Beerse, Belgium, 1st March 2018- 29th May 2018.

- Supervisors: Mathias Chintinne, Rafik Jerroudi
- Title: "Develop a model to calculate the right amount to AdditiveX to add for minimum loss of Ag to copper cathode".

University of Leicester, Leicester, UK, 9th September–31st October 2019.

- Supervisors: Andrew Abbot, Dr. Robert Harris
- Title: "Extraction of metals from DES solution (ethylene glycol and choline chloride) onto an activated carbon".